

LOW-COST REACTION WHEEL DESIGN FOR CUBESAT APPLICATIONS

A Thesis

presented to

the Faculty of California Polytechnic State University,

San Luis Obispo

In Partial Fulfillment

of the Requirements for the Degree

Master of Science in Mechanical Engineering

by

Nicholas J. Bonafede Jr.

July 2020

© 2020

Nicholas J. Bonafede Jr.

ALL RIGHTS RESERVED

## COMMITTEE MEMBERSHIP

TITLE: Low-Cost Reaction Wheel Design for  
CubeSat Applications

AUTHOR: Nicholas J. Bonafede Jr.

DATE SUBMITTED: August 2020

COMMITTEE CHAIR: William R. Murray, Ph.D.  
Professor of Mechanical Engineering

COMMITTEE MEMBER: John Bellardo, Ph.D.  
Professor of Computer Science

COMMITTEE MEMBER: John Ridgely, Ph.D.  
Professor of Mechanical Engineering

## ABSTRACT

### Low-Cost Reaction Wheel Design for CubeSat Applications

Nicholas J Bonafede Jr.

As science instruments on CubeSats become more sensitive to the attitude of the spacecraft, better methods must be employed to provide the accuracy needed to complete the planned mission. While systems that provide the accuracy required are available commercially, these solutions are not cost-effective, do not allow the design to be tailored to a specific mission, and most importantly, do not give students hand-on experience with attitude control actuators. This thesis documents the design, modeling, and simulation of a low-cost, student-fabricated, reaction wheel system for use in 3U CubeSat satellites. The entire design process for the development of this reaction wheel is based on fundamental design principles and can be replicated for either larger or smaller spacecraft as needed. Additionally, plans for bringing this design up to a prototyping and testing phase are outlined for continued use of this design in the Cal Poly CubeSat Laboratory.

Keywords: Reaction wheel, CubeSat, PolySat, attitude determination and control system, ADCS, ACS, actuator, space vehicle, spacecraft, motor, flywheel, mechanical design, MATLAB, Simulink, simulation, modeling, fabrication, assembly

## ACKNOWLEDGMENTS

This work was supported in part by The Aerospace Corporation through industry relations with the Cal Poly CubeSat Laboratory. Thank you for the mentorship and industry experience you have provided.

Dr. William R. Murray, thank you for your guidance on this project and your enthusiasm in teaching. What I learned from your courses has truly spurred my interest in mechatronics and systems design.

Dr. John Bellardo, thank you for your help finding and scoping this project and for your support throughout my time in the Cal Poly CubeSat Laboratory.

Dr. John Ridgely, thank you for taking the time to be on my committee.

I would like to thank each of the individuals in the Cal Poly CubeSat Laboratory who worked with me to develop many of the requirements used in this thesis, especially Liam Bruno, Cole Gillespie, Michael Fernandez, and Nicholas Sizemore.

I would like to express my appreciation for the Cal Poly Mini-Baja team. My time spent on this team taught me the importance of looking at a problem from the ground up and that, often, the simplest solution is the best solution.

To my family and friends, thank you for your support and encouragement to continue pushing my limits and to always go after what matters.

## TABLE OF CONTENTS

|   | Page |
|---|------|
| LIST OF TABLES.....                                 | xi   |
| LIST OF FIGURES .....                               | xii  |
| CHAPTERS  |      |
| 1. INTRODUCTION.....                                | 1    |
| 1.1 Overview of the CubeSat Program .....           | 1    |
| 1.2 CubeSat Design Challenges .....                 | 3    |
| 1.3 Attitude Determination and Control Systems..... | 4    |
| 1.4 Purpose .....                                   | 5    |
| 1.4 Methodology.....                                | 6    |
| 2. BACKGROUND.....                                  | 8    |
| 2.1 Attitude Control Systems.....                   | 8    |
| 2.2 Magnetorquers.....                              | 10   |
| 2.3 Reaction Wheels.....                            | 12   |
| 2.4 Control Moment Gyroscopes.....                  | 15   |
| 2.5 Reaction Control Thrusters .....                | 17   |
| 2.6 Solar Pressure and Aerodynamic Drag .....       | 21   |
| 2.7 Passive Attitude Stability .....                | 21   |
| 3. TRADE STUDY .....                                | 24   |
| 3.1 Pointing Performance.....                       | 25   |

|                               |    |
|-------------------------------|----|
| 3.2 Cost.....                 | 26 |
| 3.3 Mass and Volume.....      | 26 |
| 3.4 System Complexity.....    | 27 |
| 3.5 Design Comparisons.....   | 27 |
| 4. DESIGN REQUIREMENTS.....   | 30 |
| 4.1 Precision.....            | 31 |
| 4.2 Torque .....              | 36 |
| 4.3 Momentum Storage.....     | 38 |
| 4.4 Mass and Volume.....      | 39 |
| 4.5 Rotor Imbalance.....      | 39 |
| 4.6 Requirement Summary ..... | 40 |
| 5. ACTUATOR DESIGN .....      | 42 |
| 5.1 Motor.....                | 42 |
| 5.2 Wheel Material .....      | 45 |
| 5.3 Wheel Geometry.....       | 47 |
| 5.4 Wheel Balancing.....      | 50 |
| 5.5 Hole Fit.....             | 51 |
| 5.6 Motor Housing.....        | 53 |
| 5.7 Three-Axis Assembly ..... | 55 |
| 5.8 Fabrication.....          | 57 |
| 5.9 Motor Controller .....    | 60 |
| 5.10 Performance Summary..... | 63 |
| 6. SIMULATION .....           | 64 |

|   |           |
|---|-----------|
| 6.1 Model.....                              | 64        |
| 6.2 Tuning.....                             | 68        |
| 6.3 Torque Boundary.....                    | 71        |
| 6.4 Operational Range .....                 | 74        |
| 6.5 Expected Maneuver .....                 | 77        |
| <b>7. PROTOTYPING AND TESTING .....</b>     | <b>82</b> |
| 7.1 Procedure Development.....              | 82        |
| 7.2 Procedure Evaluation.....               | 83        |
| 7.3 Vacuum Operation.....                   | 85        |
| 7.4 Performance.....                        | 85        |
| 7.5 Longevity .....                         | 87        |
| 7.6 Quality Assurance.....                  | 88        |
| <b>8. DISCUSSION.....</b>                   | <b>90</b> |
| 8.1 Design.....                             | 90        |
| 8.2 Simulation.....                         | 92        |
| 8.3 Performance.....                        | 93        |
| <b>9. CONCLUSION.....</b>                   | <b>96</b> |
| <b>REFERENCES .....</b>                     | <b>98</b> |
| <b>APPENDICES</b>                           |           |
| A. Commercial CubeSat Reaction Wheels ..... | 103       |
| B. Rotor Imbalance Limits.....              | 105       |
| C. Hole Fit References .....                | 108       |
| D. Simulink Model.....                      | 111       |

|   |     |
|---|-----|
| E. MATLAB Software.....                   | 116 |
| F. Typical Maneuver Torque Requests ..... | 136 |
| G. Mechanical Drawings .....              | 141 |

## LIST OF TABLES

| Table   | Page |
|---|------|
| 1-1. CubeSat Standard Sizes .....                                     | 3    |
| 3-1. Pairwise Comparison of Design Metrics .....                      | 28   |
| 3-2. Decision Matrix to Select Actuator Type .....                    | 29   |
| 4-1. Summary of Design Requirements .....                             | 41   |
| 5-1. Evaluation of Commercial Motors for Reaction Wheel Design .....  | 44   |
| 5-2. Evaluation of Relevant Materials for Flywheel Design .....       | 46   |
| 5-3. Summary of Hole and Shaft Fit Sizes .....                        | 53   |
| 5-4. Evaluation of Maxon BLDC Motor Controllers.....                  | 62   |
| 5-5. Summary of Design Performance Expectations .....                 | 63   |
| 6-1. Motor and Flywheel Parameters Used in Simulink Model .....       | 66   |
| A-1. Examples of Commercial CubeSat Reaction Wheel Products .....     | 104  |
| B-1. Balance Quality Grades for Representative Rigid Rotors.....      | 106  |
| C-1. Descriptions of Preferred Fits Using the Basic Hole System.....  | 109  |
| C-2. Selection of International Tolerance Grades – Metric Series..... | 109  |
| C-3. Fundamental Deviations for Shafts – Metric Series .....          | 110  |

## LIST OF FIGURES

| Figure   | Page |
|--|------|
| 2-1. Diagram of an Attitude Determination and Control System.....                      | 9    |
| 2-2. Diagram of Magnetic Torque Acting on Current in a Magnetorquer.....               | 11   |
| 2-3. Diagram of Momentum Transfer in a Reaction Wheel .....                            | 14   |
| 2-4. Diagram of Momentum Transfer in a Control Moment Gyroscope.....                   | 17   |
| 2-5. Diagram of Torque Generated by Reaction Control Thrusters .....                   | 18   |
| 4-1. Spacecraft Attitude Stability with 10-bit and 12-bit Speed Controllers .....      | 35   |
| 5-1. Flywheel Design.....  | 49   |
| 5-2. Motor, Housing, and Flywheel Assembly Design.....                                 | 54   |
| 5-3. Motor Housing Design.....   | 55   |
| 5-4. Reaction Wheel Three-Axis Assembly.....   | 56   |
| 5-5. Three-Axis Assembly in Context of 1U CubeSat.....                                 | 57   |
| 6-1. Simulink Model of Physical, Electrical, and Mechanical System.....                | 66   |
| 6-2. Simulink Model of Test Input, Control Loop, and Autotuning Logic.....             | 68   |
| 6-3. System Response Before and After Tuning, Step Input.....                          | 70   |
| 6-4. System Response Before and After Tuning, Random Noise.....                        | 70   |
| 6-5. Theoretical Motor Torque Boundary Experiment .....                                | 72   |
| 6-6. Torque Boundary Simulation Compared to Operational<br>Limits, Torque Domain ..... | 73   |
| 6-7. Torque Boundary Simulation, Timeseries Results .....                              | 73   |

|  |     |
|--|-----|
| 6-8. Operation Range Simulation, Speed Setpoints.....  | 75  |
| 6-9. Operational Range Simulation, Torque Domain .....   | 75  |
| 6-10. Operational Range Simulation, Timeseries Results.....                                    | 76  |
| 6-11. Typical CubeSat Attitude Maneuver, ADCS Torque Requests.....                             | 79  |
| 6-12. Typical CubeSat Attitude Maneuver, Timeseries Results.....                               | 79  |
| 6-13. Typical CubeSat Attitude Maneuver, Timeseries Results (Detail).....                      | 80  |
| 6-14. Typical CubeSat Attitude Maneuver, Torque Domain .....                                   | 80  |
| 6-15. Typical CubeSat Attitude Maneuver, Torque Domain (detail).....                           | 81  |
| B-1. Maximum Permissible Residual Unbalance .....  | 107 |
| D-1. Top Level Simulink Model .....  | 112 |
| D-2. Simulink Speed Controller Setpoints for Tuning and Torque<br>Boundary Tests.....          | 113 |
| D-3. Simulink Speed Controller Setpoints for Operational Range Test .....                      | 113 |
| D-4. Simulink Speed Controller Setpoint Integrator for Typical<br>Maneuver Torque Inputs ..... | 114 |
| D-5. Simulink Autotuning Logic Block.....  | 114 |
| D-6. Simulink Universal DC Motor Parameters .....  | 115 |

## CHAPTER 1

### INTRODUCTION

#### 1.1 Overview of the CubeSat program

When a large satellite is designed and a launch vehicle is selected, the mass of the satellite is often less than the payload capacity of the vehicle. Due to the extremely high cost, about \$10,000 per kilogram, to put satellites into orbit, several methods were developed for the primary payload to share the remaining payload capacity with other satellite manufacturers at a reduced price. These “seats” as secondary payloads became commonplace on orbital launches allowing SmallSats to be delivered to orbit without the need to purchase an entire launch vehicle. However, even with the drastic reduction in cost, SmallSats were still too large and costly for most universities to develop. To further reduce the barrier to entry for university students, The CubeSat standard was created by California Polytechnic State University, San Luis Obispo and Stanford University's Space Systems Development Lab in 1999 [1].

The CubeSat standard creates a common platform for nanosatellites, from 1 to 10 kg, allowing universal integration with launch vehicles and simplified construction by the manufacturer. This classification of satellites comes in multiples of  $10 \times 10 \times 10 \text{ cm}$  cubes (1U) with a maximum mass of 1.33 kg per U [16]. These miniature satellites allow academia and industry to participate in rideshares to Low Earth Orbit (LEO). Typically, CubeSat missions are used as a low-cost way to gather preliminary science data, gain flight heritage on specific

components in preparation for a larger mission, or simply when miniaturization of instruments is possible. Many universities, companies, and even some countries use CubeSats as their primary access to space.

Low earth orbit is an excellent place for CubeSats, particularly below 600 km, because of its proximity to earth. This proximity allows for several optimizations to be made that reduce the cost of developing the spacecraft considerably. First, these altitudes are still within the outer wisps of the atmosphere, creating a minute but measurable aerodynamic drag on the spacecraft. This drag slows the spacecraft down over time, reducing its altitude and further increasing its drag. This cycle continues until the spacecraft no longer has the velocity necessary to maintain orbit and burns up in the atmosphere. This cycle occurs over the course of several months up to 25 years and helps keep space debris to a minimum. Second, the lower altitude requires less energy from the spacecraft to send transmissions to earth. The transmission power requirement is important because the spacecraft is limited by the power it can collect via solar panels on its outer faces. Due to the small surface area of CubeSat, the power is often limited to between 1 W and 5 W. Third, the proximity to earth allows the spacecraft to conduct high quality earth observations. Since the spacecraft is so close to the earth it does not require the use of a telescope to get close-up images. Finally, the orbit requires less energy from the launch vehicle to get there, allowing greater payload capacity for other secondary and primary payload(s).

## 1.2 CubeSat Design Challenges

While beneficial to lower budget satellite programs, the CubeSat standard comes with a few design challenges. Typically, the primary constraint on a CubeSat is either volume or power, followed closely by mass. As mentioned previously, a CubeSat must be 10 cm x 10 cm x 10 cm and 1.33 kg per U [16]. These constraints pose challenges in designing a satellite as most space-rated COTS systems (electrical, communications, attitude control) are designed for much larger communications satellites (typically over 1000 kg). Since CubeSats still require all of these mission critical systems to function, they must be redesigned for the much smaller form factor and power requirements.

Several miniature spacecraft components are available as COTS devices. It is even possible to purchase an entire CubeSat prefabricated and designed to specification. However, these services are both expensive and counterproductive to the Cal Poly spirit of Learn By Doing. In the case of spacecraft, this spirit manifests by student designed, built, and tested CubeSats as an extra-curricular teaching exercise.

Table 1-1. CubeSat Standard Sizes [16]

|                | 1U       | 1.5U     | 2U       | 3U       | 6U       |
|----------------|----------|----------|----------|----------|----------|
| Mass [kg]      | 1.33     | 2.00     | 2.66     | 4.00     | 12.00    |
| Dimension [cm] | 10x10x10 | 10x10x15 | 10x10x20 | 10x10x30 | 10x20x30 |

### 1.3 Attitude Determination and Control Systems

One of the primary systems in spacecraft design is the Attitude Determination and Control System (ADCS). As the name of the system suggests, it uses sensors throughout the spacecraft to determine the current orientation of the spacecraft, compares this information with the desired orientation, and uses actuators throughout the spacecraft to adjust the current orientation to match the desired orientation. This functionality can be used to orient the spacecraft relative to the local azimuth (vertical) or horizon, a star cluster, a point on the ground as the craft flies overhead, or even a target moving through space [29].

There are many reasons why a spacecraft might need to orient itself in a specific direction. If a vehicle has a directional antenna for communication with the ground, the antenna must be pointed at the corresponding ground station to communicate with it. As the spacecraft flies over the earth at 28,000 kph, the relative positions of the two devices change and the craft must compensate by changing orientation to track the ground station. Most satellites contain some form of science payload, such as an imager or spectrometer. These devices, and many others, require that they be pointed at a specific target and the orientation held for the duration of the image or test.

For many reasons, it is desirable for CubeSats to be in low earth orbit. As mentioned previously, the small aerodynamic drag causes the spacecrafsts in LEO to slowly deorbit [22]. The deorbiting of CubeSats helps keep space debris to a minimum, but it also limits the life of a spacecraft that could otherwise operate for a longer period. Some CubeSats, and many larger spacecrafsts use

small thrusters to perform “station-keeping” maneuvers to overcome this aerodynamic drag. These thrusters allow the spacecraft to raise its orbit slightly to counteract the drag from the thin atmosphere. However, to perform these maneuvers without losing control of the spacecraft, the vehicle requires precise attitude control.

#### 1.4 Purpose

Cal Poly CubeSat Laboratory presently has the capability to design, build, test, and fly CubeSats that utilize basic attitude control actuators like magnetorquers. These actuators do not allow for 3-axis control and are usually not accurate enough for high-precision scientific measurements to be made. To complete a mission that requires higher precision attitude control, a more precise attitude control actuator must be either developed or purchased.

This project is aiming to develop a low-cost, precision attitude control actuator for use in 3U CubeSat development. To accomplish this task, this project answers several additional questions. Is a reaction wheel the right type of actuator for this application? What is an appropriately-sized reaction wheel for this application? Is it reasonable to have these reaction wheels fabricated by students? How are these reaction wheels expected to perform in benchtop and on-orbit operations?

The scope of this project is limited to design and analysis the actuator itself. The design of control hardware is limited to the selection of existing or commercial hardware for benchtop testing. Additionally, while the final product and the process by which it is developed will certainly be usable in larger or smaller

spacecraft, the design and analysis conducted will be limited to the application of 3U CubeSats.

## 1.5 Methodology

The purpose of this thesis is of a dual nature. Most importantly, it is intended to develop a practical solution to a specific problem. As such, the methods employed here are primarily of an applied nature. However, to understand the problem at hand and the potential solutions, the background research is necessarily fundamental. Additionally, a portion of this work is intended to provide a generalized structure to allow the work to be recreated as needed for other applications and form factors.

In general, the research follows the basic principles of fundamental design. First, a generalized understanding and analysis of the problem is developed using a combination of textbook and industry sources. This process leads to the development of the qualitative requirements necessary to solve this problem. Then, a survey of possible solutions to the defined problem is conducted. The result of this survey allows bias in decision making to be both quantified and mitigated to ensure that justification of the final design path is not premature. Once the decision on the design path is finalized, the requirements are then tailored to specific values relevant to the chosen design track and will be used to drive the design of the product.

With the performance requirements of the design formalized, the design is then executed one component at a time. The design starts with the component that

has the least number of prerequisite decisions to be made. Starting with the most independent design choices allows the design of each component to be based solely on the formalized requirements developed and the other components that have already gone through this process.

With the design complete, the expected performance specifications are summarized and evaluated against the original requirements. The system is then modeled and simulated using a software suite designed for this type of analysis. This model will both allow a detailed analysis of how the system would perform in situ and provide an additional confirmation that the system performance expectations were not made in error.

## Chapter 2

### BACKGROUND

#### 2.1 Attitude Control Systems

There are many reasons for a spacecraft to require pointing in either a specific direction or to track a moving point in space. To accomplish this task a spacecraft must be equipped with an attitude determination and control system (ADCS). The job of the ADCS on a spacecraft is to measure and control what direction the vehicle is pointing. To measure the current orientation, a spacecraft uses a suite of sensors such as accelerometers, gyroscopes, magnetometers, star trackers, and solar angle sensors. Information from available sensors is combined to allow the spacecraft to predict its current orientation and rotational velocity in space. Additional information from ground tracking stations is typically uploaded to the spacecraft to give the vehicle knowledge of its orbit, position, and velocity. Because a system can only control as precisely as the sum of its measurement errors, these systems need to be very precise to meet the mission requirements for pointing accuracy. Fortunately, development of these technologies is both well understood in industry and being adapted to CubeSat applications at the collegiate level. While the systems for measuring the location and orientation of the spacecraft are relatively scalable, the mechanisms to control location and orientation are more difficult to scale [29].

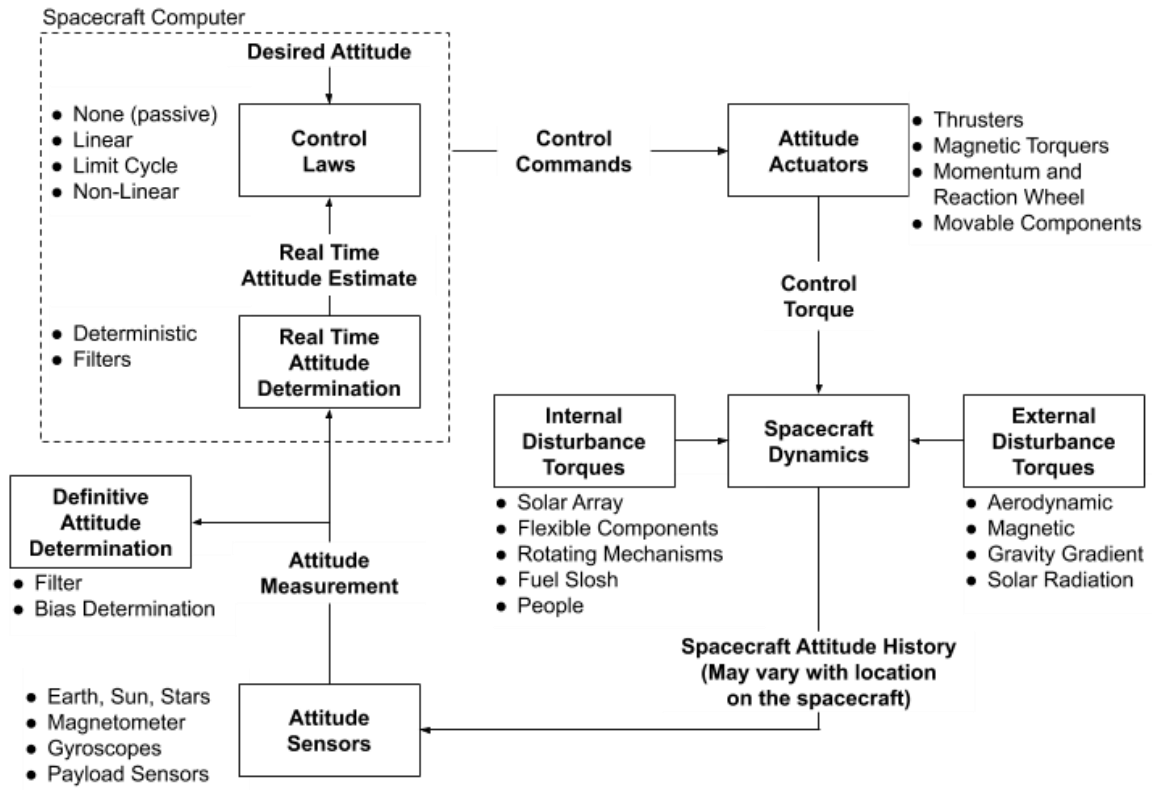


Figure 2-1. Diagram of an Attitude Determination and Control System [29]

According to the law of conservation of momentum, for an object to change its momentum, either translational or rotational, that momentum must be transmitted from one object to another. The measure of this change in momentum is known as an impulse. An impulse is the time integral of the force or torque between the objects. Land, sea, and air vehicles each have a medium that they travel through (or on). The wheels on a car generate an impulse with the ground. The propeller on a boat generates an impulse with the water. The wings on a plane generate an impulse with the air. These impulses allow these vehicles to effectively exchange momentum with the medium of their environment to control their movement. In space, however, there is extremely little land, sea, or air for the spacecraft to exchange momentum with.

For a spacecraft to control its momentum, it must exchange momentum with another object or medium. This process can be done by interacting with the magnetic or gravitational field of the earth, solar radiation pressure, or the extremely thin atmosphere. Other options for generating an impulse in space require the spacecraft to have another object, or propellant, on board to exchange momentum with. The latter options are typically more costly, but usually yield better results.

## 2.2 Magnetorquers

Magnetorquers are the most common attitude control device on CubeSats because of their low-cost, high-reliability, and simple implementation.

Magnetorquers are electrical devices that allow a spacecraft to interact with the local magnetic field, usually the that of the earth [29]. They function by sending current through a coil that is within this magnetic field. Current travelling through a magnetic field creates a force. Current returning on the other side of the coil, creates an opposing force. Diagram and fundamental equations are shown in Figure 1-2 and equations 2.1 through 2.7.

By using magnetorquers in a 3-axis configuration, this device allows the spacecraft to generate torque in any direction perpendicular to the magnetic field. However, since the coils can only generate moments perpendicular to the magnetic field, magnetorquer systems will always be underactuated. More specifically, magnetorquers cannot directly control the spin of the spacecraft around the axis of the magnetic field.

The pointing accuracy of magnetorquer systems is typically limited to about  $\pm 5$  deg. Additionally, magnetorquers require proximity to a body with a strong magnetic field to function. Since CubeSats are usually in LEO, magnetic field strength is generally not an issue. However, CubeSats are beginning to be used for missions beyond LEO, where a magnetic field strong enough for magnetorquers is not present. Examples of deep space CubeSats include MarCO and several advanced concepts projects currently in development [19].

Despite their limitations, the relative simplicity and low cost of magnetorquers makes them the default actuator for most CubeSat missions. Additionally, magnetorquers are often used as secondary actuators for situations when precision attitude control is only needed intermittently, or when desaturation of reaction wheels or control moment gyroscopes becomes necessary.

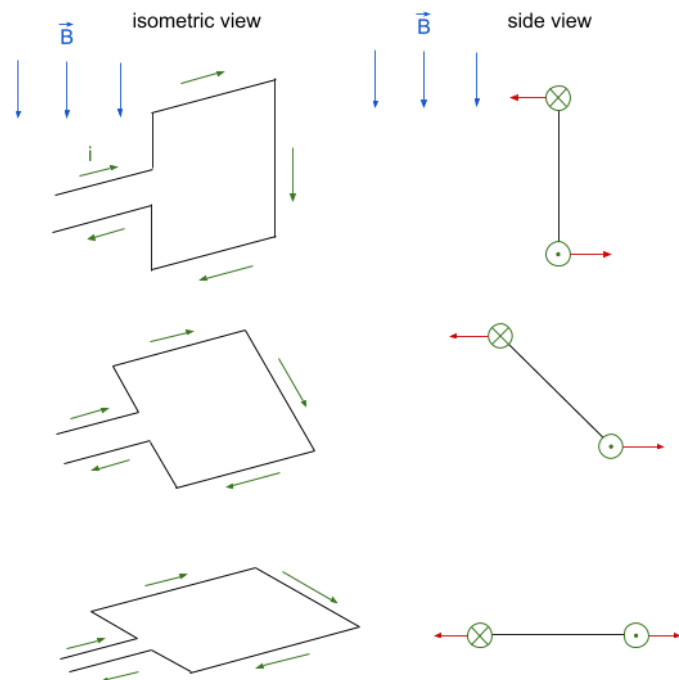


Figure 2-2. Magnetic Torque Acting on Current in a Magnetorquer [23]

$$\vec{F}_0 = (\vec{I} L) \times \vec{B} \quad (2.1)$$

$$\vec{T}_0 = \vec{F}_0 \times \vec{d} \quad (2.2)$$

$$\vec{T}_0 = ((\vec{I} L) \times \vec{B}) \times \vec{d} \quad (2.3)$$

$$\vec{T} = n(\vec{F} \times \vec{d}) \quad (2.4)$$

$$\vec{T} = n((\vec{I} L) \times \vec{B}) \times \vec{d} \quad (2.5)$$

$$\Delta \vec{L} = \int_{t_2}^{t_2} \vec{T} dt \quad (2.6)$$

$$\Delta \vec{L} = \int_{t_2}^{t_2} ((\vec{I} L) \times \vec{B}) \times \vec{d} dt \quad (2.7)$$

where  $\vec{F}_0$  is the force generated by a single wire,  $\vec{I}$  is the current through the wire,  $L$  is the length of the wire,  $\vec{B}$  is the magnetic field,  $\vec{d}$  is the vector between wires on opposing sides of the coil,  $\vec{T}_0$  is the torque generated by a single coil,  $n$  is the number of coils,  $\vec{T}$  is the torque generated by the entire device, and  $\vec{L}$  is the angular momentum of the spacecraft.

### 2.3 Reaction Wheels

It is often necessary for a spacecraft to maintain more control authority than what magnetorquers alone can provide. When additional control authority is required, another body or propellant must be present for the spacecraft to exchange momentum with. The simplest of these devices is the reaction wheel. The device consists of a motor attached to a flywheel. As the motor applies torque to the

flywheel, an equal and opposite torque is applied to the spacecraft. By positioning multiple reaction wheels in a 3-axis configuration and controlling the torque output of each, the ADCS can control the attitude of the spacecraft precisely [29].

The benefits of a reaction wheel system include improved control authority, 3-axis control, no need for propellants, and less complex design when compared to alternatives. The increased power of a motor, compared to magnetorquers allows the system to output much larger torques which, in turn, allows the system to adequately control a much larger vehicle. Since the system does not rely on the magnetic field of the Earth to function, 3-axis control of the spacecraft is possible whether it is near the Earth or out in deep space. Additionally, reaction wheels do not require the use of propellants. Therefore, pressure vessels, valves, and controllers, which add to the development time, cost, mass, and volume used within the spacecraft, are unnecessary. Due to the simplicity of the design, it is also less prone to design and manufacturing errors, further improving reliability and longevity.

The main limitation of reaction wheels is that the wheels have a maximum speed. Over time, the spacecraft experiences disturbances that cause the reaction wheel speed to slowly climb. When the wheel reaches the maximum speed, it cannot go any faster and is said to be saturated. A saturated reaction wheel can only provide torque in one direction. Saturation events usually happen during a maneuver where the wheel was spinning up but was unable to reach the desired speed before saturating. Saturation can result in a failed maneuver and loss of

spacecraft stability that must be recovered using a different attitude control actuator.

To overcome this limitation, reaction wheels must be regularly desaturated.

Desaturation is typically done in one of two ways: (1) applying a known torque to the spacecraft using another actuator, like a magnetorquer, or through careful design of the spacecraft to allow controlled torques from aerodynamic drag or solar radiation pressure; or (2) command the wheels to stop, allowing the spacecraft to tumble from the induced instability, and de-tumbling the spacecraft using other actuators, such as magnetorquers or reaction control thrusters. In either case, the result is the same: a reaction wheels with speeds much further from their saturation points, increasing the useful life of the devices.

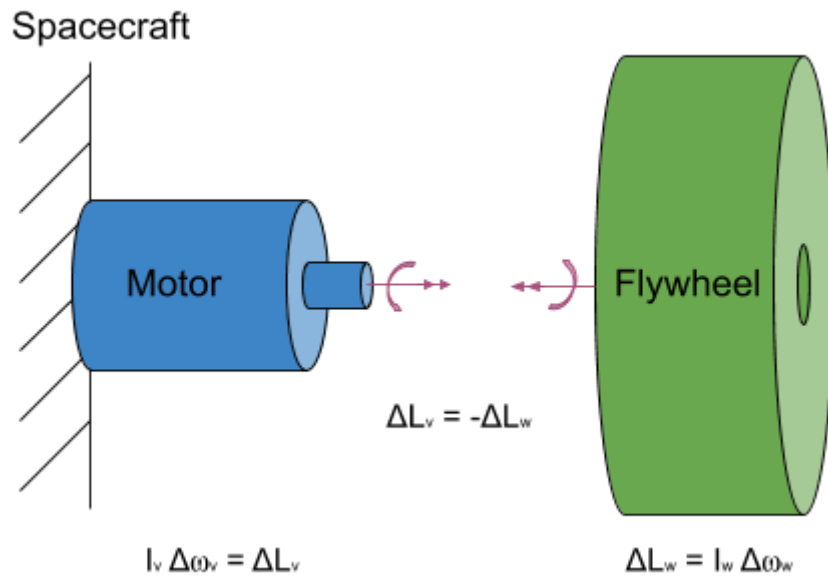


Figure 2-3. Diagram of Momentum Transfer in a Reaction Wheel

$$\vec{L}_1 + \int_{t_2}^{t_2} \vec{T} dt = \vec{L}_2 \quad (2.8)$$

$$\Delta \vec{L} = \int_{t_2}^{t_2} \vec{T} dt \quad (2.9)$$

$$\vec{L}_1 = \vec{L}_2 \quad (2.10)$$

$$\vec{L} = \vec{L}_w + \vec{L}_v \quad (2.11)$$

$$\vec{L}_{1,w} + \vec{L}_{1,v} = \vec{L}_{2,w} + \vec{L}_{2,v} \quad (2.12)$$

$$\Delta \vec{L}_v = -\Delta \vec{L}_w \quad (2.13)$$

Reaction wheels control  $\vec{L}_w$  by changing the magnitude of the vector, not the direction.

$\vec{L}$  is angular momentum,  $\vec{T}$  is torque, and  $\vec{\omega}$  is angular velocity, and  $t$  is time. Subscripts  $v$  and  $w$  denote reference to vehicle or wheel, respectively. Subscripts  $1$  and  $2$  denote state 1 or state 2, respectively.

## 2.4 Control Moment Gyroscopes

Another device that is often used to control the attitude of a spacecraft is a control moment gyroscope. Like a reaction wheel, a control moment gyroscope uses a flywheel to store momentum. However, unlike a reaction wheel, a control moment gyroscope applies torque to change the axis of rotation of the flywheel. The change in direction of the angular momentum of the flywheel causes momentum to be transferred between the device and the spacecraft. The torque applied to the flywheel axis generates an equal and opposite torque on the spacecraft and can be used by the ADCS to control its attitude [29].

Like reaction wheels, control moment gyroscopes allow precise control of a attitude of the spacecraft without the need for propellant and related systems. Additionally, because the wheels are not directly connected to the motors, they generally can be much larger without adversely affecting the life of the motor. Further, since the actuators to change the axis of the gyroscope do not need to be high-speed actuators, they are able to generate larger torques and control larger spacecraft for minimal additional mass. However, control moment gyroscopes must be regularly spun up to recover momentum lost to friction over long periods of time. Additionally, control moment gyroscopes require complex gimbaling systems to change the orientation of the flywheel and operators must be careful to avoid gimbal lock.

Gimbal lock occurs when multiple axes of a gimbal system become co-axial. Gimbal lock results in a situation where the system can only provide torque on two of the axes, the third remaining uncontrolled until the gimbal lock is resolved. Modern control algorithms can handle this situation relatively easily by avoiding situations where this situation would occur preemptively.

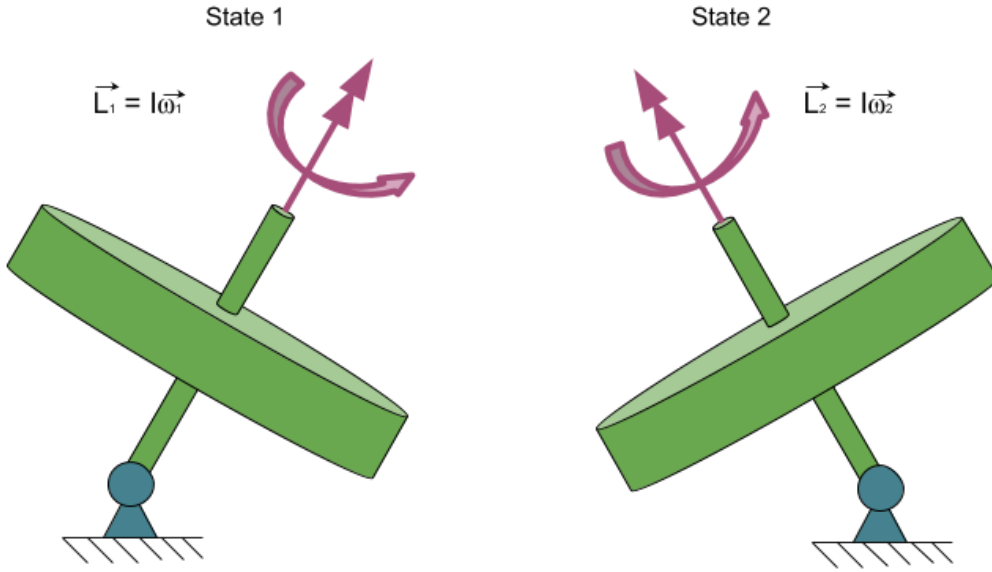


Figure 2-4. Diagram of Momentum Transfer in a Control Moment Gyroscope

$$\Delta \vec{L}_v = -\Delta \vec{L}_w \quad (2.14)$$

Control Moment Gyroscopes control  $\vec{L}_w$  by changing the direction of the vector, not the magnitude.

## 2.5 Reaction Control Thrusters

One of the classic solutions to spacecraft attitude control is to use small thrusters to generate reaction forces on the spacecraft. Firing thrusters in opposing directions separated by a distance generates a moment. A pair of thrusters on each axis can be actuated and throttled up or down to control spacecraft roll, pitch, or yaw independently or even make minor adjustments in trajectory. A thruster-based attitude control is known as a reaction control system (RCS). Reaction control thrusters can be designed to achieve large torques and precision control to effectively control large spacecraft, like the space shuttle [29].

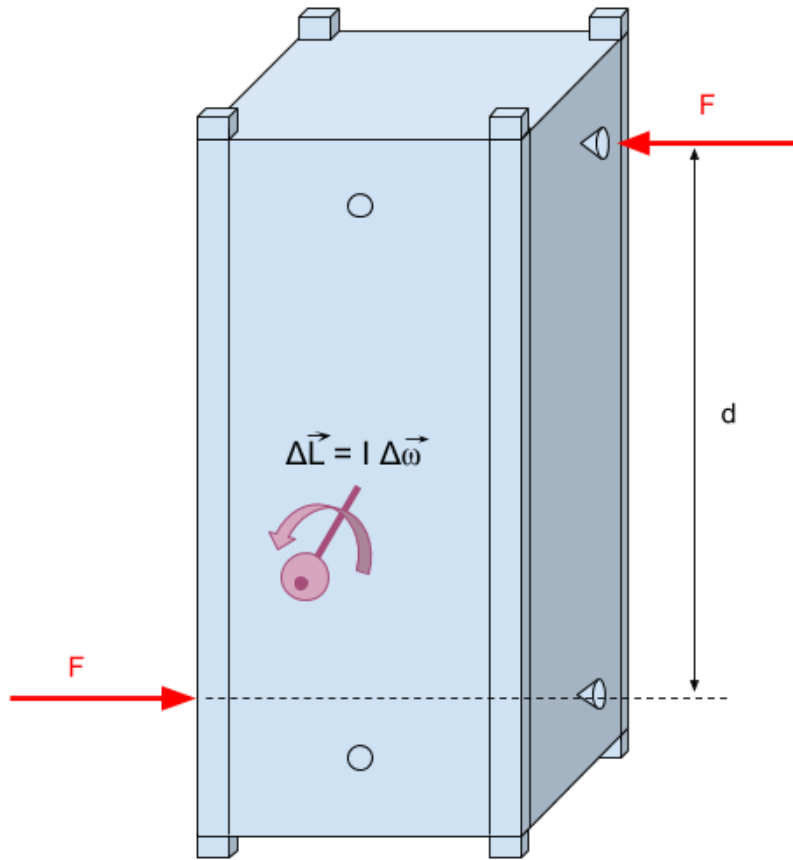


Figure 2-5. Diagram of Torque Generated by Reaction Control Thrusters

$$\Delta \vec{L} = \int_{t_1}^{t_2} \vec{T} dt \quad (2.15)$$

$$\vec{T} = \vec{F} \times \vec{d} \quad (2.16)$$

Reaction control thrusters are small rocket motors. There are many propellant options to choose from when designing a reaction control system. The simplest form of thruster is a cold gas thruster. A propellant, usually inert, is stored in a pressure vessel and released through the desired nozzle to create thrust. Since there is no combustion or heating, there is no need to manage thermal systems. Since the propellant is inert, there is little risk of corrosive materials damaging the

spacecraft. However, due to the low energy density of a simple pressurized gas, such a thruster is not very efficient.

When efficiency becomes more important than simplicity, there are many alternatives that can provide much more thrust for the same amount of propellant. This metric is known as specific impulse. It is a measure of the total impulse delivered per unit of propellant used and is measured in seconds. Generally, a rocket nozzle converts pressure and temperature into linear momentum as the propellant exits the nozzle. The momentum exiting the vehicle creates thrust, causing the vehicle to accelerate. This thrust can be increased by increasing the velocity or the mass of the propellant exiting the nozzle.

There are many ways to increase the exit velocity of a propellant. The most common solution is to increase the temperature of the propellant prior to the nozzle. A monopropellant system uses the heat generated during an exothermic decomposition while flowing the propellant over a catalyst bed to generate heat. A hypergolic system uses two separate propellants that combust spontaneously on contact. These systems are often very corrosive and difficult to store for long periods of time. Other bipropellant systems use less reactive propellants but require an ignition source to start combustion. Other forms of propellant heating involve electrical heating either by flowing the propellant over a resistive element or using micro or radio waves to put the propellant into an energized state, like a plasma. In each case, the heated exhaust is then accelerated out of the nozzle to generate thrust.

A very different type of thruster has also been developed that ionizes its propellant and then accelerates the charged particles to relativistic speed before ejecting them out of the vehicle. This process is known as ion propulsion and can operate at extremely high efficiency for long periods of time. However, this method also operates at very low thrust output and is thus not well suited as an attitude control actuator.

The chemical methods work well at the scale of rockets but see diminishing returns or combustion instability when miniaturizing. The electrical methods have been shown to miniaturize easier than their chemical counterparts. However, even the electric methods experience extremely diminishing returns when trying to miniaturize beyond the size of a primary booster for 3U CubeSat. Which means that the only reasonable propellant option for attitude thrusters on a 3U CubeSat is cold gas.

The primary reason reaction control thrusters are used is to take advantage of their ability to achieve both large torques and precise control, especially with larger spacecraft. Additionally, because the energy used for propulsion is generally stored chemically, the operation of reaction control thrusters consumes little power. Further, reaction control systems do have to worry about saturation, gimbal lock, or running friction. However, reaction control thrusters do require propellant and many complex subsystems, such as plumbing, valves, and heating, to function.

## 2.6 Solar Pressure and Aerodynamic Drag

While normally only considered to be disturbance torques, under careful conditions, solar pressure and atmospheric drag can be used to intentionally apply small torques to a spacecraft. These torques can be used to desaturate reaction wheels or control moment gyroscopes when the lack of a strong magnetic field precludes the use of magnetorquers. This method of attitude control is not common because it produces very little torque and requires that the spacecraft be oriented properly before this method can function properly. The spacecraft must also be designed in such a way that the aerodynamic or illuminated surfaces are oriented to produce the desired torque. Intentionally designing to increase drag torque is counter to the typical design philosophy since, if the spacecraft is not oriented correctly, such a design would generate unusually large disturbance torques [20, 29].

## 2.7 Passive Attitude Stability

All the methods up to this point are active control systems. Active control means that they must be directly controlled by the spacecraft to function properly. However, several methods exist for passive attitude stability in space. The most common of these are spin stability, gravity gradient, aerodynamic stability, and magnetic stabilization. These methods allow the spacecraft design to allow the vehicle to have a natural orientation that it will gravitate toward. This natural orientation is usually very weak, does not provide precise attitude control, and does not easily allow the spacecraft to change the orientation it is drawn toward.

Spin stability operates on the principle of angular momentum. If you cause the spacecraft to spin in a known orientation, it should maintain that orientation for a long period of time without external input. Spin stability is how spacecraft in deep space can power down for long periods of time while maintaining orientation toward Earth for communications. The ability to power down while maintaining attitude stability is useful for saving power and propellant, but it does not actively control the spacecraft and fine adjustments are needed periodically [29].

Gravity gradient stabilization takes advantage of the varied strength of gravity over changes in altitude. Normally this effect is not noticeable on Earth because the difference is so small. However, in space there are a lot less disturbances and this effect can begin to be used effectively. Operationally, the spacecraft extends either one or two long booms (typically between 1 m to 10 m) with mass at the end. The long axis that acts as a pendulum in the microgravity environment. The higher gravity on the radial-in side of the spacecraft causes a torque that acts to center the long axis toward a radial orientation. Gravity gradient stabilization is a simple solution to maintaining an attitude relative to a nearby body, but it does not easily allow the spacecraft to maneuver to an orientation other than radial. Additionally, the pendulum will continue to oscillate at angles near the desired radial orientation resulting in relatively poor stability (typically between  $\pm 5$  deg and  $\pm 10$  deg)

Aerodynamic stability is a concept that allows a spacecraft in low orbit to maintain its attitude relative to its direction of motion. Aerodynamic stability is achieved by creating a high-drag surface toward the rear of the vehicle which

causes that section to naturally drift rearward. While this orientation could be useful, it is not often used because the increased drag also causes the spacecraft to deorbit much sooner than it would otherwise.

Magnetic stabilization is rarely used, but the concept is similar to gravity gradient stabilization using magnetism instead of gravity. Permanent magnets are mounted to the spacecraft. These magnets cause the spacecraft to naturally align its magnetic axis to that of the Earth. This design results in a situation similar to the gravity gradient pendulum where the spacecraft will tend to oscillate around the magnetic field orientation. However, if the spacecraft travels near the poles, the magnetic field direction changes quickly and reverses often. The quickly changing field results in very poor attitude stability in most cases except those near the equator.

## Chapter 3

### TRADE STUDY

When searching for a solution to an engineering problem, first the problem itself must be properly defined. Once there is a clear statement of what factors are important when solving the problem, possible solutions can then be evaluated to determine the best course of action. These solutions should be evaluated based on the metrics determined during the development of requirements. This evaluation is conducted using a pairwise comparison to determine the relative importance of each metric and a decision matrix to compare each design alternative with respect to the weighted decision metrics. Upon analysis, there should be at least one solution that would perform adequately for the desired mission, otherwise, the problem definition and/or constraints must be re-evaluated.

The stated goal of this project is to “develop a low-cost, precision attitude control actuator for use in 3U CubeSat development.” Breaking down this goal, there are three main elements. First, the solution should be capable of precision attitude control for a 3U CubeSat. Secondly, the system should be low-cost to allow for many prototypes and iterations to be made. Additional requirements are implied by the phrase “for the use in 3U CubeSat development.” The system should be of appropriate size and mass for this size CubeSat. Further, the system solution chosen should not be unnecessarily complex as to reduce the cost of implementation into future designs and the likelihood of manufacturing errors.

### 3.1 Pointing Performance

The first and most important requirement is that the actuator must allow the spacecraft to operate with both adequate control authority and sufficient pointing accuracy. If the solution does not meet this requirement, the entire system is not worth developing because it would be simpler, cheaper, and more effective to use the current magnetorquer solutions. Current solutions are both underactuated and only capable of about  $\pm 5 \text{ deg}$  of pointing accuracy. The solution developed here is intended to be used in a full attitude control system with the goal of achieving better than  $\pm 1 \text{ deg}$  of pointing accuracy. There are many other sources of errors in the attitude control system (i.e. sensor orientation, sensor inaccuracy, or actuator location) that compound to produce a total system error. Given that there are many other sources of error, the goal is for the actuator design itself to produce no more than  $\pm 0.1 \text{ deg}$  of pointing inaccuracy.

Breaking it down further, the requirement is shown to be quite nuanced. First, the solution should have large enough torque that the attitude control system has adequate control authority over the spacecraft. Second, the solution should be precise enough to introduce less than  $\pm 0.1 \text{ deg}$  of error into the system. Third, the system must be able to store enough momentum that it will allow the system to perform maneuvers and attitude corrections for an adequate amount of time without requiring desaturation. Finally, the system should be able to survive the duration of the mission with little risk of malfunction and minimal loss in performance.

### 3.2 Cost

Minimizing monetary cost is important because we do not want future development to be unnecessarily hindered by the cost of producing prototypes, test articles, and design iterations. As cost of this custom solution increases, it becomes more and more beneficial to use a commercially available solution because of the reduction of development time. However, as this system is intended to be both a useful instrument for spacecraft design and a learning opportunity for future student teams, it is desired for this solution to be both economical and high performing. The goal for this project is to develop a system that costs less than \$2000 in components for a full 3-axis system.

### 3.3 Mass and Volume

The next consideration is volume and mass. A 3U CubeSat is  $10x10x30\text{ cm}$  with a mass of less than  $4\text{ kg}$  [16]. The attitude control actuator should remain a small portion of this volume and mass to allow the spacecraft enough remaining volume and mass for other mission-critical systems. As a rough goal, it is desired for the system to take up less than a  $\frac{1}{2}\text{U}$  of volume and mass. This goal means that the entire 3-axis system should have a mass of less than  $665\text{ g}$  and take up less than  $10x10x5\text{ cm}$ , or  $500\text{ cm}^3$ .

### 3.4 System Complexity

It is important to minimize the amount of work that needs to be repeated for future mission designers. Everything from mounting of actuators to design of ancillary hardware like propellant tanks and plumbing will require some amount of bespoke design on a per mission basis. Some solutions will require more redesign and others will require less. The less redesign required for a solution to be implemented in future missions will reduce the time cost of using that solution. Time cost, particularly for student designers, is often more valuable than monetary cost.

Additionally, it is also important to minimize the time spent jumping through regulatory hoops. Some designs will require more regulatory steps than others. For example, a system that requires onboard pressure vessels requires more stringent documentation that could easily add months to a project.

### 3.5 Design Comparisons

By comparing the relative importance of each of these considerations, metrics and weights are generated for comparing each solution directly. The results from this exercise show that the most important criteria are max torque, precision, and total momentum storage followed distantly by system mass, longevity, and volume. A normalization factor of four is used to make sure that no one metric takes too much of the relative weighting.

Solutions are compared across these weighted metrics. Solutions being compared are the following: (1) reaction control thrusters, (2) control moment

gyroscopes, and (3) reaction wheels. Each solution is assumed to have additional magnetorquers for low precision maneuvers and desaturation of wheels. Additionally, these solutions are compared against the current solution, magnetorquer only, as a baseline. Results from this decision matrix show that in missions where precision attitude control is required, the reaction wheel solution is the favored configuration followed closely by the control moment gyroscope solution. When precision attitude control is not required, magnetorquers alone are the optimal choice because of their ease of design and low mass, volume, and cost.

Upon review of this information in the context of this application, it is found that the initial assumption of reaction wheels as the primary actuator for a precision 3U attitude control system was optimal.

Table 3-1. Pairwise Comparison of Design Metrics

|            | Torque | Precision | Duration | Momentum | Redesign | Regulation | Volume | Mass | Cost | Normalization | Weight      |
|------------|--------|-----------|----------|----------|----------|------------|--------|------|------|---------------|-------------|
| Torque     | 1      | 1/2       | 4        | 1        | 2        | 4          | 2      | 2    | 4    | 4             | 24.5        |
| Precision  | 2      | 1         | 4        | 1        | 2        | 4          | 2      | 2    | 4    | 4             | 26          |
| Duration   | 1/4    | 1/4       | 1        | 1/4      | 2        | 4          | 1/2    | 1/2  | 2    | 4             | 14.75       |
| Momentum   | 1      | 1         | 4        | 1        | 2        | 4          | 2      | 2    | 4    | 4             | 25          |
| Redesign   | 1/2    | 1/2       | 1/2      | 1/2      | 1        | 2          | 1      | 1/2  | 2    | 4             | 12.5        |
| Regulation | 1/4    | 1/4       | 1/4      | 1/4      | 1/2      | 1          | 2      | 1/2  | 2    | 4             | 11          |
| Volume     | 1/2    | 1/2       | 2        | 1/2      | 1        | 1/2        | 1      | 1    | 2    | 4             | 13          |
| Mass       | 1/2    | 1/2       | 2        | 1/2      | 2        | 2          | 1      | 1    | 2    | 4             | 15.5        |
| Cost       | 1/4    | 1/4       | 1/2      | 1/4      | 1/2      | 1/2        | 1/2    | 1/2  | 1    | 4             | 8.25        |
|            |        |           |          |          |          |            |        |      |      |               | Total 150.5 |

Table 3-2. Decision Matrix to Select Actuator Type

|               | Reaction Control<br>Thrusters | Control Moment<br>Gyroscope | Reaction Wheel | Magnetorquer | Weight |
|---------------|-------------------------------|-----------------------------|----------------|--------------|--------|
| Precision     | 2                             | 4                           | 2              | 1            | 26     |
| Momentum      | 2                             | 2                           | 4              | 1/4          | 25     |
| Torque        | 4                             | 4                           | 4              | 1/4          | 24.5   |
| Mass          | 1/4                           | 1/2                         | 2              | 4            | 15.5   |
| Duration      | 1/4                           | 1                           | 2              | 4            | 14.75  |
| Volume        | 1/4                           | 1/2                         | 2              | 4            | 13     |
| Redesign      | 1/4                           | 1/2                         | 2              | 4            | 12.5   |
| Regulation    | 1/4                           | 2                           | 2              | 4            | 11     |
| Cost          | 1/4                           | 1                           | 2              | 4            | 8.25   |
| <b>Totals</b> | <b>219</b>                    | <b>318</b>                  | <b>400</b>     | <b>338</b>   |        |

## CHAPTER 4

### DESIGN REQUIREMENTS

After reaction wheels are selected as the primary actuation device, requirements need to be developed before iteration on specific actuator design can be conducted. These requirements will be developed from several different sources. First and foremost, the requirements are driven by performance expectations from spacecraft system leads. The most important feature of this system is that it should be useful to these designers in the future. However, prior to development of a specific mission concept, it is not always known what the requirements of a specific mission will be. To overcome this problem, the performance expectations are compared to that of similar products available on the market. While these products are not sized perfectly for this application, they should give good approximations on the order of magnitude of performance required to complete this task.

From the pairwise comparison, it is shown that the key requirements to drive the design of this reaction wheel system are precision, total momentum storage, and maximum torque. Mass and volume requirements are already defined to be less than  $\frac{1}{2}U$ . Cost guidelines are already defined to be less than \$2000 per 3-axis system. Due to the complexity of predicting system life in a thermal vacuum environment, longevity will need to be evaluated by destructive testing of prototypes. System integration and regulatory considerations will be evaluated as

appropriate during the design phase; however, there are no hard requirements regarding this consideration.

#### 4.1 Precision

Attitude precision while using a reaction wheel system is related to precision and type of the wheel controller, the rotational inertia of the flywheel, and the rotational inertia of the spacecraft itself. Since the momentum being transferred from the spacecraft to the wheel is conserved for the entire system, it is simple to show that the change in momentum of the wheel is equal and opposite to the change in momentum of the spacecraft (4.6). Further, the change in angular velocity of the spacecraft is causally related to the change in angular velocity of the wheel by the negative of the ratio of rotational inertias of the two bodies (4.9). This result gives a direct relationship between the accuracy of the wheel speed to the accuracy of the spacecraft angular velocity.

$$L = \sum I\omega = I_w\omega_w + I_v\omega_v \quad (4.1)$$

$$L_1 + \int_{t_1}^{t_2} Mdt = L_2 \quad (4.2)$$

since no external moments are applied to the system,

$$L_1 = L_2 \quad (4.3)$$

$$I_w\omega_{w,1} + I_v\omega_{v,1} = I_w\omega_{w,2} + I_v\omega_{v,2} \quad (4.4)$$

rearranging,

$$I_v \omega_{v,1} - I_v \omega_{v,2} = I_w \omega_{w,2} - I_w \omega_{w,1} \quad (4.5)$$

$$\Delta L_v = -\Delta L_w \quad (4.6)$$

$$I_v (\omega_{v,2} - \omega_{v,1}) = -I_w (\omega_{w,2} - \omega_{w,1}) \quad (4.7)$$

$$I_v \Delta \omega_v = -I_w \Delta \omega_w \quad (4.8)$$

finally,

$$\Delta \omega_v = -\left(\frac{I_w}{I_v}\right) \Delta \omega_w \quad (4.9)$$

where  $L$  is angular momentum,  $I$  is moment of inertia;  $\omega$  is rotational velocity,  $M$  is external moment, and  $t$  is time. Subscripts  $v$  and  $w$  refer the vehicle or flywheel, respectively. Subscripts  $1$  and  $2$  refer to state 1 or 2, respectively. Note that values are scalar since reaction wheels are fixed to a specific axis during installation.

A motor can typically be controlled in one of two methods: torque control or speed control. The flight computer is outputting new torque requests for the reaction wheel to provide at a rate of once per second. Because of the nature of control systems, there is always a lag between when a setpoint is requested and when the plant reaches that setpoint. This lag means that, if this setpoint were a torque setpoint, the total impulse applied would be less than what the flight computer is expecting to have been applied over the second between setpoint updates.

It is for this reason that controlling a reaction wheel is typically done via speed control. The torque request from the flight computer is integrated in software and

divided by the inertia of the wheel to obtain a speed setpoint that accounts for the lag in the control loop. The motor controller receives the speed setpoint, measures the speed of the motor with an encoder, compares the motor speed to the setpoint, and changes the voltage applied to the motor based on the error until the motor is spinning at the desired speed. Because this speed setpoint is changing at the same rate as the motor would if it were producing the desired torque, when the motor catches up, it will have generated an equivalent impulse to what would have been generated if the torque requested could have been applied instantaneously. Additionally, if this process happens faster than the one second update period of the attitude controller, the flight computer never needs to deal with any of these inaccuracies.

Speed controllers typically have either 10, 12, or 16-bit accuracy resulting in either 1024, 4096, or 65,536 possible speeds, respectively. These speeds are divided evenly across the range possible setpoints for the motor and controller. For example, a motor with a max speed of  $1024 \text{ rpm}$  and a 10-bit speed controller would be capable of receiving setpoints with an accuracy of  $1 \text{ rpm}$  (4.10). This concept is known as the minimum speed bit, or least significant bit, and can cause some issues since the floating-point speed is usually not exactly on one of these setpoints. This problem is handled quite simply by rounding the desired speed to the nearest setpoint. The result is quite simple and effective with respect to motor control. However, with regards to spacecraft control, this solution can result in some undesirable effects.

$$\frac{1024 \text{ rpm}}{1024 \text{ possible setpoints}} = 1 \frac{\text{rpm}}{\text{bit}} \quad (4.10)$$

Quantization, the rounding of the speed command to the nearest bit, can cause large issues in stability if the command bit size is too large. For example, when the flight computer commands the motor to stop changing speed at the end of a maneuver, if the motor controller integrates the previous torque requests to an *(integer + 0.6) rpm* speed and the speed bit size is *1 rpm*, the system will produce a *1 rpm* wheel speed change. This *0.6 rpm* static, wheel-speed error will cause the spacecraft to have a non-zero rotational speed. Its attitude will drift until the error in the pointing causes the flight computer to update the torque setpoint to correct. Regardless of how small the torque request is, the smallest change that the motor controller can make is *1 rpm*. This quantization results in a *0.4 rpm*, static, wheel speed error causing the spacecraft to drift again in the opposite direction. The result on the spacecraft is an oscillation between the nearest speed bits and may cause faulty sensor readings if this oscillation is too large or too fast.

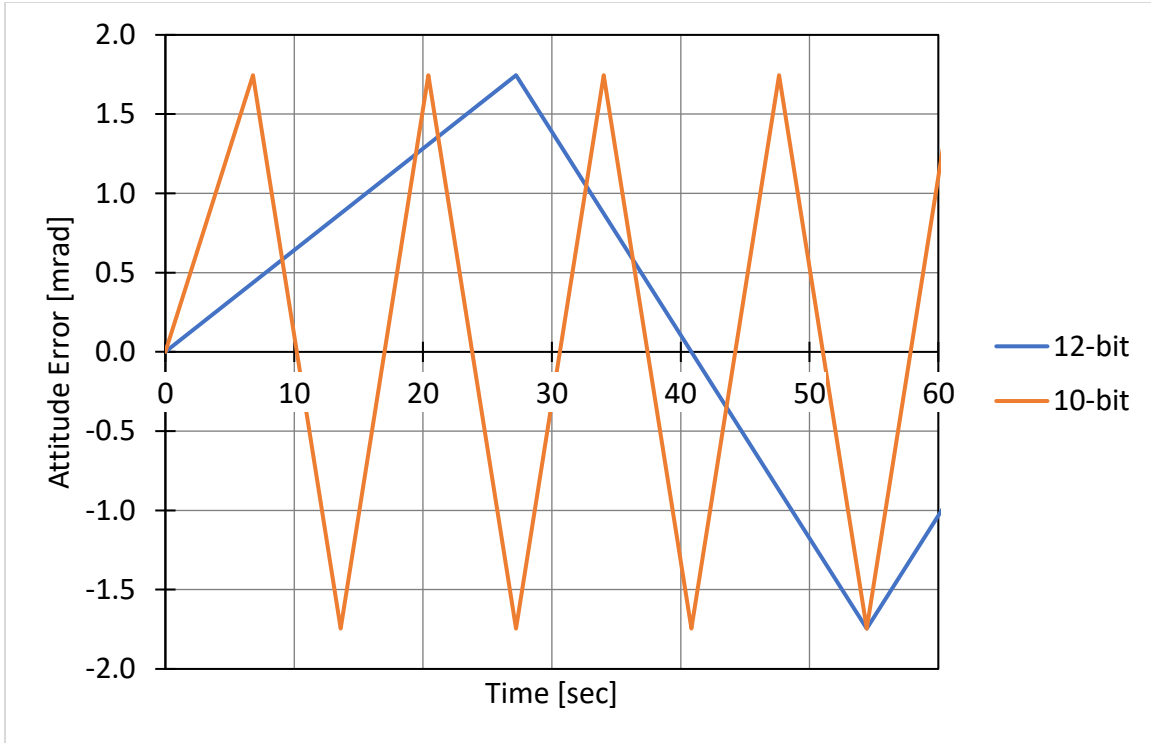


Figure 4-1. Spacecraft Attitude Instability with 10-bit and 12-bit Speed Controllers

Although it is generally not possible to achieve perfectly static pointing due to quantization of speed setpoints, it is important to determine the bounds on the minimum drift of the spacecraft. Since it has been determined that this system should induce less than 0.1 *deg* of inaccuracy and that the torque command update rate from the flight computer is 1 *Hz*, it can be concluded that, under the worst condition, the spacecraft should drift less than 0.1 *deg/s*. As shown in equation 4.9, the change in rotational speed of the spacecraft is directly related to both the change in speed of the reaction wheel and the ratio of their respective rotational inertias. Given that the approximate rotational inertia of a 3U about its long axis is  $100 \text{ kg cm}^2$ , it is shown that the reaction wheel system is required to have momentum bit of less than  $17.5 \mu\text{N m s}$  (4.15), where the momentum bit is rotational inertia times the speed bit (4.11). This metric is most relevant to the

design of the speed controller but is dependent on both the rotational inertia of the wheel and the saturation speed of the motor.

$$dL = I_w \Delta \omega_w \quad (4.11)$$

$$dL = |-I_v \Delta \omega_v| \quad (4.12)$$

$$dL = (100 \text{ kg cm}^2) \left( 0.1 \frac{\text{deg}}{\text{s}} \right) \quad (4.13)$$

$$dL = (10) \left( \frac{\text{kg cm}^2 \text{ deg}}{\text{s}} \right) \left( \frac{\text{m}}{100 \text{ cm}} \right)^2 \left( \frac{\pi \text{ rad}}{180 \text{ deg}} \right) \quad (4.14)$$

$$dL = (10)(10^{-4}) \left( \frac{\pi}{180} \right) \left( \frac{\text{kg m}^2}{\text{s}} \right) \left( \frac{N}{\left( \frac{\text{kg m}}{\text{s}^2} \right)} \right) \quad (4.15)$$

$$dL = 17.5 \mu\text{N m s} \quad (4.16)$$

where  $dL$  is the minimum change in momentum,  $I_w$  is the wheel inertia, and  $\Delta \omega_w$  is the minimum change in motor speed.

## 4.2 Torque

Maximum torque is important to the design because it sets a limit on how much angular acceleration the ADCS can request at any given time. If the torque is too low, it will take a long time for the spacecraft to begin/stop rotating during a maneuver. Conversely, if the max torque is too high, it may be difficult to control the spacecraft because the minimum applicable torque may also be too high. The minimum torque issue is greatly mitigated through the use of speed control, as discussed above. Additionally, due to the characteristics of electric motor torque

curves, the maximum torque issue only becomes a problem at the extremes of the speed range. There will always be plenty of torque available for the attitude controller, so long as the wheel is not saturated.

According to the PolySat mission leads, the attitude controller is tuned to request approximately  $0.1 \text{ mN m}$  of peak torque during a typical maneuver. In order to maintain a safety factor of 10 to account for performance degradation over the life of the mission, the motor must be able to output approximately  $1.0 \text{ mN m}$  of torque at the maximum speed prior to saturation. Given that the rotational inertia of a 3U CubeSat is approximately  $400 \text{ kg cm}^2$  about one of the short axes and  $100 \text{ kg cm}^2$  about one of the long axes, the  $1.0 \text{ mN m}$  torque from the motor would allow for maximum angular accelerations of  $0.1 \frac{\text{rad}}{\text{s}^2}$  or  $0.025 \frac{\text{rad}}{\text{s}^2}$ , respectively (4.21). This metric is only relevant to the motor selection and is not dependent on any other reaction wheel design decisions.

$$T = I_v \alpha_v \quad (4.17)$$

$$\alpha_v = \frac{T}{I_v} \quad (4.18)$$

$$\alpha_{v,s} = \frac{(1.0 \text{ mN m})}{(100 \text{ kg cm}^2)} \quad (4.19)$$

$$\alpha_{v,s} = (10^{-5}) \left( \frac{N \text{ m}}{kg \text{ cm}^2} \right) \left( \frac{100 \text{ cm}}{1 \text{ m}} \right)^2 \left( \frac{\left( \frac{kg \text{ m}}{s^2} \right)}{N} \right) \quad (4.20)$$

$$\alpha_{v,s} = 0.1 \frac{\text{rad}}{\text{s}^2} \quad \text{OR} \quad \alpha_{v,l} = 0.025 \frac{\text{rad}}{\text{s}^2} \quad (4.21)$$

where  $T$  is maximum motor torque,  $I_v$  is rotational inertia of the vehicle, and  $\alpha_v$  is maximum angular acceleration of the vehicle. Subscript  $s$  and  $l$  reference the vehicles short or long axis, respectively.

### 4.3 Momentum Storage

When the motor reaches a speed where it can no longer output the required torque, it is said to be saturated. When the motor can no longer produce the required torque, the attitude of the spacecraft is not adequately control. This situation can be avoided by having the ADCS software limit the maximum slew rate in a maneuver to one that would not cause the wheels saturate. Over time, however, wheels correcting spacecraft attitude from disturbances such as air resistance and solar pressure will cause the wheel speed to drift toward saturation. This drift will eventually make the desired maneuver impossible without first desaturating the wheels. Desaturation can be done using alternate attitude control actuators, such as magnetorquers, but typically results in a period of reduced pointing accuracy. The more momentum storage available, the less frequently desaturation is required.

The maximum momentum storage of a reaction wheel is the rotational inertia times the maximum speed of the wheel (4.22). According to PolySat mission leads, based on typical disturbance torques on 3U spacecraft in low earth orbit, a total momentum storage of  $5 \text{ mN m s}$  would be adequate for maintaining spacecraft pointing accuracy for sufficient time between desaturation events. This metric affects both the rotational inertia of the wheel and the maximum

speed of the motor. However, since rotational inertia of the wheel is related to both the volume and the mass of the system as a whole, the motor will be chosen to maximize saturation speed subsequently minimizing the rotational inertia required to achieve the desired  $5 \text{ mN m s}$ .

$$L_{max} = I\omega_{max} \quad (4.22)$$

where:

$L_{max}$  is total momentum stored,  $I$  is rotational inertia of the wheel, and

$\omega_{max}$  is maximum motor speed.

#### 4.4 Mass and Volume

The budget for both mass and volume of an entire three-axis reaction wheel system is less than  $\frac{1}{2}U$ . This requirement translates to a volume of  $5 \times 10 \times 10 \text{ cm}^3$  and a mass of  $660 \text{ g}$  to be distributed across three reaction wheels, electronics, and mounts. Assuming that the mounting and electronics consist of approximately the same mass and volume as a single reaction wheel, the volume budget is  $5 \times 5 \times 5 \text{ cm}^3$  and the mass budget is  $165 \text{ g}$  per each reaction wheel. This metric is used as the justification for minimizing the size and mass of the motor and the flywheel and, in turn, maximizing the speed of the motor.

#### 4.5 Rotor Imbalance

When the center of mass of a rotating object is not perfectly on its axis of rotation, it will generate vibrations perpendicular to the axis of rotation. This eccentricity of the center of mass is called rotor imbalance and can cause many

issues with the spacecraft. Some of these issues are oscillations induced in the spacecraft, harmonic resonance with other components in the spacecraft, and unnecessary loading of motor bearings, mounts, and other portions of the spacecraft resulting in reduced performance mission longevity. The requirement for rotor balance specifications is both dependent on the rotational inertia of the wheel and the speed of the motor.

Selecting an imbalance tolerance is typically done using the process outlined by ISO 1940/1. This process involves first selecting a balance quality grade based on the application of the rotor in question. Reference tables for these calculations are included in Appendix XX. Using Table B-1 in Appendix B, the standard recommends using balance quality grade G 6.3 for flywheels and small electric armatures. This grade is then identified on Table B-2 in Appendix B and combined with the maximum speed of the rotor to determine the permissible residual unbalance. Since the motor is yet to be defined, this requirement will remain as balance quality grade G 6.3.

#### 4.6 Requirement Summary

All of the relevant requirements for a reaction wheel system can be seen in Table 4-1. These requirements are in line with the specifications from both PolySat mission leads as well as similar product available on the CubeSat components market. Summary of similar products available commercially is available in Appendix A.

Table 4-1. Summary of design requirements

|                       |  |
|-----------------------|--|
| Momentum Bit          | $17.5 \mu N m s$   |
| Torque                | $1.0 mN m$   |
| Total Momentum        | $5 mN m s$   |
| Balance Quality Grade | G 6.3  |
| Deorbit Demise        | Does not survive reentry from LEO  |
| Mass                  | $165 g$ per wheel assembly<br>$660 g$ ( $\frac{1}{2}U$ ) total             |
| Volume                | $5x5x5 cm^3$ per wheel assembly<br>$10x10x5 cm^3$ ( $\frac{1}{2}U$ ) total |
| Cost                  | Less than \$2000 per 3-axis system   |

## CHAPTER 5

### ACTUATOR DESIGN

With the base requirements determined, the next step is to design a system that fulfills these requirements. It is important to note that this project is intended to find a simple solution that meets the requirements, not necessarily the optimum solution. The design philosophy used in this project is one attempting to fall back on first principles. The motor is selected first because the torque requirement drives this selection without requiring that any prior selections be made. After the motor selection is made, knowledge of the saturation speed of the motor and of the required total momentum storage allows rough sizing of the wheel. From this rough sizing, it is possible to determine the material viability for reentry demise, allowing material selection to be finalized. With the material for the wheel selected, the wheel's geometry can be finalized, accounting for material density as well as manufacturing and balancing concerns. After the primary functional components are designed, additional supporting components are be addressed and the entire system is evaluated against the requirements. This process maximizes the simplicity of the design by allowing each requirement to be addressed individually while only requiring the designer to focus on one component at a time.

#### 5.1 Motor

The primary requirement when selecting a motor is that is has at least  $1 \text{ mN m}$  of torque at saturation. It is important that the motor be small, lightweight, and cost-

effective. However, to minimize the required mass and volume of the flywheel while maintaining the required total momentum storage, it is most important to ensure that the motor speed at saturation is high. Additionally, the motor should be DC to take advantage of the simplicity of PWM speed control (compared to variable frequency control) and brushless to minimize wear and particulate generated in the space environment. These requirements lead to a miniature brushless DC motor as the primary choice for motor type.

With the selection field narrowed, research was conducted on what motors in this field are commercially available. The result was that most miniature high-speed motors in the  $1\text{mN m}$  torque range are approximately  $8\text{ mm}$  to  $16\text{ mm}$  in diameter. Further, there are at least four major companies that offer these products: Moog, Portescap, Faulhaber, and Maxon. Since all the options evaluated have the required  $1\text{ mN m}$ , the primary design factor is the speed at which each motor saturates to the required torque output. The motor with the highest saturation speed is easily the Maxon EC10 which will not saturate until  $53,400\text{ rpm}$ . With the torque squarely in the desired torque range, this high saturation speed means that the flywheel can be significantly lighter while maintaining the required total momentum storage. Additionally, this motor boasts a small size and weight, high efficiency, long life, and reasonable price.

Table 5-1. Evaluation of Commercial Motors for Reaction Wheel Design [6,7,11,12,22]

|                          | DBH-0472 | 16BHS 2A T .01 | 1028S012B | EC10   | ECX    |
|--------------------------|----------|----------------|-----------|--------|--------|
| Manufacturer             | Moog     | Portescap      | Faulhaber | Maxon  | Maxon  |
| Max Torque [mN m]        | 3.5      | 4.0            | 9.22      | 15.6   | 5.18   |
| Max Speed [rpm]          | 11,090   | 33,770         | 33,600    | 57,100 | 35,500 |
| Saturation Torque [mN m] |          |                | 1.0       |        |        |
| Saturation Speed [rpm]   | 9,900    | 25,300         | 29,900    | 53,400 | 28,600 |
| Diameter [mm]            | 12       | 16             | 10        | 10     | 8      |
| Mass [g]                 | 11.3     | 33             | 9.4       | 13     | 6      |

## 5.2 Wheel Material

With the motor selected, design can now proceed with the flywheel. The basic shape of the wheel is a simple ring and disk design to maximize simplicity for the initial iteration. Given the motor's maximum speed is  $50,900 \text{ rpm}$  and the required total momentum is  $5 \text{ mN m s}$ , it can be easily shown that the required moment of inertia of the rotating system is  $9.38 \text{ g cm}^2$  (equation 5.4). Since the rotor inertia from the motor is  $0.07 \text{ g cm}^2$ , the inertia from the flywheel is required to be  $9.31 \text{ g cm}^2$  (equation 5.5). Overall, this design process results in a flywheel with approximately diameter of  $22 \text{ mm}$  and length between  $8 \text{ mm}$  and  $15 \text{ mm}$  depending on density of the chosen material.

$$L = I\omega \quad (5.1)$$

$$I = \frac{L}{\omega} \quad (5.2)$$

$$I = \left( \frac{5 \text{ mN m s}}{50900 \frac{\text{rev}}{\text{min}}} \right) \left( \frac{\frac{\text{g m}}{\text{s}^2}}{\text{mN}} \right) \left( \frac{100 \text{ cm}}{1 \text{ m}} \right)^2 \left( \frac{1}{\frac{2\pi \text{ rad}}{1 \text{ rev}}} \right) \left( \frac{1}{\frac{1 \text{ min}}{60 \text{ s}}} \right) \quad (5.3)$$

$$I = 9.38 \text{ g cm}^2 \quad (5.4)$$

$$I_m = 0.07 \text{ g cm}^2 \text{ and } I_w = 9.31 \text{ g cm}^2 \quad (5.5)$$

where  $I$  is the total rotating inertia,  $\omega$  is the saturation speed of the motor, and  $L$  is the maximum momentum storage in the flywheel. Subscripts  $m$  and  $w$  reference the motor's rotor and the flywheel, respectively.

Several factors must be considered when choosing the material for the wheel. First, the chosen material is required to burn up on reentry. This requirement

reduces the risk of the spacecraft debris damaging anyone or anything on the ground and is required for compliance with the standards for mission disposal and debris from NASA [22]. Second, the chosen material should be dense to minimize volume occupied by a wheel of a given inertia. Density also reduces the mass of a wheel for a given inertia as more mass may be placed closer to the outside diameter of the wheel of a given diameter. Third, the chosen material should not be cost prohibitive to allow for many prototypes to be made and tested.

Materials considered were Aluminum, Stainless Steel, Brass, and Tungsten. Tungsten was very desirable for its high density but was eliminated because it would not burn up on re-entry. Aluminum, stainless steel, and brass of the required size were determined to be safe for reentry demise. Aluminum was desirable for its low-cost but was eliminated because of its low density. Brass was desirable for its high-density and reasonable cost increase over stainless, however it was eventually not chosen because its low hardness makes it more susceptible to damage during handling or launch that could cause rotor unbalance and pose risks to the mission. Ultimately, 316 Stainless Steel was chosen for its combination of density, manufacturability, hardness, cost, and low risk of deorbit safety non-compliance.

Table 5-2 Evaluation of Relevant Materials for Flywheel Design [24,25,28]

|                          | Aluminum                       | Stainless Steel | Brass     | Tungsten |
|--------------------------|--------------------------------|-----------------|-----------|----------|
| Alloy                    | 6061 Aluminum                  | 316 Stainless   | 360 Brass | Tungsten |
| Stock Size               | .875" OD x 12" Length (20 pcs) |                 |           |          |
| Material Price [USD/ea.] | 0.262                          | 1.111           | 1.528     | 15.388   |
| Density [g/cc]           | 2.7                            | 8.0             | 8.5       | 19.3     |
| Melting Point [K]        | 930                            | 1640            | 1300      | 3640     |
| Re-entry Demise          | Yes                            | Yes             | Yes       | No       |
| Hardness                 | HB 95                          | HRB 75          | HRB 25    | HRC 25   |
| McMaster P/N             | 8974K12                        | 89325K19        | 8953K97   | 8279K36  |

### 5.3 Wheel Geometry

Once the wheel material is selected, geometry can be designed to match the desired wheel inertia. Additional factors, such as manufacturability and mass distribution, should also be considered when designing the wheel geometry. In this design, the wheel is designed to be as simple as possible to reduce the probability of manufacturing errors and minimize the cost of prototype iterations. The flywheel is a simple ring with a solid disk spanning the inner diameter to mount the ring to the motor output shaft. Further optimization for either volume or mass efficiency would be possible through minor adjustments to ring inner and outer diameters as well as lightening of the mounting disk.

When designing the flywheel, several factors must be considered. First and foremost, the inertia of the flywheel should closely match the desired inertia. Too much inertia would be unnecessary, a waste of mass, and the increased momentum bit would result in worse pointing accuracy. However, too little inertia in the flywheel would not be able to absorb enough total momentum for the system to function long enough for the spacecraft to complete its mission objectives. Secondly, the wheel should have two balancing planes, one on either end of the ring. The two balancing allows the wheel to be balanced easily and effectively, reducing loading on the motor bearings, increasing system life, and reducing vibration transmitted to the spacecraft during operation. Third, the CG of the wheel should be located as close to the motor bearings as possible. This requirement poses a slight challenge as the actual bearing positions in the motor is not shown on the specifications sheet. As an educated guess, based on the available external CAD of the motor from the supplier, the motor bearings are assumed to be  $3\text{ mm}$  to  $5\text{ mm}$  from the front of motor housing. The CG of the flywheel is therefore positioned in this region as much as possible while still accomplishing the goals above.

The resulting design was a ring with  $21\text{ mm}$  outer diameter,  $17\text{ mm}$  inner diameter, and  $10\text{ mm}$  length and a  $1\text{ mm}$  mounting disk located  $1\text{ mm}$  from one end face of the ring. A thickened section was added to the middle of the mounting disk to allow greater engagement with the motor output shaft. As discussed previously, the flywheel will be made of 316 series stainless steel.

Reference images of the design can be seen in Figure 5-1. Drawings can be found in Appendix G.

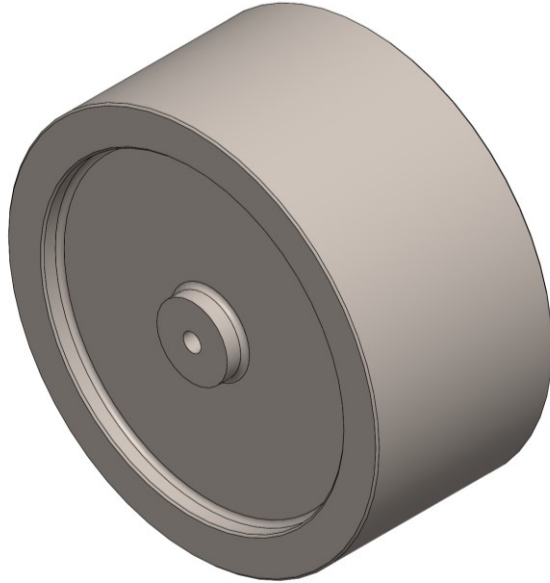


Figure 5-1. Flywheel Design

The final inertia of the flywheel is  $9.35 \text{ g cm}^2$ . Combining this inertia with the rotor inertia of the motor results in a total inertia of  $9.42 \text{ g cm}^2$ , which satisfies the goal of  $9.38 \text{ g cm}^2$  without too much excess. Final mass of the flywheel is  $11.5 \text{ g}$ .

Geometry shows that 18-20 pieces could be cut from  $7/8"$  diameter round stock 12" long. This design results in a material price of \$1.23 per wheel [20]. Additional costs would be incurred during tooling, machining, and balancing. Due to the simple design and intended fabrication by students, tooling and machining costs are assumed to be negligible.

## 5.4 Wheel Balancing

During manufacturing of the wheel and installation onto the motor, the compounding of tolerances will result in the CG of the flywheel not residing directly on the rotational axis of the motor. Rotor unbalance will cause undue loading of the bearings, vibrations transmitted to the spacecraft, and ultimately reduced life of the system. To compensate for this unbalance, the wheel must undergo balancing. Material is carefully removed either end of the ring to move the CG of the wheel to the desired location.

Because the design is an electrical armature/flywheel system, the recommended balance quality grade is G 6.3 (Table B-1). Using the grade G 6.3 line on Figure B-1, along with the saturation speed of the motor at 53,400 *rpm*, it is determined that the residual unbalance for this system must be less than  $1.4 \text{ g mm/kg}$ . Further, knowing that the flywheel design has a mass of  $11.5 \text{ g}$ , it can be concluded that the maximum residual unbalance for the system must be no more than  $16.1 \text{ g } \mu\text{m}$  [4,16].

This process is easily completed for a low fee by many commercial shops as this process must be done for many other applications. Some of these applications include rebuilding industrial and consumer turbine products. These turbines, particularly in automotive engines, have mass and speed similar to this application and many shops that do this kind of work would be willing to follow similar procedures to balance these devices.

## 5.5 Hole Fit

The mounting hole for the motor output shaft must be sized properly for a press fit. The recommended fit for this application is a *medium drive fit* H7/s6. This denotation assumes a hole basis. Since the shaft for the motor cannot be easily changed, the tolerance must be changed to S7/h6. This change results in the same interference fit while using the shaft diameter as the basis.

Breaking down the fit denotation S7/h6, the tolerance grades on the hole and shaft are IT 7 and IT 6, respectively. Since the basic size is approximately 1 *mm*, the final tolerances are 0.010 *mm* and 0.006 *mm* for the hole and shaft, respectively. Looking at the fundamental deviations, the shaft has deviation “h”, indicating no deviation, and the hole has deviation “S”. Using the basic size of 1 *mm* once again, the hole deviation is found to be 0.014 *mm* [7].

Referring to the motor specification, the shaft has size limits of 0.991 *mm* minimum and 0.997 *mm* maximum. Substituting into equation 5.7 shows that the shaft has tolerance is 0.006 *mm* (IT6), which is the same tolerance grade recommended for this fit. This matching result is further confirmation that the selected tolerance grade is appropriate for this application. Since shaft basis is being used, fundamental shaft deviation is zero and the basis size will be the same as the maximum shaft size of 0.997 *mm* (5.9).

$$d_{max} = D - \delta_d \quad (5.6)$$

$$d_{min} = d_{max} - \Delta d \quad (5.7)$$

$$\Delta d = 0.997 - 0.991 = 0.006 \text{ (IT6)} \quad (5.8)$$

$$D = 0.997 + 0 = 0.997 \quad (5.9)$$

where  $d_{max}$  is the maximum allowable shaft diameter,  $d_{min}$  is the minimum allowable shaft diameter,  $D$  is the basic fit size,  $\delta_d$  is the fundamental deviation for the shaft, and  $\Delta d$  is the tolerance grade for the shaft.

To find the size limits for the hole, similar equations are used by substituting shaft values for hole values (5.10, 5.13). Using the basic size and fundamental hole deviation with equation 5.10, the maximum diameter of the hole is shown to be 0.983 mm (5.12). Substituting this maximum diameter and the hole tolerance into equation 5.13, the minimum diameter of the hole is shown to be 0.973 mm (5.15).

$$D_{max} = D - \delta_D \quad (5.10)$$

$$D_{max} = 0.997 \text{ mm} - 0.014 \text{ mm} \quad (5.11)$$

$$D_{max} = 0.983 \text{ mm} \quad (5.12)$$

$$D_{min} = D_{max} - \Delta D \quad (5.13)$$

$$D_{min} = 0.983 \text{ mm} - 0.010 \text{ mm} \quad (5.14)$$

$$D_{min} = 0.973 \text{ mm} \quad (5.15)$$

where  $D_{max}$  is the maximum allowable size for the hole,  $D_{min}$  is the minimum allowable size for the hole,  $\delta_D$  is the fundamental deviation for the hole, and  $\Delta D$  is the tolerance grade for the hole.

Similarly, maximum and minimum interferences are determined using equations 5.14 and 5.17 and are found to be 24  $\mu\text{m}$  and 8  $\mu\text{m}$ , respectively. Summary of the

hole and shaft values are available in Table 5-3 and dimensions are included in the component drawings in Appendix G.

$$I_{max} = d_{max} - D_{min} \quad (5.14)$$

$$I_{max} = 0.973 \text{ mm} - 0.997 \text{ mm} \quad (5.15)$$

$$I_{max} = 24 \mu\text{m} \quad (5.16)$$

$$I_{min} = d_{min} - D_{max} \quad (5.17)$$

$$I_{max} = 0.983 \text{ mm} - 0.991 \text{ mm} \quad (5.18)$$

$$I_{max} = 8 \mu\text{m} \quad (5.19)$$

where  $I_{max}$  and  $I_{min}$  are the maximum and minimum interference, respectively.

Table 5-3. Summary of Hole and Shaft Fit Sizes

|         | Hole     | Shaft    | Interference     |
|---------|----------|----------|------------------|
| Maximum | 0.983 mm | 0.997 mm | 24 $\mu\text{m}$ |
| Minimum | 0.973 mm | 0.991 mm | 8 $\mu\text{m}$  |

## 5.6 Motor Housing

With the design of the rotating assembly complete, a housing was added around the motor to protect it during assembly, facilitate installation into a larger, multi-axis actuator assembly, and ease integration of EMI shielding. The bore of the housing is sized for a clearance fit with extra room for EMI shielding and

adhesive between the motor and the housing. The outer diameter is sized to allow the entire assembly to be installed into a larger 3-axis reaction wheel assembly. A flange is left near the middle of the housing to create a positive stop for locating the motor depth when installing into the 3-axis assembly. Reference images are available in Figures 5-2 and 5-3. Drawings are available in Appendix G.

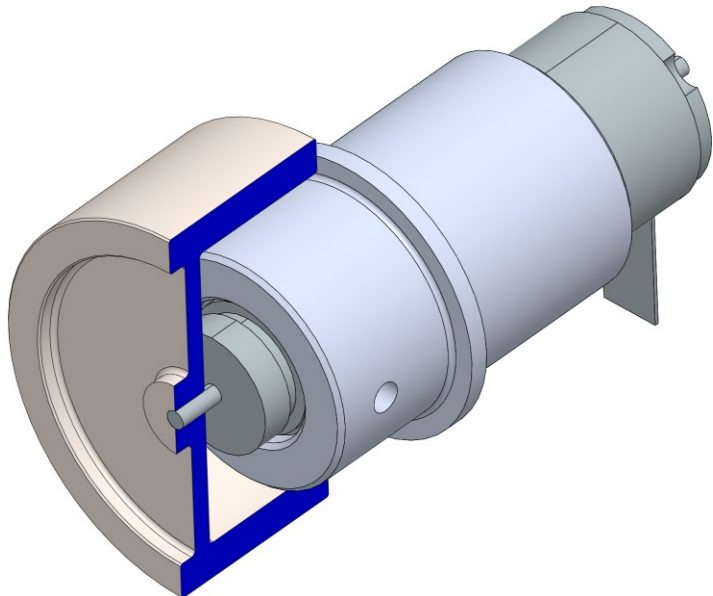


Figure 5-2. Motor, Housing, and Flywheel Assembly Design

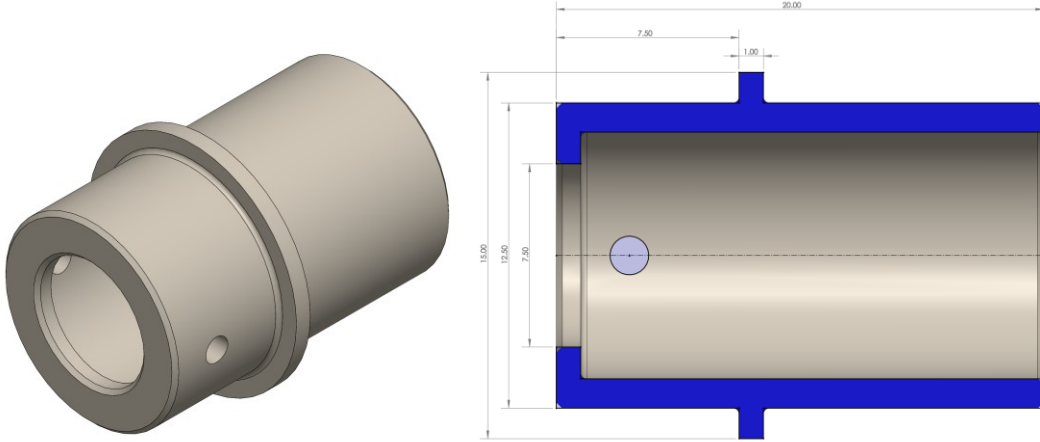


Figure 5-3. Motor Housing Design

## 5.7 Three-Axis Assembly

Each of these motor assemblies will be able to control one axis of the attitude of the spacecraft. For the spacecraft to properly control its attitude in three dimensions, at least three reaction wheel assemblies must be affixed to the spacecraft in linearly independent orientations. A simple mounting block was designed to accept these reaction wheel assemblies in a 3-axis configuration with adequate room for cabling and clearance between the rotating assemblies. Graphic representation of the assembly can be seen in Figure 5-4 and the drawing for the assembly housing can be found in Appendix G. Additionally, the system was modelled in context of a basic 1U CubeSat structure for scale (Figure 5-5). Detailed images of the assembly in this context can be seen in Appendix G. This initial design was intended to maximize simplicity while allowing for complete EMI shield testing during the prototyping stage. If the amount of material used in this design is determined to have little effect on the

shielding performance, there is much room for lightening of the structure in future iterations.

In missions where high reliability is required, a fourth reaction wheel is often used to increase redundancy and allow the spacecraft to continue operating if one of the wheels were to fail. The redundant reaction wheel is installed at an oblique angle to each of the other reaction wheels. In the event that any of the other three reaction wheels were to fail, the system still retains three functional reaction wheels on linearly independent axes. This level of reliability is not required for this design; however, this design also does not preclude the adaptation of this concept at a later date.

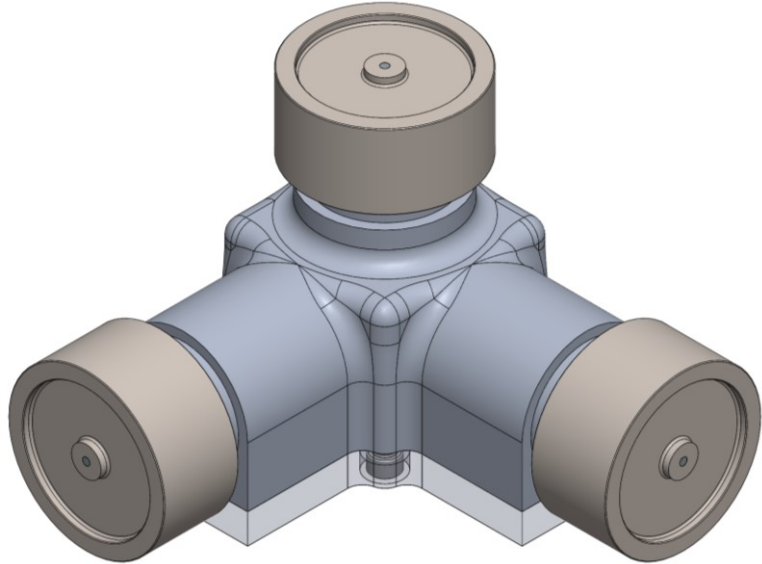


Figure 5-4. Reaction Wheel Three-Axis Assembly

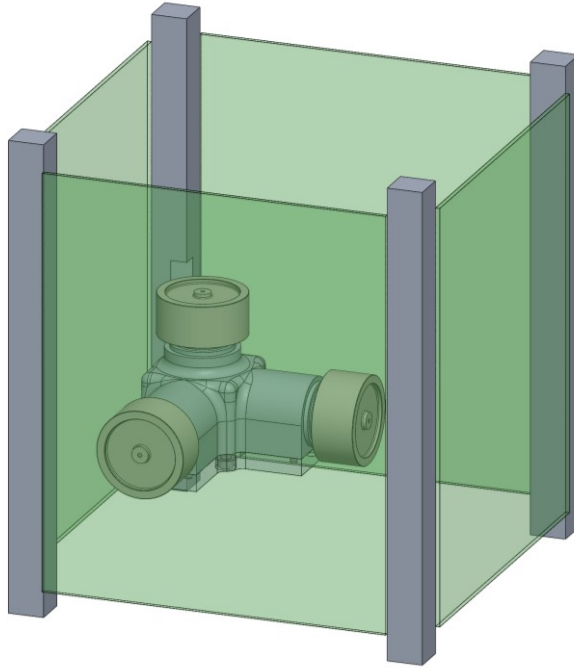


Figure 5-5. Three-Axis Assembly in Context of 1U CubeSat

## 5.8 Fabrication

[This section has been removed in compliance with the United States International Traffic in Arms Regulations]

[This section has been removed in compliance with the United States  
International Traffic in Arms Regulations]

[This section has been removed in compliance with the United States  
International Traffic in Arms Regulations]

[This section has been removed in compliance with the United States International Traffic in Arms Regulations]

## 5.9 Motor Controller

The final major component in this design is the motor controller. The ideal solution for controlling this motor would be small, lightweight, and integrated directly to the rest of the flight control electronics. However, redesigning the entire flight control board is well beyond the scope of this project. Therefore, to allow the motor and wheel to be used for benchtop and prototype testing a separate wheel speed controller is required. In the interest of simplicity and since this controller is not intended to be used as the final solution for the spacecraft integration, the motor control units recommended by Maxon, the manufacturer of the selected motor, will be evaluated for use in benchtop and prototype testing with the assumption that a future team would integrate electronics with similar (or better) specifications into the flight control board in a future project.

Several motor control units are recommended by the manufacturer and are compared in Table 5-4. All the recommended units meet the requirements for brushless DC motor control, max power, max speed, closed-loop control, and configurable speed range. The most important requirement remaining is that the momentum bit of the system be less than  $17.5 \mu N \cdot m \cdot s$ . Knowing that the inertia of the rotating assembly will be approximately  $9.42 \text{ g cm}^2$ , the saturation speed of the motor is approximately  $53,400 \text{ rpm}$ , and that the speed range of the controller is adjustable, it is simple to calculate the momentum bit of the system. Using

55,000 *rpm* as the maximum speed for the controller and assuming that the controllers use a separate command line for controlling the direction of the motor, the resulting momentum of a 10-bit or 12-bit speed controller on this system would produce momentum bits of 5.30  $\mu N \text{ m s}$  and 1.33  $\mu N \text{ m s}$ , respectively (5.25).

These are both well within the 17.5  $\mu N \text{ m s}$  requirement, and thus either a 10-bit or 12-bit controller would be satisfactory for this application. However, as the cost difference between the two is minimal and since this selection will be primarily a benchtop unit, there is little incentive to choose the less capable DEC Module 24/2. The ESCON Module 24/2 controller is selected because it is the both the least expensive option that offers 12-bit speed resolution.

$$\Delta L_w = I_w \Delta \omega_w \quad (5.20)$$

$$\Delta L_w = I_w \left( \frac{\omega_{max}}{2^n - 1} \right) \quad (5.21)$$

$$\Delta L_w = (9.42 \text{ g cm}^2) \left( \frac{55,000 \text{ rpm}}{2^{12} - 1} \right) \quad (5.22)$$

$$\begin{aligned} \Delta L_w \\ = \frac{(9.42)(55,000)}{(2^{12} - 1)} \frac{\text{g cm}^2 \text{ rev}}{\text{min}} \left( \frac{1 \text{ kg}}{10^3 \text{ g}} \right) \left( \frac{1 \text{ m}}{10^2 \text{ cm}} \right)^2 \left( \frac{2\pi \text{ rad}}{1 \text{ rev}} \right) \left( \frac{1 \text{ min}}{60 \text{ s}} \right) \end{aligned} \quad (5.23)$$

$$\Delta L_w = \frac{(9.42)(55,000)}{(2^{12} - 1)} \left( \frac{2\pi}{60} \times 10^{-7} \right) \frac{\text{kg m}^2}{\text{s}} \left( \frac{1 \text{ N}}{\frac{1 \text{ kg m}}{\text{s}^2}} \right) \quad (5.24)$$

$$\Delta L_w = 1.33 \mu N \text{ m s} \quad (5.25)$$

where n is the number of bits available for speed control

Table 5.4. Evaluation of Maxon BLDC Motor Controllers [13,14]

|                                |  |  |  |  |  |
|--------------------------------|---|---|--|---|---|
| Requirement                    | DEC<br>Module 24/2  | DEC<br>Module 36/3  | ESCON<br>Module 50/4   | ESCON<br>Module 50/4  | ESCON<br>Module 24/2  |
| Max Power<br>[W]               | > 8   | 48  | 100  | 200   | 48  |
| Max Speed<br>[rpm]             | > 53,400  | 80,000  |  | 150,000   |   |
| Configured Speed<br>[rpm]      | -   |   |  | 55,000  |   |
| Resolution                     | -   | 10-bit  |  |   | 12-bit  |
| Momentum Bit<br>[ $\mu$ N m s] | < 17.5  | 5.33  |  |   | 1.33  |
| Weight                         | -   | 4 g   | 36 g   | 11 g  | 7 g   |

## 5.10 Performance Summary

Upon completion of this design, every major requirement has been addressed. There may still be discrepancies between the final product and the expected results. Some of these discrepancies will be tenable and others may not. These discrepancies and plans for their evaluation and potential eradication are discussed in Chapter 8. A summary of the relevant performance parameters of the system, as designed, is shown in Table 5-5.

Table 5-5. Summary of Design Performance Expectations

| <u>Motor</u>   |                          | <u>Controller</u>          |            |
|----------------|--------------------------|----------------------------|------------|
| Maxon EC10-18V |                          | ESCON Module 24/2          |            |
| Stall Torque   | 15.6 mN m                | Max Speed                  | 150k rpm   |
| No-Load Speed  | 57,100 rpm               | Configurable Speed Range   | Yes        |
| Power          | 8 W                      | Input                      | 12-bit ADC |
| Voltage        | 18 V                     | Speed Bit                  | 13 rpm     |
| Diameter       | 10 mm                    | PWM Frequency              | 53.6 kHz   |
| Length         | 34.4 mm                  | PI Current Controller Rate | 53.6 kHz   |
| Shaft Diameter | 1 mm                     | PI Speed Controller Rate   | 5.36 kHz   |
| Rotor Inertia  | 0.0691 g cm <sup>2</sup> | Mass                       | 7 g        |
| Mass           | 13 g                     |                            |            |

| <u>Flywheel</u> |                        | <u>System</u>            |                        |
|-----------------|------------------------|--------------------------|------------------------|
| Material        | Stainless 316          | Saturation Torque        | 1.61 mN m              |
| Inertia         | 9.35 g cm <sup>2</sup> | Saturation Speed         | 53,400 rpm             |
| Outer Diameter  | 21 mm                  | Rotating Inertia         | 9.42 g cm <sup>2</sup> |
| Inner Diameter  | 17 mm                  | Momentum Storage         | 5.02 mN m s            |
| Length          | 10 mm                  | Momentum Bit             | 1.29 $\mu$ N m s       |
| Hole Fit        | 0.997 H7/s6            | Mechanical Time Constant | 365 ms                 |
| Mass            | 11.45 g                | Material Cost            | 1060 USD               |

## CHAPTER 6

### SIMULATION

With the design formalized, the next step is to analyze if and to what extent it will meet mission requirements. To accomplish this evaluation, a simulation must be developed and validated. This simulation should be a simplified starting point to approximate the implementation of a control system design for this application. It should be robust to accept changes in motor, wheel, electrical, and control system parameters. Many details, such as inverter, voltage controller, pulse width modulation and commutation logic, are not necessary for this level of analysis. Additionally, these components increase the complexity of the model which can both obfuscate results and increase the time it take for the simulation to solve.

The purpose of this simulation is to show that the actuator portion of this system is sufficient for consideration in future mission designs. It will also serve as a starting point for future teams to design the electrical and software control systems to complement this actuator. As with the design, the simulation will serve to prove the existence of a valid solution, not necessarily the optimal solution.

#### 6.1 Model

The simulation is a simplified model of the motor, flywheel, voltage supply, and speed controller. The control loop is a classic closed-loop control system with rpm feedback. Additionally, the model includes autotuning logic that allows the

system to be tuned easily and accurately. The model can be broken into two main subsections: the plant and the controller. The plant is the model of the physical system and how it responds to changing inputs. The controller is the part of the model that collects feedback information from the plant and processes it to determine appropriate changes in the plant input to achieve the desired response. Additionally, rpm setpoint, response, and torque are exported to the workspace for data processing and plotting.

The plant is the physical portion of the model and is intended to be the analogue for the reaction wheel system designed in this project. It consists of three main components: voltage source, motor, and flywheel. The voltage source is modeled as ideal and simply converts voltage requests from the speed controller into voltage in the electrical domain with no losses or time delay. This simplification is done to bypass the complexities inherent in the design of the electrical subsystem used to drive the motor. Upon completion of a future project to design this electrical subsystem, components like a voltage controller, amplifier, pulse width modulator, and 3-phase power inverter along with the associated encoder logic on the motor would be added to this simulation to ensure that the system continues to operate as expected with the increased complexity of the design.

The motor is modelled as a universal motor using the appropriate motor constants from the datasheet. This simplification, from a physically simulated 3-phase BLDC to a standard brushed motor is commonly done in motor modelling both to simplify the commutation logic and the physical simulation solver. It is generally considered to be a valid assumption when modelling similar systems.

The flywheel is modelled as a simple rotational inertia that creates a grounding path for the torque generated by the motor. In addition to the main components, the plant model also includes rotational and torque sensors used for closed-loop feedback and simulation output. The plant model can be seen in Figure 6-1. Motor and wheel constants used are included in Table 6-1.

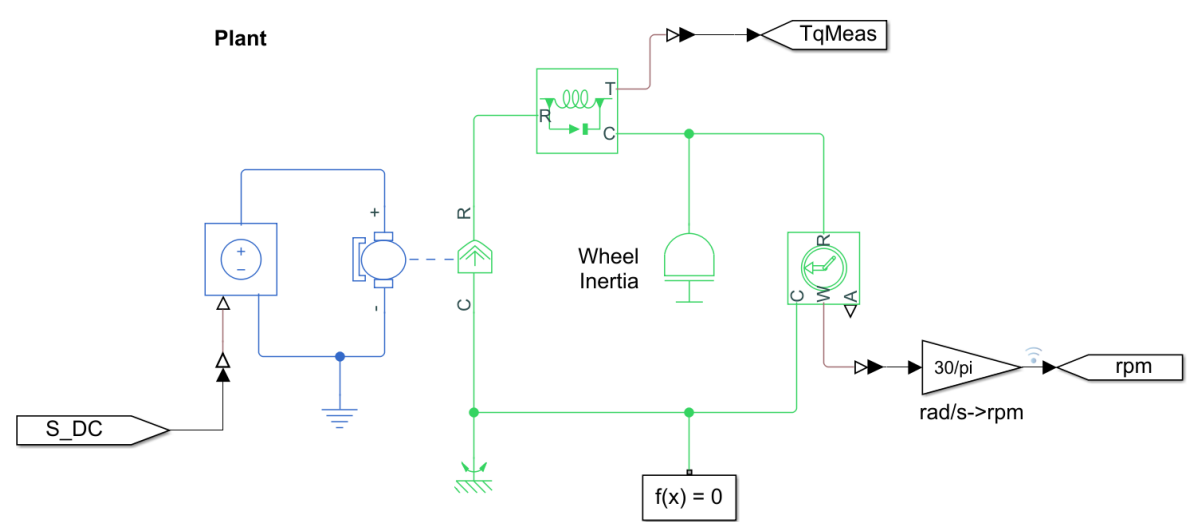


Figure 6-1 Simulink Model of Physical, Electrical, and Mechanical System

Table 6-1 Motor and Flywheel Parameters Used in Simulink Model

|                                  |                                 |
|----------------------------------|---------------------------------|
| Armature Inductance              | 0.0671 <i>mH</i>                |
| Stall torque                     | 15.6 <i>mN m</i>                |
| No-load speed                    | 57,100 <i>rpm</i>               |
| Rated DC supply voltage          | 24 <i>V</i>                     |
| No-load current                  | 67.3 <i>mA</i>                  |
| Supply voltage @ no-load current | 18 <i>V</i>                     |
| Rotor inertia                    | 0.0691 <i>g cm</i> <sup>2</sup> |
| Flywheel inertia                 | 9.35 <i>g cm</i> <sup>2</sup>   |

The control loop portion of the simulation also consists of three main sections. The left-hand portion of the simulation defines the test parameters. This portion includes flags and logic switches to control which input is applied to the system and timeseries data to define the motor controller setpoints at continuously throughout the simulation. The midsection of the controller model is the closed-loop feedback controller. Motor speed is fed back from the speed sensor on the plant and compared to the speed setpoint from the input blocks. The right-hand side of the model is an autotuning subsystem which was sourced from various Simulink control systems examples [4]. Additionally, there are two time-step conversion blocks that allow the control loop to update at a slower rate than the physical simulation and a gain block to scale the speed controller output ( $\pm 1$ ) to the voltage input range for the motor ( $\pm 18V$ ). The controller section of the model can be seen in Figure 6-2.

The input blocks contain the timeseries rpm setpoints for each of the tests that are used to validate the model and design performance. The first test is a simple step input from 0 *rpm* to 30,000 *rpm*. This test is used as the baseline for the autotuning process. The second test is a step input to max speed, followed by another step input to max reverse speed, and finally a step back to zero speed. This step allows the simulation to determine the maximum torque in either direction at every speed in the available range. This information is used to determine the saturation torque and speed of the system. The third test is ramp input at the max operational torque found from the previous test. The ramp

continues up to max speed, back down to max reverse speed, and finally ramps back to zero speed. The fourth test consists of recorded torque requests from a full PolySat ADCS simulation. The torques are integrated to get speed setpoints and the setpoints are passed forward to the simulation. The details of each of these test inputs can be found in Appendices D and E and summarized in their respective results sections.

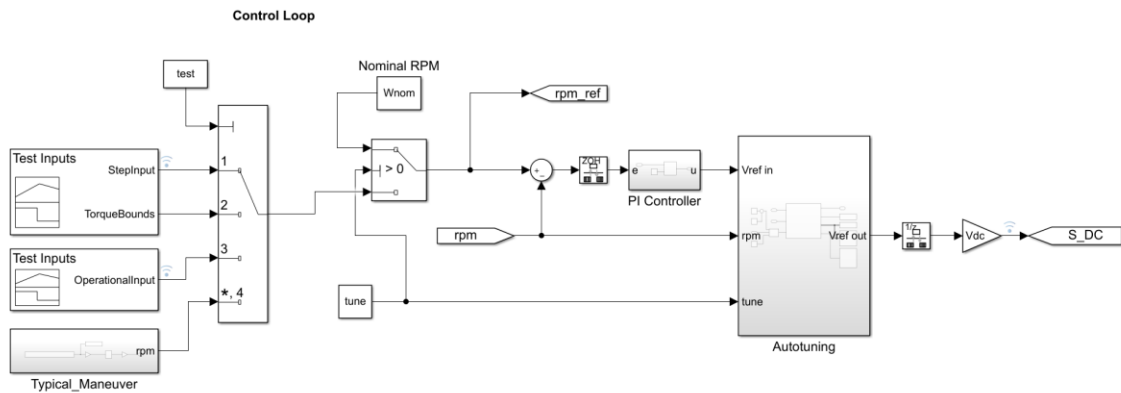


Figure 6-2 Simulink Model of Test Input, Control Loop, and Autotuning Logic

## 6.2 Tuning

Before simulations can be run to estimate the performance of the system, the controller must first be tuned. To accomplish this task, the system is fed a constant speed setpoint, allowed to normalize to this setpoint, then disturbances are injected, quantified, and control constants are generated. Most of this process is handled by the autotuning system. However, some setup is needed for the system to function properly. First, the nominal speed setpoint,  $W_{nom}$ , is set to 30,000 rpm and the *tune* parameter is set to *True*. When system is run, it applies  $W_{nom}$  as the rpm setpoint and waits one second to allow the system to

reach steady state. After the system settles, the autotuning subsystem injects disturbances into the system and measures the response to find the appropriate constants for the PI controller. These results are then used to update the constants in the speed controller for further simulations.

Figure 6-3 and Figure 6-4 show the system response before and after tuning to the step response and random disturbances, respectively. Before tuning, issues included both steady state error and an overdamped response curve. After tuning, the response is quick, has slight overshoot, and has little steady state error. While changes to the control logic and implementation of this system in a future designed product suite will require this tuning to be redone for the new system, the drastic improvement of this response indicates that this process was incredibly successful for the purpose of this project.

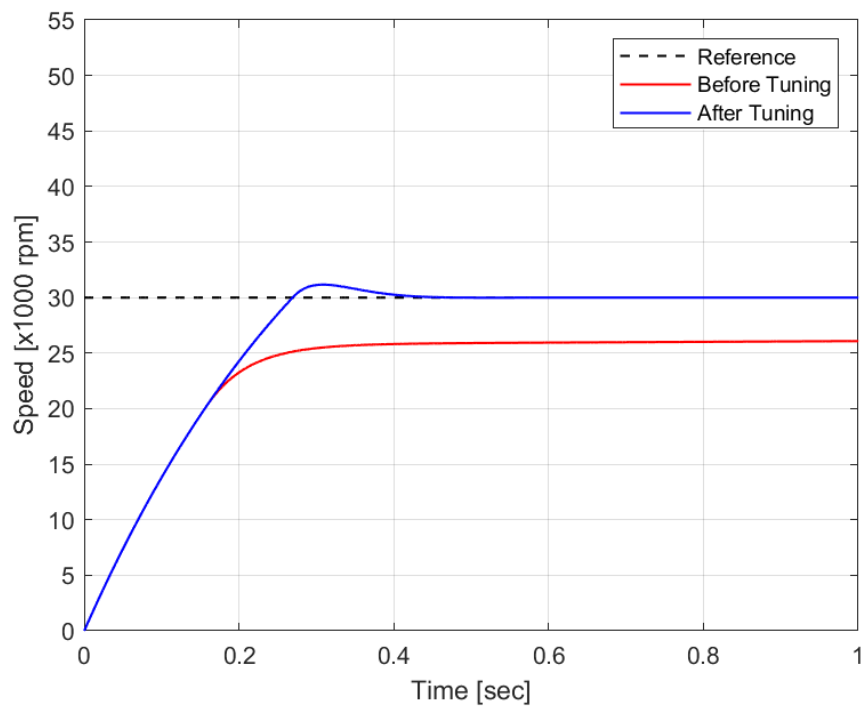


Figure 6-3 System Response Before and After Tuning, Step Input

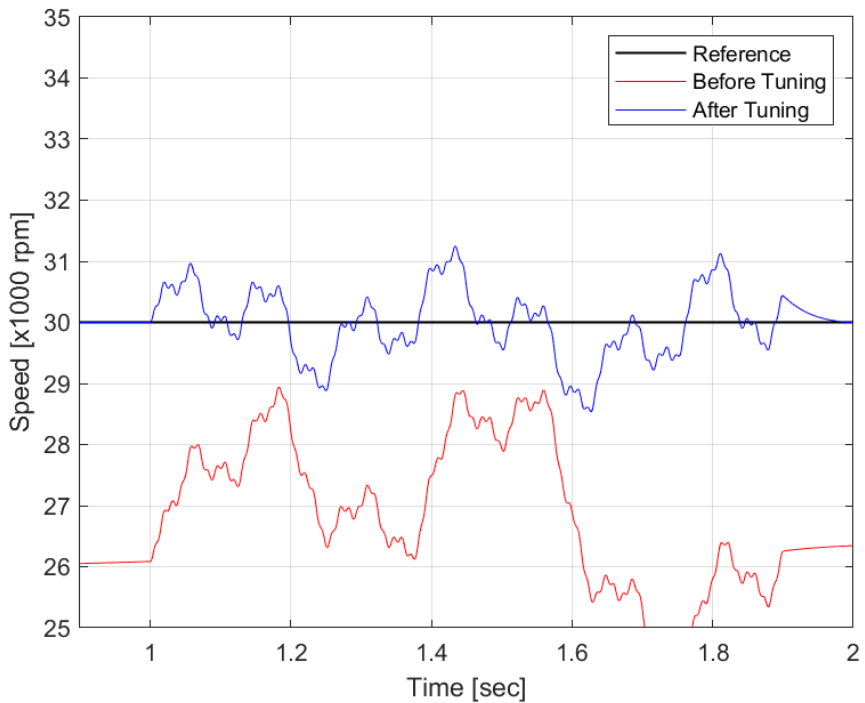


Figure 6-4 System Response Before and After Tuning, Random Noise

### 6.3 Torque Boundary

With the control loop and plant system tuned, the system can now be evaluated to show that it meets the design expectations. This second test is designed to determine the bounds on the available torque output at any speed. This test is conducted by applying the maximum voltage input to the motor and allowing it to run up to its maximum speed. The maximum voltage is generated by exposing the system to a maximum speed setpoint. Since the motor speed will always be much less than the maximum speed, the error term in the controller should always be maximized and the controller should always output the maximum voltage.

Since the motor is at maximum voltage, it is known that the torque provided will be the maximum available at any given speed. When the motor achieves the desired maximum speed, the input is then reversed to determine the torque available in the opposing direction at positive speeds. The motor is subjected to reverse voltage until it reaches its maximum reverse speed. At this point the motor is then subjected to positive voltage again to determine the positive torque available with the motor in the negative speed regime. The process is summarized in Figure 6-5.

Results from running this procedure show that the system will produce at least  $\pm 1.0 \text{ mN m}$  of torque in the range of  $\pm 53,400 \text{ rpm}$ . This result exactly matches expectations of this design and simulation, especially considering the simplified and idealized nature of this model. Work still needs to be done to confirm that the physical system matches these results. However, there is no reason to indicate

that they will not match expectations beyond typical motor manufacturing tolerances at this time. Torque values from the simulation alongside the expected bounds of torque requests during flight are shown in Figure 6-6. Timeseries results are shown in Figure 6-7. The script used to run this simulation is available in Appendix E.

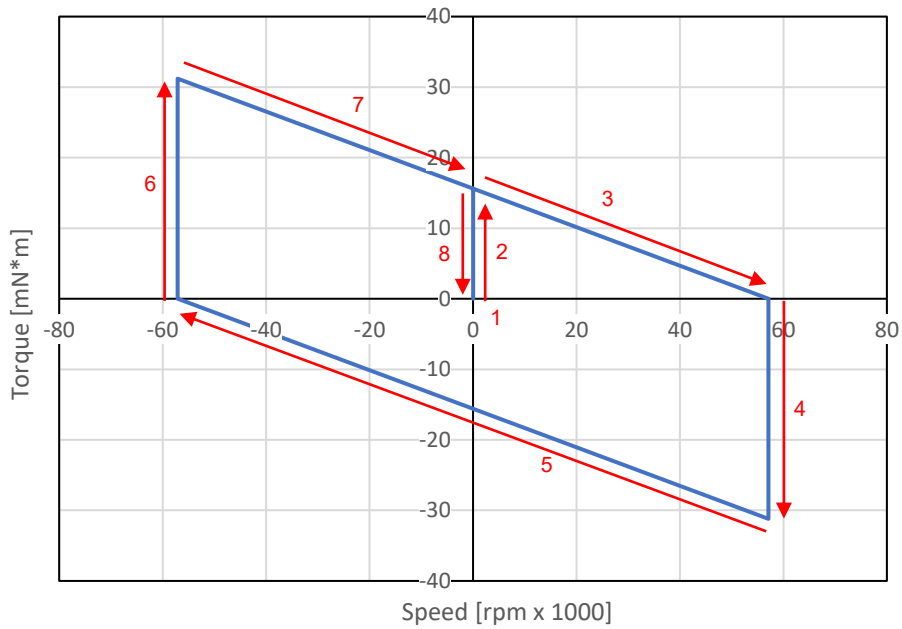


Figure 6-5 Theoretical Motor Torque Boundary Experiment

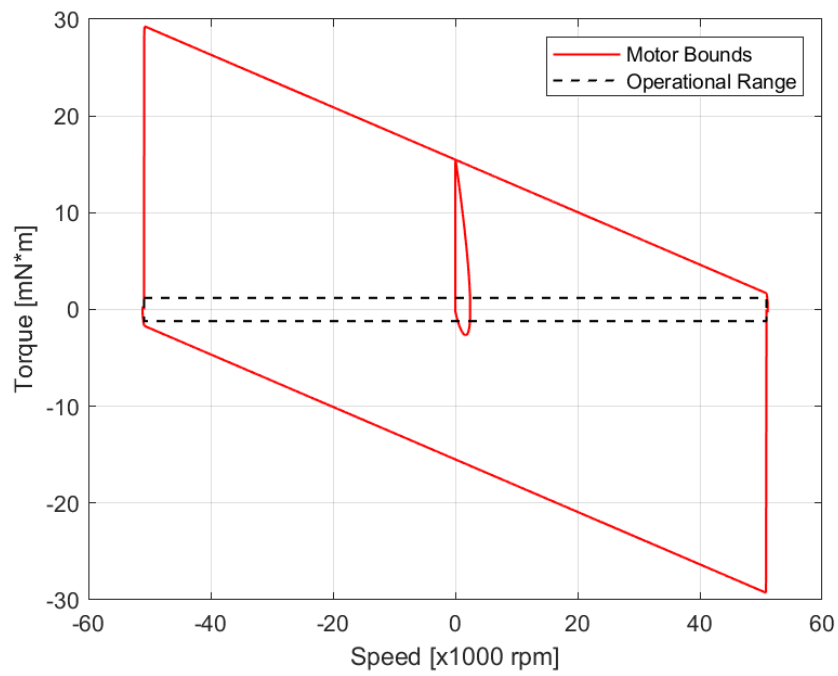


Figure 6-6 Torque Boundary Simulation Compared to Operational Limits, Torque Domain

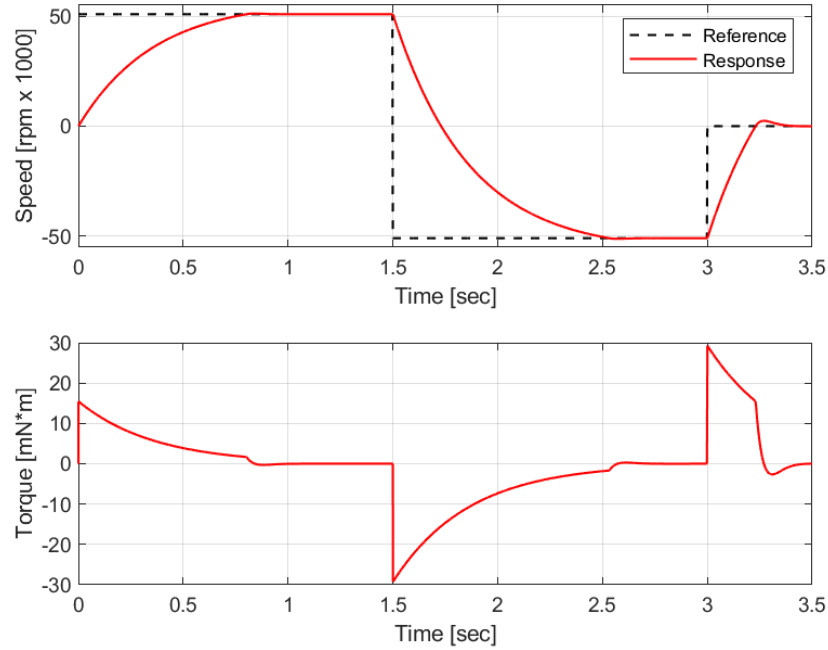


Figure 6-7 Torque Boundary Simulation, Timeseries Results

## 6.4 Operational Range

The simulation has been shown to give the expected results for maximum voltage torque bounds. The system should also be able to run a simulation showing how it would perform sweeping through its operational range. This third test scenario is similar to the previous one with the main difference being the input rpm setpoint. The setpoint for this test is designed to mimic a constant, maximum torque request from the ADCS program. As such, a speed ramp was calculated to approximate  $1.0 \text{ mN m}$  from zero to maximum speed, return to max reverse speed, then back to zero. The procedure and setpoints are summarized in Figure 6-8.

Results from running this simulation show that the modelled system closely follows the requested setpoints. Discrepancies from the setpoints are shown, by inspection, to be artifacts of control system tuning and the mechanical time response of the system. Measured torque values alongside requested torque values are shown in Figure 6-9. Time series data for measured speed, measured torque, and speed setpoints are shown in Figure 6-10. The script to run this simulation is included in Appendix E.

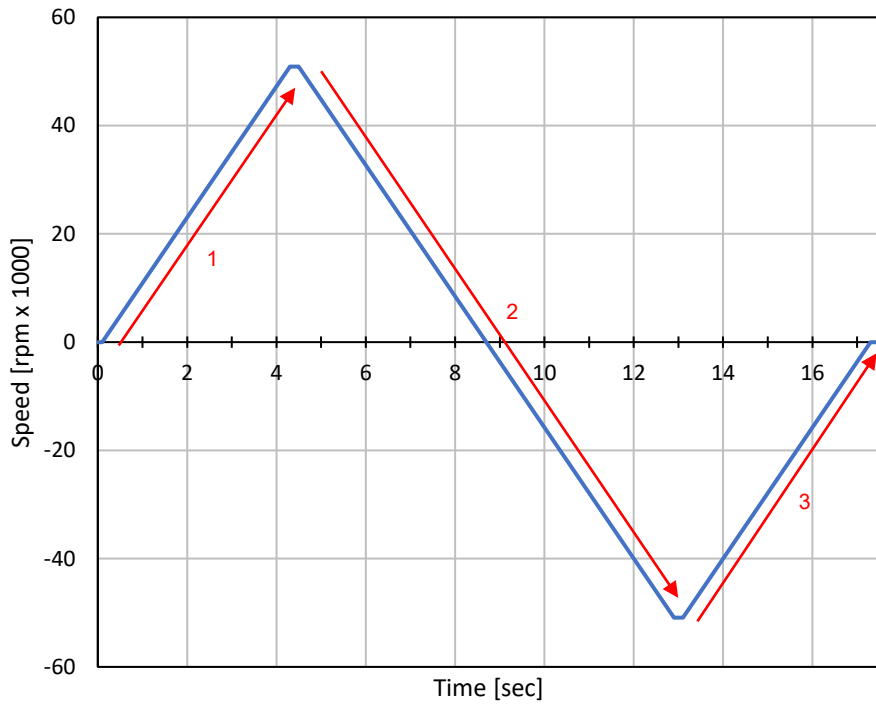


Figure 6-8 Operation Range Simulation, Speed Setpoints

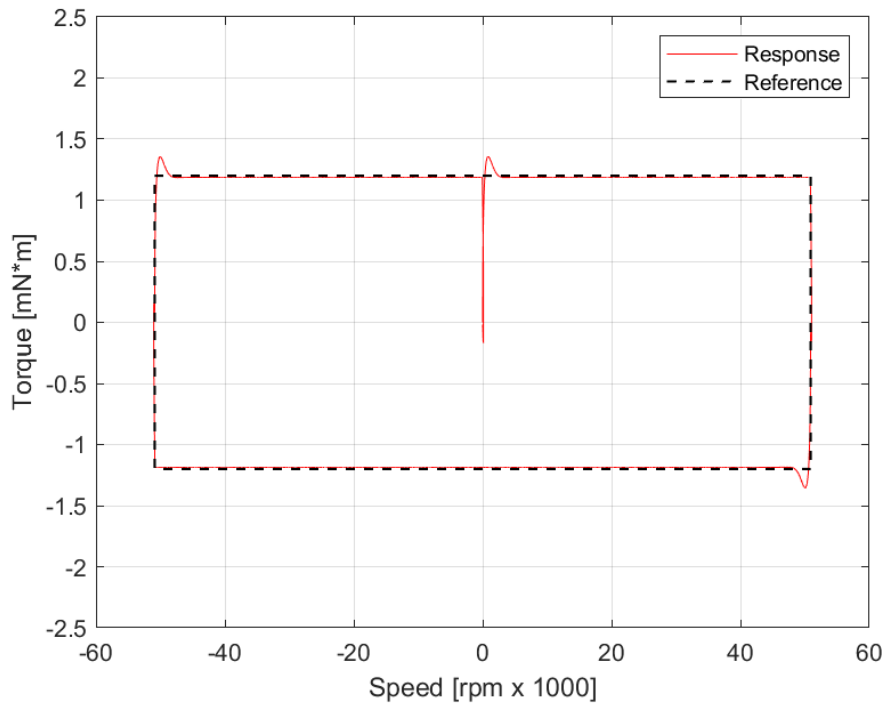


Figure 6-9 Operational Range Simulation, Torque Domain

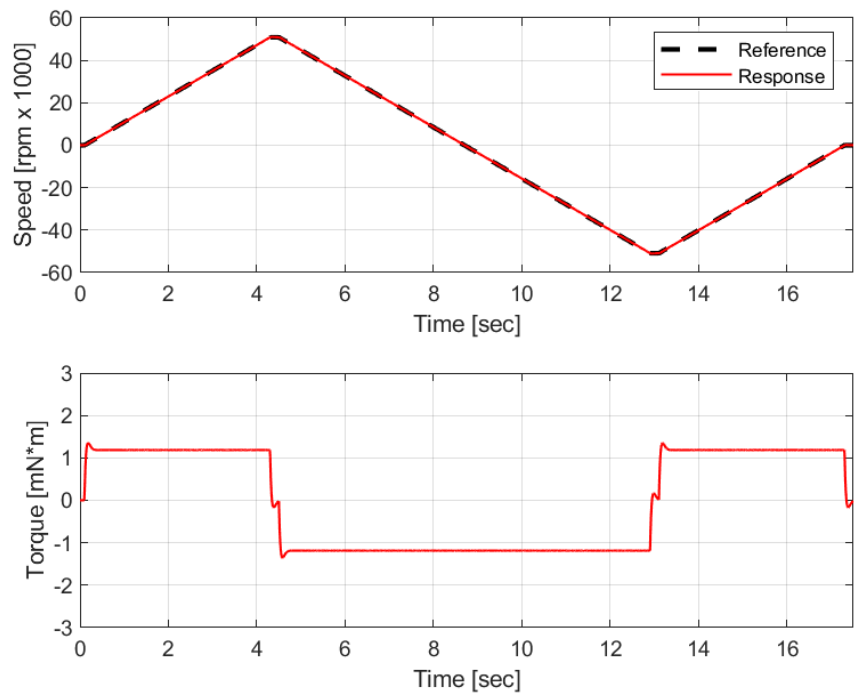


Figure 6-10 Operational Range Simulation, Timeseries Results

## 6.5 Expected Maneuver

The fourth and final test scenario is a typical torque request curve from a full ADCS simulation. The ADCS simulation is tuned to require low torques. This tuning is done to improve stability and accuracy in spacecraft attitude and allow for the control loop to be updated less frequently. Additionally, this tuning makes it easier for the ADCS software and sensors to keep track of the attitude of the spacecraft. From the perspective of the reaction wheel, this tuning means that the ADCS is requesting much less than the maximum torque of the motor. This lower torque puts the torque requests well within the operational limits set on the system allowing generous margins for the performance of the system to degrade over time or for the ADCS to be re-tuned for a more aggressive control scheme.

The main complication of this situation is that the motor controller functions on speed setpoints, not torque setpoints. To overcome this problem, the torque requests, which are imported from a CSV file, are processed into speed setpoints. This solution is accomplished through the same process that would be conducted in the flight computer of the spacecraft that will eventually use this system. The motor driver logic receives a torque request and knowing the inertia of the flywheel, integrates the speed setpoint according to this torque. This solution causes the speed setpoint to constantly track the speed that the wheel should be at if it were constantly producing the requested torque. This outcome means that, while the wheel will have a small delay in achieving this speed, it will be able to make up for the missing torque impulse because the ideally integrated speed setpoint will have already accounted for this loss. With the torque

commands converted into speed commands, the commands are inputted to the speed controller and the simulation is run as normal. Input torque commands are summarized in Figure 6-11 and detailed in Appendix F. Diagram of torque integration model is detailed in Appendix D.

The results from this simulation show that the system closely follows the requested setpoints. The speed of the motor follows the converted setpoints with minimal lag. The torque has the expected tuned second-order response with slight overshoot and no little steady state error. While the torque cannot exactly follow the requested setpoints, the conversion to idealized speed setpoints allows the controller to overshoot the step inputs from the torque commands to maintain the total angular impulse requested by the ADCS. Timeseries data for this test is summarized in Figure 6-12 with the first five seconds shown in greater detail in Figure 6-13.

Additionally, results from this simulation confirm that the torque requests are well within the operational limits of this design. This maneuver could easily be accommodated with the motor starting at any point within the operational range and remain within the operational range as long as the starting speed of the motor is at less than the saturation speed minus the max speed change during the maneuver. Further, because the requested torques are low, the motor could even provide the required torque outside the defined operational range, thereby increasing the effective operational range of the system. If all maneuvers for a spacecraft are expected to require low torques like this example, it may be prudent to increase the max operational speed of the system at the cost of

maximum torque. Torque domain results are shown in Figure 6-14 and in greater detail in Figure 6-15.

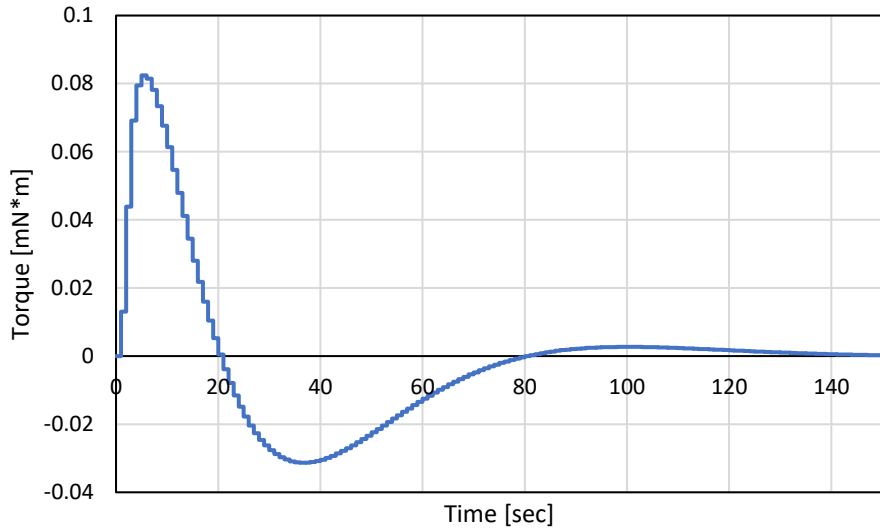


Figure 6-11 Typical CubeSat Attitude Maneuver, ADCS Torque Requests

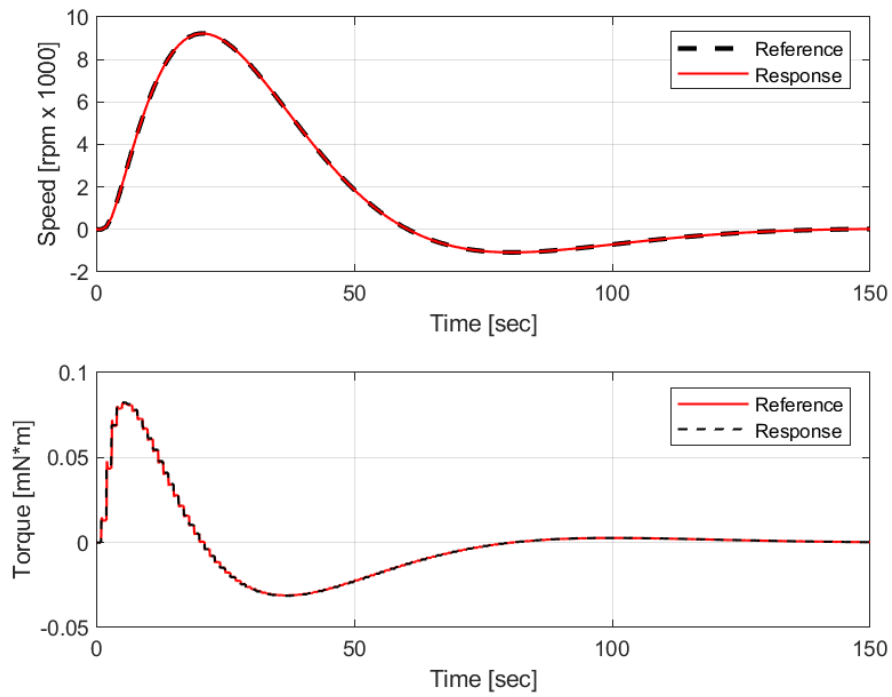


Figure 6-12 Typical CubeSat Attitude Maneuver, Timeseries Results

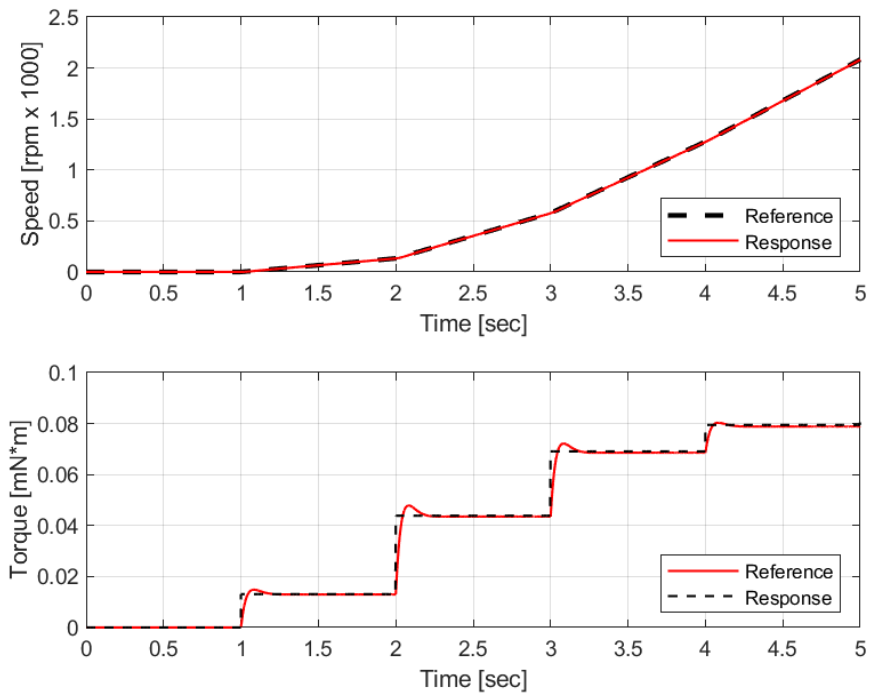


Figure 6-13 Typical CubeSat Attitude Maneuver, Timeseries Results (Detail)

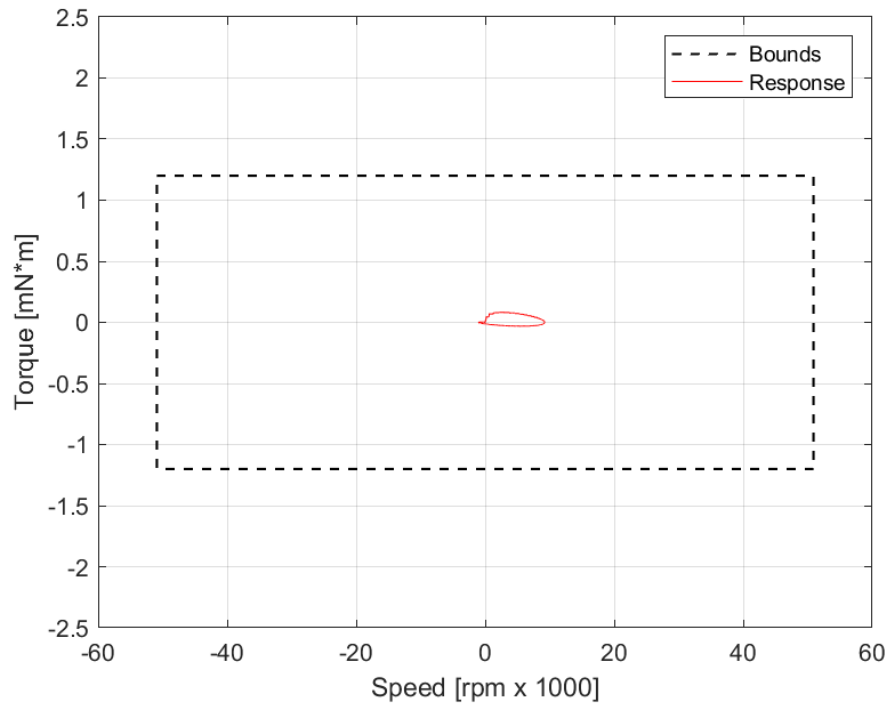


Figure 6-14 Typical CubeSat Attitude Maneuver, Torque Domain

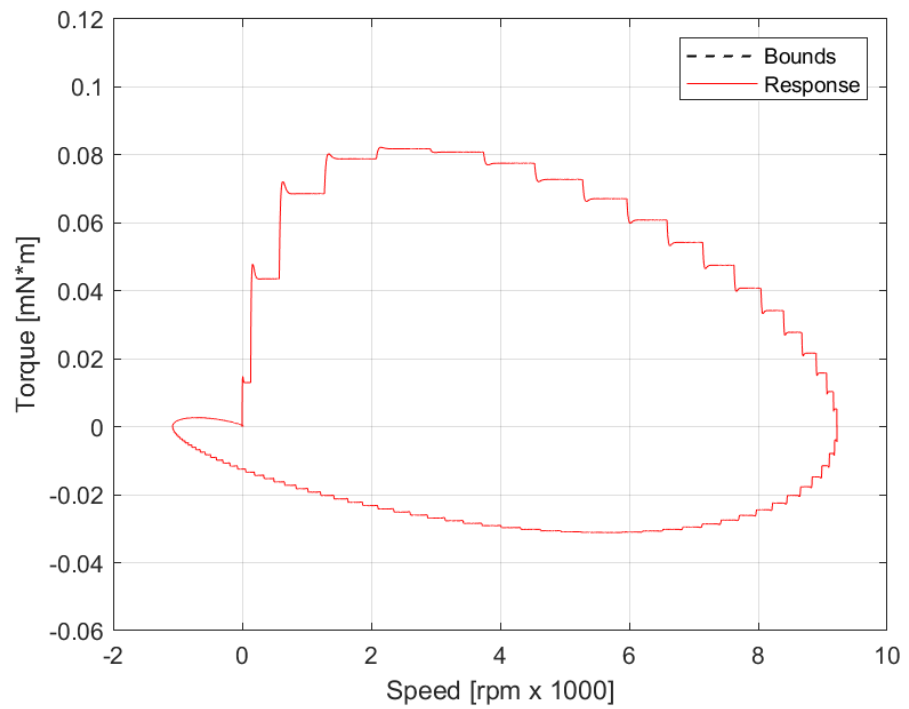


Figure 6-15 Typical CubeSat Attitude Maneuver, Torque Domain (detail)

## CHAPTER 7

### PROTOTYPING AND TESTING

Originally, the intention of this project was to complete a large portion of this prototyping, conduct initial benchtop tests, and evaluate the results against the simulation. Additionally, this would have delivered a functional prototype for testing to whomever is going to continue this work going forward. Unfortunately, this became impossible when Cal Poly campus shut down in response to the COVID-19 pandemic in Spring 2020. Considering the inability for this project to proceed tangibly at this time, this section will outline a procedure for which this work could expeditiously take place upon the re-opening of Cal Poly research facilities.

#### 7.1 Procedure Development

With the design complete and the simulation results promising, the next steps to developing a functional system are prototyping and benchtop testing. The prototyping process is one of trial and error that will inform the design stage and drive changes to dimensions and proposed procedures. With motor samples and raw materials in hand, custom components are fabricated and assembled. Not unexpectedly, some of these components will not fit as well as intended. Further, when they do fit together, they may produce a product with sub-optimal performance due to unforeseen complications in processing. These issues inform design changes, design changes are implemented in another round of

prototyping, and more imperfections are discovered in the design. This process continues until no further issues can be identified.

## 7.2 Procedure Evaluation

Once the assembly prototyping has removed any issues apparent in the assembly process, the prototypes need to be tested to confirm the accuracy of the performance model. Each of the simulations above should be run on the benchtop prototype sample. The results should be compared to the simulation results and analyzed to determine the origins of discrepancies between the simulation and the prototype. Discrepancies in test results can be caused by issues in either design, fabrication, testing, or simulation.

Errors in the initial design should be limited to either the requirements or the implementation of the features designed to satisfy the requirement. The inherent issues in each of these is discussed in detail throughout the first five chapters of this thesis. Changes to initial requirements should prompt investigation into whether to redesign the system to meet the new requirements or not. Errors in design implementation are generally manifested as discrepancies between the intended performance and tested performance that remain constant across many components and assemblies. It is very difficult to diagnose these issues until variation in fabrication and testing have been addressed.

Errors in fabrication are generally easy to diagnose. These Issues typically manifest as a mechanical defect during testing, such as parts that do not fit or assemblies with radically varying test results. Some examples of these issues

are adhesive joints not curing properly or tolerances on flywheel manufacturing not being held properly. Fabrication issues like these examples would most likely show up as components that do not fit together properly, rattle loose early during life testing, or have significantly different performance curves during benchtop testing. Often, fabrication issues can be identified by careful measurement of components and assemblies at each step of the fabrication process.

Errors caused by issues in test design are more difficult to diagnose. Testing issues will often appear as a single assembly having drastically different test results on repeated tests. However, sometimes issues in the test design can result in a bias in the results it provides. This type of error can be very difficult to distinguish from errors inherent in the design that cause overall changes in performance.

Additionally, there are many errors inherent to simulations. Simplification reduces the accuracy of a simulation. Every simplification made is an intentional departure from realism. This is necessary to reduce the computational cost of the simulation. Often, these simplifications have little effect on the quality of the simulation. However, each simplification needs to be addressed on a case-by-case basis to determine whether the effect on the result is acceptable.

Additionally, rounding errors on these simplifications can add up to cause the simulation to perform in a way that the physical system would not. Unfortunately, adding complexity intended to enhance the realism of a simulation can also create unintended consequences. These issues tend to manifest in simulation results as singularities or variation due to variables that should have little effect.

### 7.3 Vacuum Operation

There are some tests that do not make sense to conduct in simulation form. One of these is operation in a vacuum environment. These tests would identify issues that may occur in space. Vacuum testing procedures should follow standard thermal vacuum (TVAC) procedures for bake-out during fabrication of test samples. Initial tests should be exploratory to identify unknown issues related to vacuum or thermal operations. Issues concerning internal motor component compatibility, especially grease, plastic, and rubber, are expected. Solutions to these issues may require discussion with the manufacturer to replace these components with vacuum-compatible replacements. However, it is possible that the best solution may be a procedure to remove these incompatible components during the fabrication process.

For example, it is likely that the plastic cover on the rear of the selected motor will not pass outgassing regulations for vacuum operation. If this plastic cover is removed, the system may meet the requirements. However, the motor electronics may be exposed more than acceptable. In this situation, a metal cover should be added to the custom motor assembly to cover the exposed area of the motor.

### 7.4 Performance

Once all reasonable inaccuracies are identified and removed, the prototypes can be evaluated against the simulation results. Tests to be run should be identical to the tests run in the simulation. First, the system should be tuned using some form

of autotuning or tuning procedure. This procedure will likely change to reflect updates in the electrical hardware and control loop driving the system. Second, the motor should be subjected to the maximum voltage, torque bounds experiment to determine the effective torque of the system at relevant speeds speed. Third, the system should be put through the constant torque, ramp speed test to confirm that the system reacts as expected to torque requests within the operational bounds. Fourth, the system should be put through its paces with the simulated maneuver test. This test should be well within the performance bounds of the system and should instead be evaluated on how quickly the system reacts to the more gradually changing inputs. Additionally, it will be important to evaluate the entire system during a “day in the life” test with an entire spacecraft. Issues at this level could also drive minor changes to the design and require re-evaluation of the testing conducted up to that point.

From each of these tests, it will be possible to compare the prototype to the simulation result. Results are expected to be slightly worse performance than the claimed values on the datasheet due to many minor flaws in the motor, manufacturing, and testing setups. Variations from 5% to 10% below stated performance are expected. These variations should be compared across several units from differing motor production batches and several in-house fabricators. Since the system design, even with 10% reduced performance, is still within acceptable parameters for use in 3U CubeSat missions, such a result will not be an issue. However, it is still important to understand how well the system functions before relying on it for mission critical operations.

Benchtop performance analysis is great for comparing the designed system to datasheet results. However, performance studies should also be run in a TVAC environment to ensure that the assembly will perform adequately in-flight. The results of this testing are expected to be within nominal performance metrics. However, it is expected that the lack of atmosphere will cause the system to run much hotter than normal. This problem should be counteracted by reducing the allowable duty cycle until temperatures remain within the allowable ranges on the motor datasheet.

## 7.5 Longevity

There are several additional system parameters that need to be tested physically because they do not allow for easy simulation. One of these parameters is longevity, or system life. It is important to know how long the system is expected to last to confirm whether it will survive the duration of a mission of the spacecraft. Fortunately, this test is quite simple. Unfortunately, it takes a long time to conduct and requires that several assemblies be tested destructively. Longevity tests consist of running the system until it fails and measuring the point at which it fails. This test should be conducted for many assemblies to get a statistical model for the expected life of any assembly given the same manufacturing process.

For example, if 50% of assemblies last for 100-200 hours and the other 50% last for more than 200 hours, it is quite easy to justify a 100-hour mission lifetime for these assemblies. However, if the mission requires a 200-hour lifetime for the

same assembly, the design only has a 50% chance of completing the mission.

This level of confidence is generally not acceptable for spacecraft design.

Ideally, this test would be run on at least 10 units and all assemblies would be run until failure. Any assemblies that failed significantly sooner than the others should be investigated for manufacturing errors. After errors are corrected, the lowest measured longevity can be used as a conservative value for the minimum expected life of a flight unit. If infant mortality, longevity of some units outside of the statistical norm, persists, burn-in procedures can be developed to catch these early failures before the assemblies are selected as flight units. However, it is worth noting that while burn-in procedures can help identify infant mortality failures, they can also put unnecessary load on the unit prior to use in a mission environment and can reduce the effective life of the rest of these nominal units.

## 7.6 Quality Assurance

The testing described above is to verify that the design is sound. Additional testing is required to prove that each assembly is manufactured to the required specifications. This testing should be simple and streamlined to avoid unnecessary wear on the unit prior to flight while remaining robust enough to identify assemblies that would be likely to fail during the mission. Recommended quality testing is as follows:

1. Controller tuning and basic performance check on benchtop (each unit)
2. TVAC bake-out, burn-in\*, and performance check in vacuum chamber (each unit)

3. Longevity test in vacuum chamber (one unit per batch)
4. “Day in the Life” test with entire vehicle prior to mission

\*burn-in only required if intermittent early-life failures are undetectable during basic performance checks.

## CHAPTER 8

### DISCUSSION

#### 8.1 Design

The design presented here consists of a low-cost, commercially available motor, magnetic shielding tape, an easily manufactured flywheel, and housing components to hold the motor in place. The motor is selected to provide enough torque up to a high speed to maximize the useful life of the system without requiring desaturation. The wheel is sized to provide the inertia necessary for the system to be able to take advantage of the high speed of the motor. The motor housing is designed to allow for magnetic shielding to be placed around the motor while holding the motor securely to the three-axis housing. The three-axis housing is designed to hold three motor assemblies at three independent axes, allowing the spacecraft to control its attitude precisely in any orientation.

This design is intended to be as simple as possible while achieving the goal of providing three-axis control to the spacecraft. By designing for simplicity, the design reduces the risk for errors to go unnoticed during fabrication or for critical features to be forgotten during design iterations. Additionally, the simplified design also reduces both the time and cost barriers for prototyping, testing, and iterating on the design. The reduced barriers should allow future teams to take this work and push forward to prototypes and, eventually, integration into a spacecraft much easier than would be possible with a more complex design.

The design presented is intended to be a well-defined starting point, not the final design. Motor samples need to be acquired, tested, and the results evaluated. Assembly processes are outlined here, but they need to be formalized into proper procedures. Adhesives and curing processes need to be selected and tested. Rotor balancing is known to be achievable, however, a relationship with a shop that can accomplish this rotor balancing needs to be developed and the results evaluated. Additionally, electronics to drive the motors and software to run these electronics need to be developed, simulated, and integrated into the full system.

Three main projects can overcome most of these limitations. First, prototyping motor assemblies and benchtop testing would allow the simulation model to be verified and the hardware to be proven. This process would require little electronics work as most of the tests required could be run using benchtop electronic testing hardware (power supplies and oscilloscopes). Next, development of electronics to drive these motors would allow the system to be controlled by the spacecraft and is necessary for use in missions. This process is also a required step on the path to getting assemblies balanced because the balancing shop will need a way to interface with the motor when balancing. Third, a relationship with a high-speed balancing shop needs to be developed prior to high-speed testing can be performed.

## 8.2 Simulation

This simulation is a simplified model of a one-dimensional motor, wheel, and speed controller system. The motor is modeled as an ideal brushed DC motor with the same motor constants as the electronically commutated brushless DC motor. This simplification removes the need for electronic commutation logic, 3-phase power inverter, and voltage controller logic. Further, any excess motor load due to imbalance in the flywheel is assumed to be negligible. The model was then run through an automatic tuning procedure and a gamut of tests to show that the system designed is expected to perform adequately for advancing to the prototyping stage of development.

These simplifications allow designers to easily experiment with different motor and flywheel parameters and allows the simulation to run much faster. This simplification, in turn, allows more iterations to be made on motor and wheel parameters. Additionally, this one-dimensional model could easily be replicated to a three-dimensional system and used as part of the plant in a full spacecraft simulation. By making these changes, the ADCS can be tuned to effectively use these actuators to control the attitude of the spacecraft. After tuning of the ADCS, the actuator system can be further evaluated and iterated upon to either improve performance or reduce mass or volume as needed.

These simplifications do not come without their drawbacks. While the model runs much faster without the more complex solving of the electronics portion of the system, it sacrifices accuracy for this simplification. It would be prudent to include a detailed model of the electronics that are intended to be used to drive this

actuator in the final system and compare the results to the simplified model to obtain either a relative error or a correction factor for the simplified model. It is recommended that the simplified version of this model be integrated into the full spacecraft model to further validate the efficacy of this design and the robustness of the related ADCS. This modeling task does not require prototyping of test samples to be complete and therefore would be well suited to parallel development with physical test articles.

### 8.3 Performance

The simulation developed here was run through several test scenarios designed to determine how well the design would perform in a realistic spacecraft application. First, the control loop and actuator system is tuned using an autotuning feature in the simulation program. Next, the model is given input such that a maximum torque response would be elicited across the entire spectrum of speeds desired for use in the spacecraft system. The result from this test is used to find the maximum operational torque for the ADCS. Third, the model was put through a scenario to simulate the ADCS requesting maximum operational torque constantly until the system is saturated. This torque is significantly less than the torque in the previous test and these results easily matched expectations. Finally, the system was given a series of realistic torque requests derived from a full ADCS simulation. Through all these simulations, there were no technical or performance issues other than inaccuracy due to model simplification discussed above.

The simulation of the designed system performed exactly as expected. This result is not surprising because if all the design parameters are inputted correctly, the simplified nature of this simulation leaves little room for divergence from theoretical results. The theoretical results matching the simulation results does, however, improve the confidence that neither were conducted in error. Additionally, the performance of the motor, flywheel, and controller in this idealized configuration have been shown to be more than adequate for the intended application.

As mentioned above, the idealized nature of the simulation can lead to discrepancies from the physical system. Correcting for these imperfections through prototype testing should give designers a better idea of the true performance of the system. Further, the confidence in the requirements for maximum torque and total momentum storage is low. These values were chosen conservatively to allow the greatest chance for developing a system that would be a useful for future designers.

Further work needs to be done to evaluate the true requirements for maximum torque and total momentum storage in a realistic CubeSat application. When these requirements get ironed out, it may be possible to tweak this design to use a smaller, lighter wheels or even a less expensive motor. Additionally, using flywheels with less inertia would allow for improved pointing accuracy at the cost of less total momentum storage. Another possibility is to tweak the operational range of the proposed design by reducing the torque required and increasing the saturation speed. It is worth noting, however, that while increasing the maximum

speed increases the total momentum storage, it also increases the momentum bit and thereby reduces pointing accuracy. Further, there is much more torque available toward the mid-range of the motor speed that could be taken advantage of, if desired. Overall, increasing the confidence that these requirements are both sufficient and not overly conservative would be beneficial to the future engineers involved in this work.

## CHAPTER 9

### CONCLUSION

It has been thoroughly shown both that a reaction wheel system is the optimal solution for a low-cost high-precision attitude control system for 3U CubeSats and that it is eminently possible to develop a such a system to be fabricated by university students. An example of such a system has been demonstrated in this thesis. The design presented, as well as many more like it, could be manufactured by students and used in university or other research applications that desire to achieve high-precision instrumentation in low earth orbit with limited funding. Additionally, development of this design into an instructional program would greatly reduce the barrier to entry of hands-on learning for university students seeking further exposure to the space industry and subsequently improve the quality of their education.

The research required to make the design decisions was primarily based on the synthesis of textbook spacecraft attitude control knowledge and application of basic design principles. This research culminated in a solution that leverages decades of industry knowledge and lessons learned regarding large satellites and applies this knowledge to the relatively less developed CubeSat form factor. Recommended future work falls int four main categories. First, the proposed design needs to be prototyped, tested, and evaluated in a laboratory environment before it can be considered as a viable solution for mission development. Second, the accompanying electronics and driving software need to be developed before the system can be used in concert with the rest of a spacecraft.

Third, it would be beneficial to future designers if an ADCS testing chamber were developed. Such a device would consist of a low-resistance three-degree-of-freedom mount for a spacecraft and some form of star, sun, and planet simulator to allow the spacecraft to track its orientation and rotate freely under its own power. Finally, if it is determined that this type of hands-on learning is desired for more than the occasional laboratory student, it would be highly beneficial to formalize some of this knowledge into an easily digestible form, such as a primer that would be more approachable prior to diving directly into textbooks and fundamental research.

The knowledge generated here should be viewed in two distinct ways. First, the design presented is a valid solution to common design hurdle in the CubeSat development process. This design can be taken and iterated on as needed for application to future missions or for instructional activities. Second, the process of developing such a system is documented in such a way that allows the recreation of the process to develop new designs that are not predicated on the availability of the specific components listed in this design. Further, even though this design is intended for applications with the 3U CubeSat form factor, the process could easily be applied to spacecraft of varying size and complexity to either scale up or down the design at the fundamental level, prior to the selection of any specific components.

## REFERENCES

- [1] “About the CubeSat Program.” CubeSat,  
<https://www.cubesat.org/about>
- [2] ANSI B4.2-1978, “American National Standard Preferred Hole Basis Metric Clearance Fits.” American National Standards Institute.
- [3] “Balance Quality Requirements of Rigid Rotors. The Practical Application of ISO 1940/1.” *IRD Balancing*, 2009,  
[http://www.irdbalancing.com/assets/balance\\_quality\\_requirements\\_of\\_rigid\\_rotors.pdf](http://www.irdbalancing.com/assets/balance_quality_requirements_of_rigid_rotors.pdf)
- [4] “BLDC Motor Speed Control with Cascade PI Controllers.” MathWorks,  
<https://www.mathworks.com/help/slcontrol/ug/bldc-motor-speed-control-with-cascade-pi-controllers.html>
- [5] “Brushless DC-Servomotors.” Faulhaber,  
[https://www.faulhaber.com/fileadmin/Import/Media/EN\\_1028\\_B\\_FMM.pdf](https://www.faulhaber.com/fileadmin/Import/Media/EN_1028_B_FMM.pdf)
- [6] “Brushless DC Slotless Motors.” Portescap,  
[https://www.portescap.com/-/media/project/automation-specialty/portescap/portescap/pdf/specification-pdfs/specifications\\_16bhs.pdf](https://www.portescap.com/-/media/project/automation-specialty/portescap/portescap/pdf/specification-pdfs/specifications_16bhs.pdf)
- [7] R. Budynas, and J. Nisbett. *Shigley's Mechanical Engineering Design*. 9th ed., The McGraw-Hill Companies, Inc., 2011.

- [8] “CubeSat Reaction Wheels Control System SatBus 4RW.” NanoAvionics,  
<https://www.nanoavionics.com/cubesat-components/cubesat-reaction-wheels-control-system-satbus-4rw/>
- [9] “CubeWheel High Reliability Reaction Wheel with Integrated Electronics.”  
CubeSatShop, CubeSpace, The LaunchLab,  
[https://www.cubesatshop.com/wp-content/uploads/2016/06/CubeWheel\\_Specsheet\\_V1.1.jpg](https://www.cubesatshop.com/wp-content/uploads/2016/06/CubeWheel_Specsheet_V1.1.jpg)
- [10] “EC10.” Maxon Group,  
[https://www.maxongroup.us/medias/sys\\_master/root/8841182052382/EN-225.pdf](https://www.maxongroup.us/medias/sys_master/root/8841182052382/EN-225.pdf)
- [11] “ECX SPEED 8 M.” Maxon Group,  
[https://www.maxongroup.us/medias/sys\\_master/root/8841177628702/EN-176.pdf](https://www.maxongroup.us/medias/sys_master/root/8841177628702/EN-176.pdf)
- [12] “DEC Modules 24/2.” Maxon Group,  
[https://www.maxongroup.us/medias/sys\\_master/root/8831202623518/2018EN-448-449.pdf](https://www.maxongroup.us/medias/sys_master/root/8831202623518/2018EN-448-449.pdf)
- [13] “ESCON Overview.” Maxon Group,  
[https://www.maxongroup.us/medias/sys\\_master/root/8831199346718/2018EN-442-443-445.pdf](https://www.maxongroup.us/medias/sys_master/root/8831199346718/2018EN-442-443-445.pdf)
- [14] P. Hughes. *Spacecraft Attitude Dynamics*. Dover Publ., 2004.

[15] ISO 1940/1, "Balance Quality Requirements of Rigid Rotors." International Organization for Standardization.

[16] S. Lee, et al. "CubeSat Design Specification." *CubeSat*, 2014.

[https://static1.squarespace.com/static/5418c831e4b0fa4ecac1bacd/t/56e9b62337013b6c063a655a/1458157095454/cds\\_rev13\\_final2.pdf](https://static1.squarespace.com/static/5418c831e4b0fa4ecac1bacd/t/56e9b62337013b6c063a655a/1458157095454/cds_rev13_final2.pdf)

[17] "LOCTITE Hysol 1C." Ted Pella, Inc.,

[https://www.tedpella.com/technote\\_html/891-60%20TN.pdf](https://www.tedpella.com/technote_html/891-60%20TN.pdf)

[18] "LOCTITE 648." Henkel Adhesives,

[https://tdsna.henkel.com/americas/na/adhesives/hnaut/tds.nsf/web/1716575D28E43176882571870000D860/\\$File/648-EN.pdf](https://tdsna.henkel.com/americas/na/adhesives/hnaut/tds.nsf/web/1716575D28E43176882571870000D860/$File/648-EN.pdf)

[19] "Mars Cube One (MarCO)." NASA Jet Propulsion Laboratory, NASA,

<https://www.jpl.nasa.gov/cubesat/missions/marco.php>

[20] "McMaster-Carr Online Catalog." McMaster-Carr,

<https://www.mcmaster.com/>

[21] "Miniature Brushless DC Motors." MOOG,

[https://www.moog.com/content/dam/moog/literature/MCG/DBH-0472\\_Model\\_DtS.pdf](https://www.moog.com/content/dam/moog/literature/MCG/DBH-0472_Model_DtS.pdf)

[22] NASA-STD-8719.14B, "Process for Limiting Orbital Debris." National

Aeronautics and Space Administration,

<https://standards.nasa.gov/standard/nasa/nasa-std-871914>

- [23] M. Richmond. “Magnetic Torques and Amp's Law.” *Rochester Institute of Technology*.

[http://spiff.rit.edu/classes/phys213/lectures/amp/amp\\_long.html](http://spiff.rit.edu/classes/phys213/lectures/amp/amp_long.html)

- [24] “Online Materials Information Resource.” MatWeb,

<https://www.matweb.com/>

- [25] “PSSCT-2 (Pico Satellite Solar Cell Testbed-2).” ESA Earth Observation Portal.

<https://directory.eoportal.org/web/eoportal/satellite-missions/content/-/article/pssct-2>

- [26] “Reaction Wheels.” Sinclair Interplanetary,

[www.sinclairinterplanetary.com/reactionwheels](http://www.sinclairinterplanetary.com/reactionwheels)

- [27] “RW210.” Hyperion Technologies B.V., 2020,

<https://www.hyperiontechnologies.nl/products/rw210/>

- [28] N. Sizemore. “Reaction Wheel Material Demise Data.” 2020.

- [29] S. Starin, and J. Eterno. “Spacecraft Attitude Determination and Control Systems.” *Space Mission Engineering: The New SMAD*, by J Wertz et al., Microcosm Press, 2011, pp. 565-591.

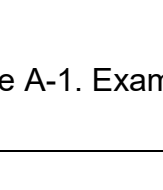
[30] J. Wertz. *Spacecraft Attitude Determination and Control*. Kluwer Academic Pub, 1999.

## APPENDICES

## APPENDIX A

### COMMERCIAL CUBESAT REACTION WHEELS

Table A-1. Examples of Commercial CubeSat Reaction Wheel Products

| SatBus 4RW0   | CubeWheel Medium  | RW210   | RW-0.01   |
|---|---|---|---|
|  |  |  |  |
| Manufacturer  | Nano Avionics   | Cube Space  | Hyperion Technologies   |
| Dimensions [mm]   | 43.5 x 43.5 x 24  | 46 x 46 x 31.5  | 25 x 25 x 15  |
| Mass [g]  | 137   | 150   | 21  |
| Max Speed [rpm]   | 6500  | 6000  | ???   |
| Speed Accuracy [rpm]  | ±1  | ±2.5  | ???   |
| Max Torque [mN m]   | 3   | 1   | 0   |
| Max Momentum [mN m s]   | 20  | 10.8  | 1.5   |
|   | [8]   | [9]   | [27]  |
|   |   |   | [26]  |

## APPENDIX B

### ROTOR IMBALANCE LIMITS

Table B-1. Balance Quality Grades for Representative Rigid Rotors [4,16]

| Balance Quality Grade | Product of the Relationship ( $e_{per} \times \omega$ ) <sup>(1) (2)</sup><br>mm/s | Rotor Types - General Examples   |
|-----------------------|--|--|
| G 4 000               | 4 000  | Crankshaft/drives <sup>(3)</sup> of rigidly mounted slow marine diesel engines with uneven number of cylinders <sup>(4)</sup>  |
| G 1 600               | 1 600  | Crankshaft/drives of rigidly mounted large two-cycle engines   |
| G 630                 | 630  | Crankshaft/drives of rigidly mounted large four-cycle engines<br>Crankshaft/drives of elastically mounted marine diesel engines  |
| G 250                 | 250  | Crankshaft/drives of rigidly mounted fast four-cylinder diesel engines <sup>(4)</sup>  |
| G 100                 | 100  | Crankshaft/drives of fast diesel engines with six or more cylinders <sup>(4)</sup><br>Complete engines (gasoline or diesel) for cars, trucks and locomotives <sup>(5)</sup>  |
| G 40                  | 40   | Car wheels, wheel rims, wheel sets, drive shafts<br>Crankshaft/drives of elastically mounted fast four-cycle engines with six or more cylinders <sup>(4)</sup><br>Crankshaft/drives of engines of cars, trucks and locomotives   |
| G 16                  | 16   | Drive shafts (propeller shafts, cardan shafts) with special requirements<br>Parts of crushing machines<br>Parts of agricultural machinery<br>Individual components of engines (gasoline or diesel) for cars, trucks and locomotives<br>Crankshaft/drives of engines with six or more cylinders under special requirements  |
| G 6.3                 | 6.3  | Parts of process plant machines<br>Marine main turbine gears (merchant service)<br>Centrifuge drums<br>Paper machinery rolls; print rolls<br>Fans<br>Assembled aircraft gas turbine rotors<br>Flywheels<br>Pump impellers<br>Machine-tool and general machinery parts<br>Medium and large electric armatures (of electric motors having at least 80 mm shaft height) without special requirements<br>Small electric armatures, often mass produced, in vibration insensitive applications and/or with vibration-isolating mountings<br>Individual components of engines under special requirements |
| G 2.5                 | 2.5  | Gas and steam turbines, including marine main turbines (merchant service)<br>Rigid turbo-generator rotors<br>Computer memory drums and discs<br>Turbo-compressors<br>Machine-tool drives<br>Medium and large electric armatures with special requirements<br>Small electric armatures not qualifying for one or both of the conditions specified for small electric armatures of balance quality grade G 6.3<br>Turbine-driven pumps   |
| G 1                   | 1  | Tape recorder and phonograph (gramophone) drives<br>Grinding-machine drives<br>Small electric armatures with special requirements  |
| G 0.4                 | 0.4  | Spindles, discs and armatures of precision grinders<br>Gyroscopes  |

1)  $\omega = 2\pi n/60 \approx n/10$ , if  $n$  is measured in revolutions per minute and  $\omega$  in radians per second.

2) For allocating the permissible residual unbalance to correction planes, refer to "Allocation of  $U_{per}$  to correction planes."

3) A crankshaft/drive is an assembly which includes a crankshaft, flywheel, clutch, pulley, vibration damper, rotating portion of connecting rod, etc.

4) For the purposes of this part of ISO 1940/1, slow diesel engines are those with a piston velocity of less than 9 m/s; fast diesel engines are those with a piston velocity of greater than 9 m/s.

5) In complete engines, the rotor mass comprises the sum of all masses belonging to the crankshaft/drive described in note 3 above.

PERMISSIBLE RESIDUAL UNBALANCE,  $e_{per}$  in g-mm/kg of rotor weight  
OR  
CENTER OF GRAVITY DISPLACEMENT,  $e_{per}$  in  $\mu\text{m}$

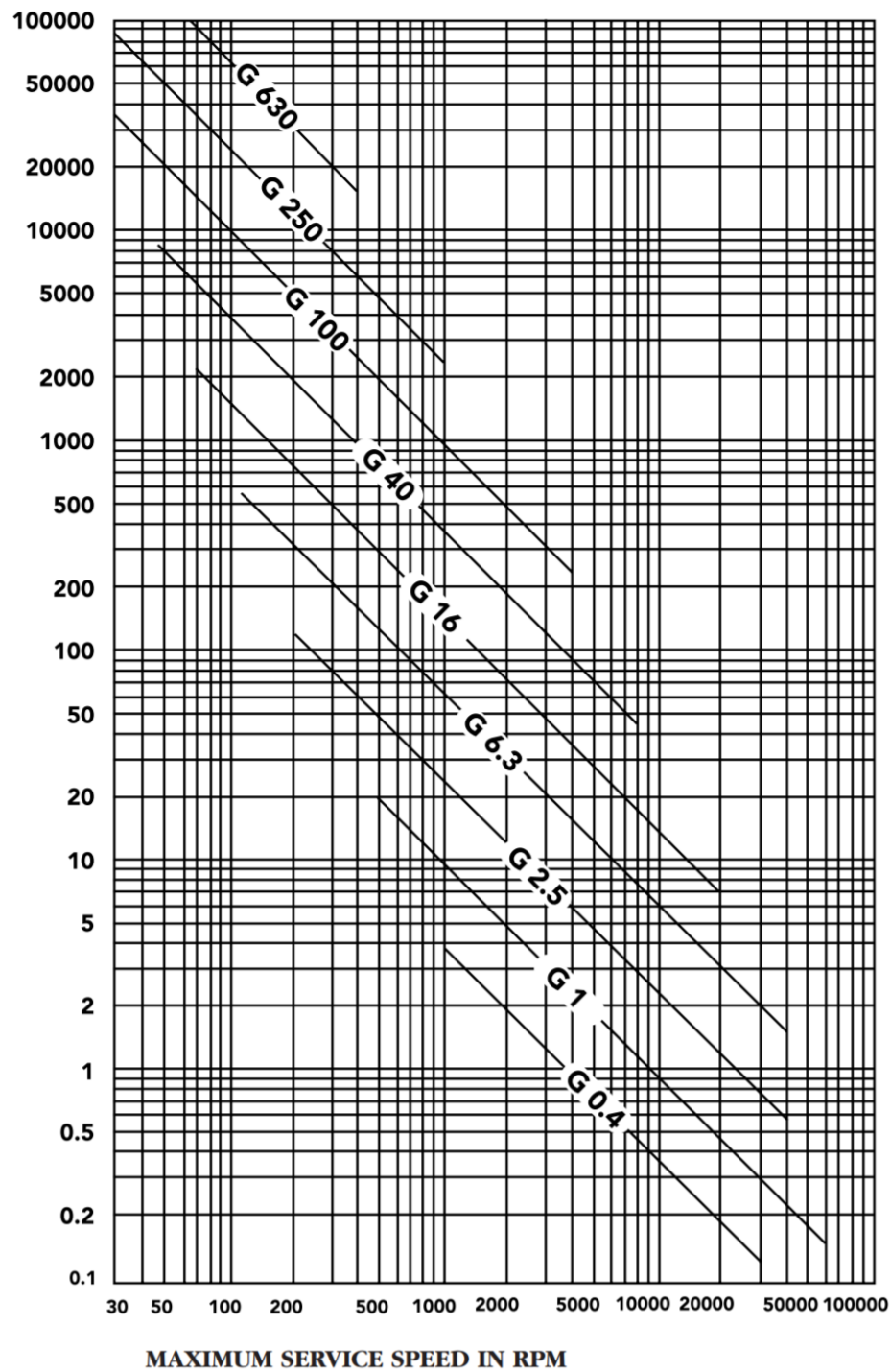


Figure B-1. Maximum Permissible Residual Unbalance [4,16]

## APPENDIX C

### HOLE FIT REFERENCES

Table C-1. Descriptions of Preferred Fits Using the Basic Hole System [3,8]

| Type of Fit  | Description   | Symbol  |
|--------------|---|---------|
| Clearance    | <i>Loose running fit:</i> for wide commercial tolerances or allowances on external members  | H11/c11 |
|              | <i>Free running fit:</i> not for use where accuracy is essential, but good for large temperature variations, high running speeds, or heavy journal pressures  | H9/d9   |
|              | <i>Close running fit:</i> for running on accurate machines and for accurate location at moderate speeds and journal pressures                                 | H8/f7   |
|              | <i>Sliding fit:</i> where parts are not intended to run freely, but must move and turn freely and locate accurately   | H7/g6   |
|              | <i>Locational clearance fit:</i> provides snug fit for location of stationary parts, but can be freely assembled and disassembled                             | H7/h6   |
| Transition   | <i>Locational transition fit:</i> for accurate location, a compromise between clearance and interference  | H7/k6   |
|              | <i>Locational transition fit:</i> for more accurate location where greater interference is permissible  | H7/n6   |
| Interference | <i>Locational interference fit:</i> for parts requiring rigidity and alignment with prime accuracy of location but without special bore pressure requirements | H7/p6   |
|              | <i>Medium drive fit:</i> for ordinary steel parts or shrink fits on light sections, the tightest fit usable with cast iron                                    | H7/s6   |
|              | <i>Force fit:</i> suitable for parts that can be highly stressed or for shrink fits where the heavy pressing forces required are impractical                  | H7/u6   |

Table C-1. Selection of International Tolerance Grades – Metric Series [3,8]

| Basic Sizes | IT6   | IT7   | IT8   | IT9   | IT10  | IT11  |
|-------------|-------|-------|-------|-------|-------|-------|
| 0–3         | 0.006 | 0.010 | 0.014 | 0.025 | 0.040 | 0.060 |
| 3–6         | 0.008 | 0.012 | 0.018 | 0.030 | 0.048 | 0.075 |
| 6–10        | 0.009 | 0.015 | 0.022 | 0.036 | 0.058 | 0.090 |
| 10–18       | 0.011 | 0.018 | 0.027 | 0.043 | 0.070 | 0.110 |
| 18–30       | 0.013 | 0.021 | 0.033 | 0.052 | 0.084 | 0.130 |
| 30–50       | 0.016 | 0.025 | 0.039 | 0.062 | 0.100 | 0.160 |
| 50–80       | 0.019 | 0.030 | 0.046 | 0.074 | 0.120 | 0.190 |
| 80–120      | 0.022 | 0.035 | 0.054 | 0.087 | 0.140 | 0.220 |
| 120–180     | 0.025 | 0.040 | 0.063 | 0.100 | 0.160 | 0.250 |
| 180–250     | 0.029 | 0.046 | 0.072 | 0.115 | 0.185 | 0.290 |
| 250–315     | 0.032 | 0.052 | 0.081 | 0.130 | 0.210 | 0.320 |
| 315–400     | 0.036 | 0.057 | 0.089 | 0.140 | 0.230 | 0.360 |

Table C-3. Fundamental Deviations for Shafts – Metric Series [3,8]

| Basic Sizes | Upper-Deviation Letter |        |        |        |   | Lower-Deviation Letter |        |        |        |        |
|-------------|------------------------|--------|--------|--------|---|------------------------|--------|--------|--------|--------|
|             | c                      | d      | f      | g      | h | k                      | n      | p      | s      | u      |
| 0–3         | –0.060                 | –0.020 | –0.006 | –0.002 | 0 | 0                      | +0.004 | +0.006 | +0.014 | +0.018 |
| 3–6         | –0.070                 | –0.030 | –0.010 | –0.004 | 0 | +0.001                 | +0.008 | +0.012 | +0.019 | +0.023 |
| 6–10        | –0.080                 | –0.040 | –0.013 | –0.005 | 0 | +0.001                 | +0.010 | +0.015 | +0.023 | +0.028 |
| 10–14       | –0.095                 | –0.050 | –0.016 | –0.006 | 0 | +0.001                 | +0.012 | +0.018 | +0.028 | +0.033 |
| 14–18       | –0.095                 | –0.050 | –0.016 | –0.006 | 0 | +0.001                 | +0.012 | +0.018 | +0.028 | +0.033 |
| 18–24       | –0.110                 | –0.065 | –0.020 | –0.007 | 0 | +0.002                 | +0.015 | +0.022 | +0.035 | +0.041 |
| 24–30       | –0.110                 | –0.065 | –0.020 | –0.007 | 0 | +0.002                 | +0.015 | +0.022 | +0.035 | +0.048 |
| 30–40       | –0.120                 | –0.080 | –0.025 | –0.009 | 0 | +0.002                 | +0.017 | +0.026 | +0.043 | +0.060 |
| 40–50       | –0.130                 | –0.080 | –0.025 | –0.009 | 0 | +0.002                 | +0.017 | +0.026 | +0.043 | +0.070 |
| 50–65       | –0.140                 | –0.100 | –0.030 | –0.010 | 0 | +0.002                 | +0.020 | +0.032 | +0.053 | +0.087 |
| 65–80       | –0.150                 | –0.100 | –0.030 | –0.010 | 0 | +0.002                 | +0.020 | +0.032 | +0.059 | +0.102 |
| 80–100      | –0.170                 | –0.120 | –0.036 | –0.012 | 0 | +0.003                 | +0.023 | +0.037 | +0.071 | +0.124 |
| 100–120     | –0.180                 | –0.120 | –0.036 | –0.012 | 0 | +0.003                 | +0.023 | +0.037 | +0.079 | +0.144 |
| 120–140     | –0.200                 | –0.145 | –0.043 | –0.014 | 0 | +0.003                 | +0.027 | +0.043 | +0.092 | +0.170 |
| 140–160     | –0.210                 | –0.145 | –0.043 | –0.014 | 0 | +0.003                 | +0.027 | +0.043 | +0.100 | +0.190 |
| 160–180     | –0.230                 | –0.145 | –0.043 | –0.014 | 0 | +0.003                 | +0.027 | +0.043 | +0.108 | +0.210 |
| 180–200     | –0.240                 | –0.170 | –0.050 | –0.015 | 0 | +0.004                 | +0.031 | +0.050 | +0.122 | +0.236 |
| 200–225     | –0.260                 | –0.170 | –0.050 | –0.015 | 0 | +0.004                 | +0.031 | +0.050 | +0.130 | +0.258 |
| 225–250     | –0.280                 | –0.170 | –0.050 | –0.015 | 0 | +0.004                 | +0.031 | +0.050 | +0.140 | +0.284 |
| 250–280     | –0.300                 | –0.190 | –0.056 | –0.017 | 0 | +0.004                 | +0.034 | +0.056 | +0.158 | +0.315 |
| 280–315     | –0.330                 | –0.190 | –0.056 | –0.017 | 0 | +0.004                 | +0.034 | +0.056 | +0.170 | +0.350 |
| 315–355     | –0.360                 | –0.210 | –0.062 | –0.018 | 0 | +0.004                 | +0.037 | +0.062 | +0.190 | +0.390 |
| 355–400     | –0.400                 | –0.210 | –0.062 | –0.018 | 0 | +0.004                 | +0.037 | +0.062 | +0.208 | +0.435 |

## APPENDIX D

### SIMULINK MODEL

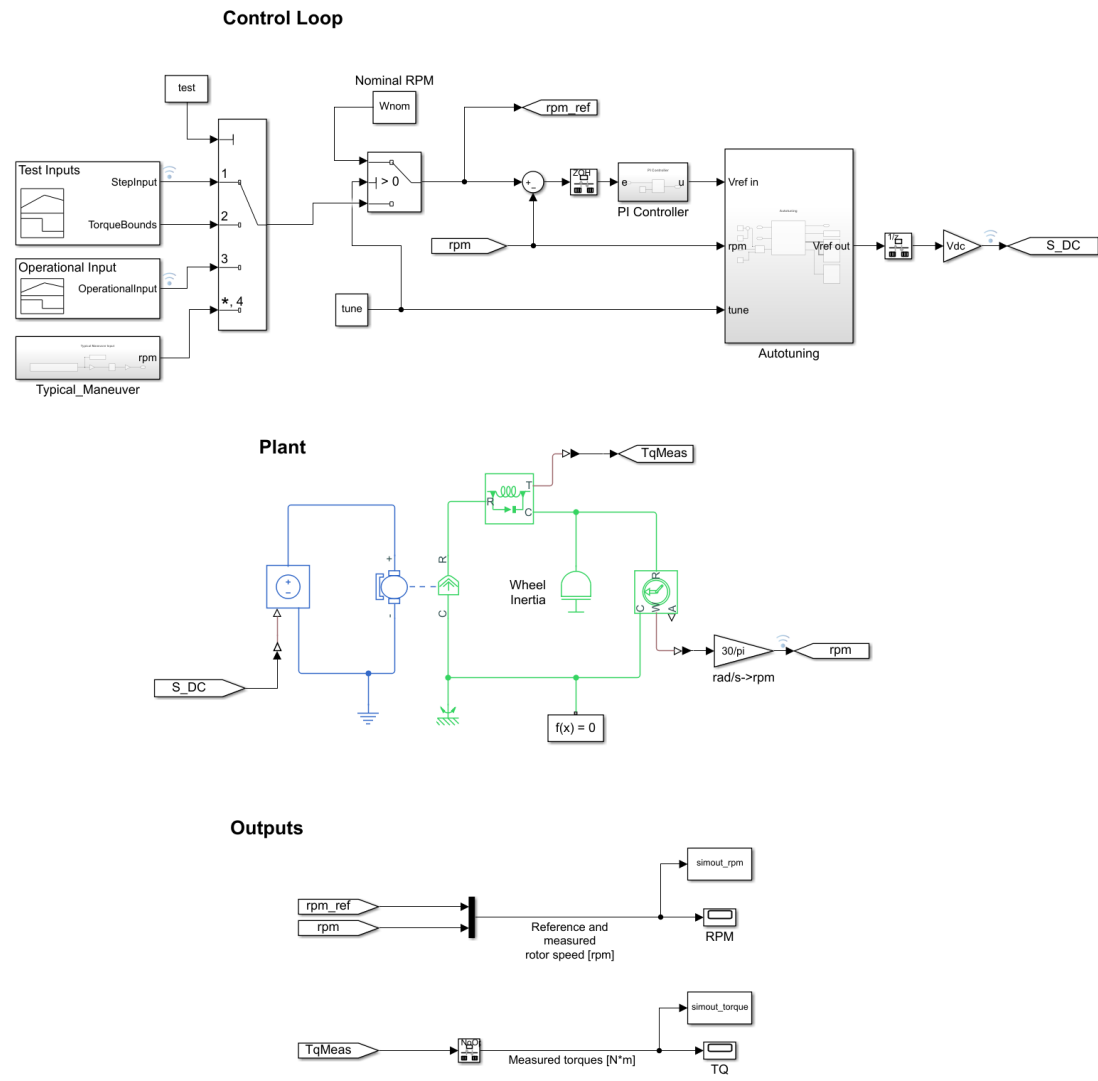


Figure D-1. Top Level Simulink Model

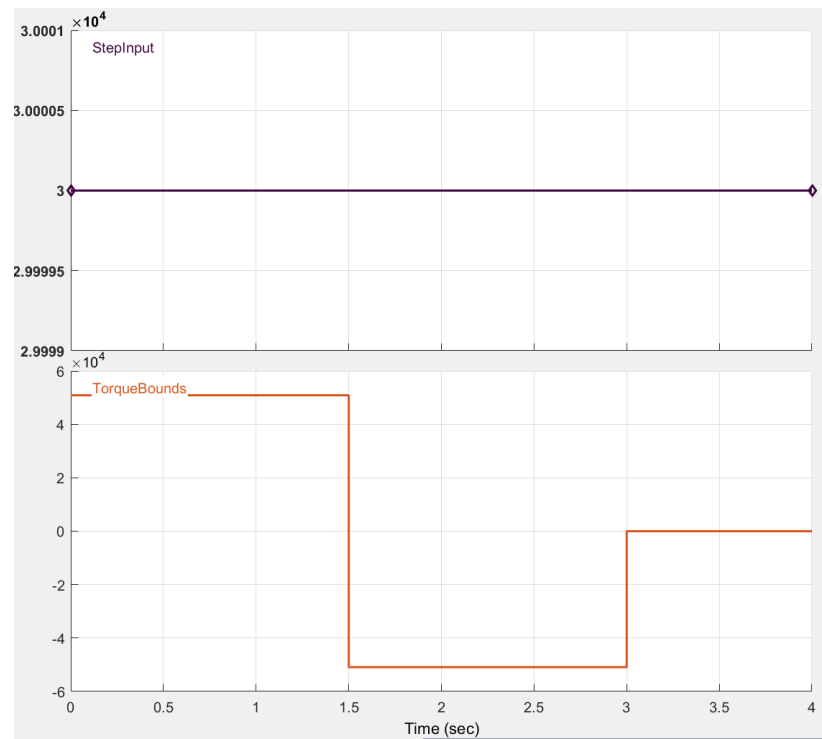


Figure D-2. Simulink Speed Controller Setpoints for Tuning and Torque

### Boundary Tests

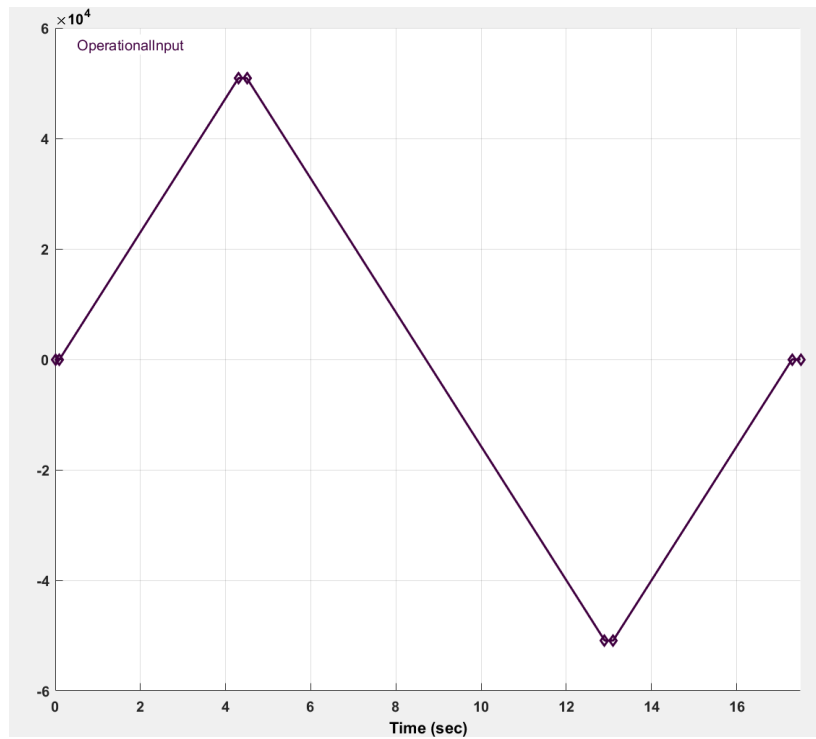


Figure D-3. Simulink Speed Controller Setpoints for Operational Range Test

### Typical Maneuver Input

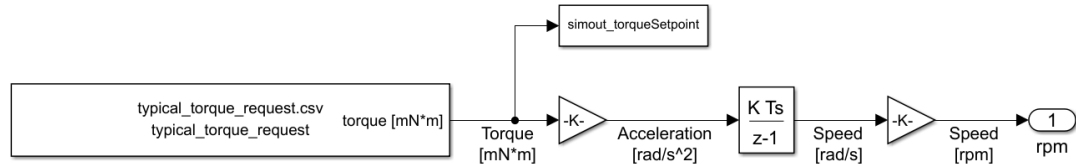


Figure D-4. Simulink Speed Controller Setpoint Integrator for Typical Maneuver

### Torque Inputs

### Autotuning

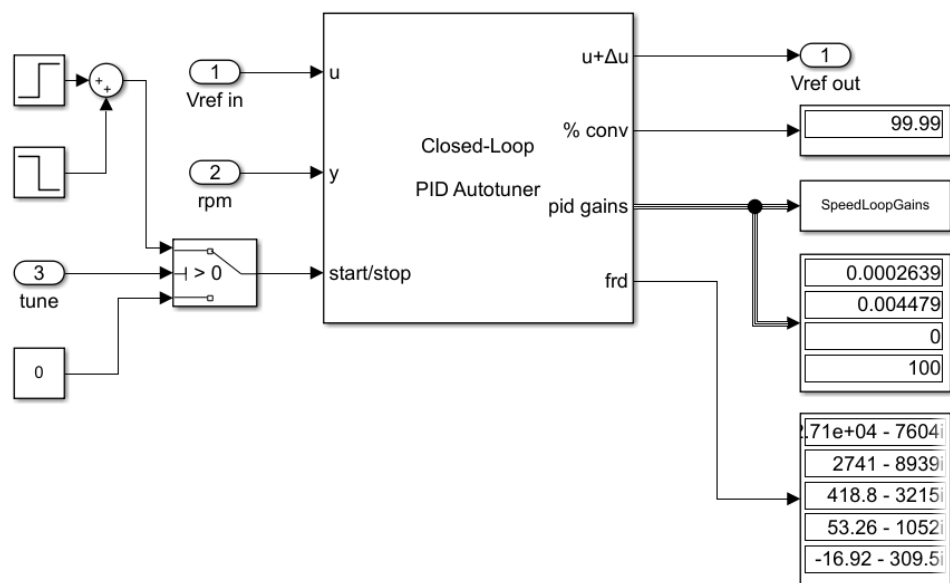


Figure D-5. Simulink Autotuning Logic Block [4]

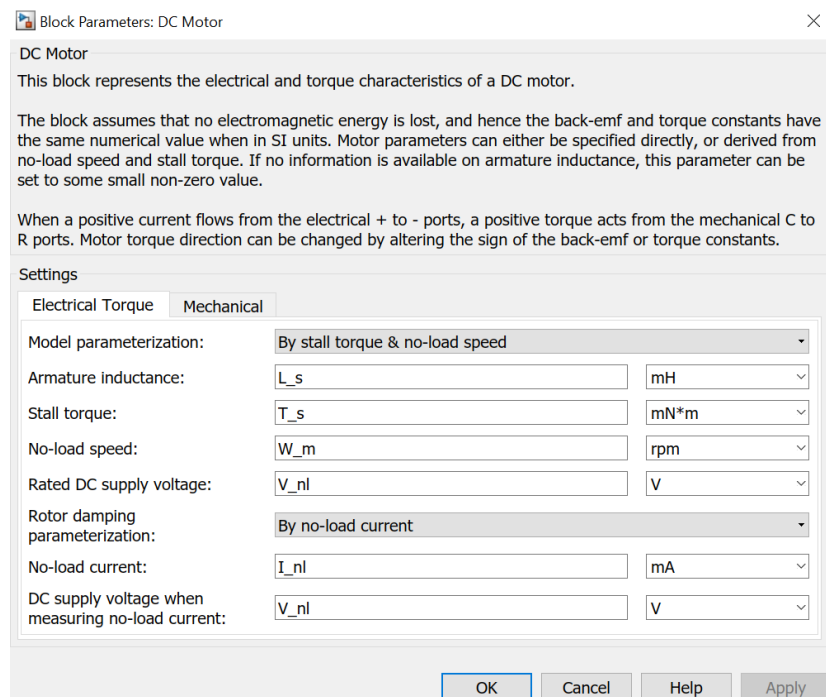


Figure D-6. Simulink Universal DC Motor Parameters [4]

## APPENDIX E

### MATLAB SOFTWARE

## E-1. Autotuning Simulation Script

```
% BLDC Motor Control - Tuning
% Nick Bonafede
% 4/29/2020
clc; clear;
```

### System Setup

```
mdl = 'scdbldcspeedcontrolThesis4';
open_system(mdl);
```

### Initial Parameters

```
L_s = 0.0671; % Armature inductance [mH]
T_s = 15.6; % Stall torque [mN*m]
W_m = 57100; % No-load speed [rpm]
V_r = 24; % Rated DC supply voltage [V]
I_nl = 67.3; % No load current [mA]
V_nl = 18; % Volatge at no load current [V]

J_r = 0.0691; % Rotor inertia [g*cm^2]
J_w = 9.35; % wheel inertia [g*cm^2]

Ts = 5e-5; % Fundamental sample time [s]
Tsc = 2e-4; % Sample time for control loop [s]

Vdc = 18; % Maximum DC link voltage [V]
Wnom = 30000; % Nominal motor speed, autotuning [rpm]

Kp = 1e-4; % Proportional gain
Ki = 1e-5; % Integrator gain

Tb = 50; % Target bandwidth

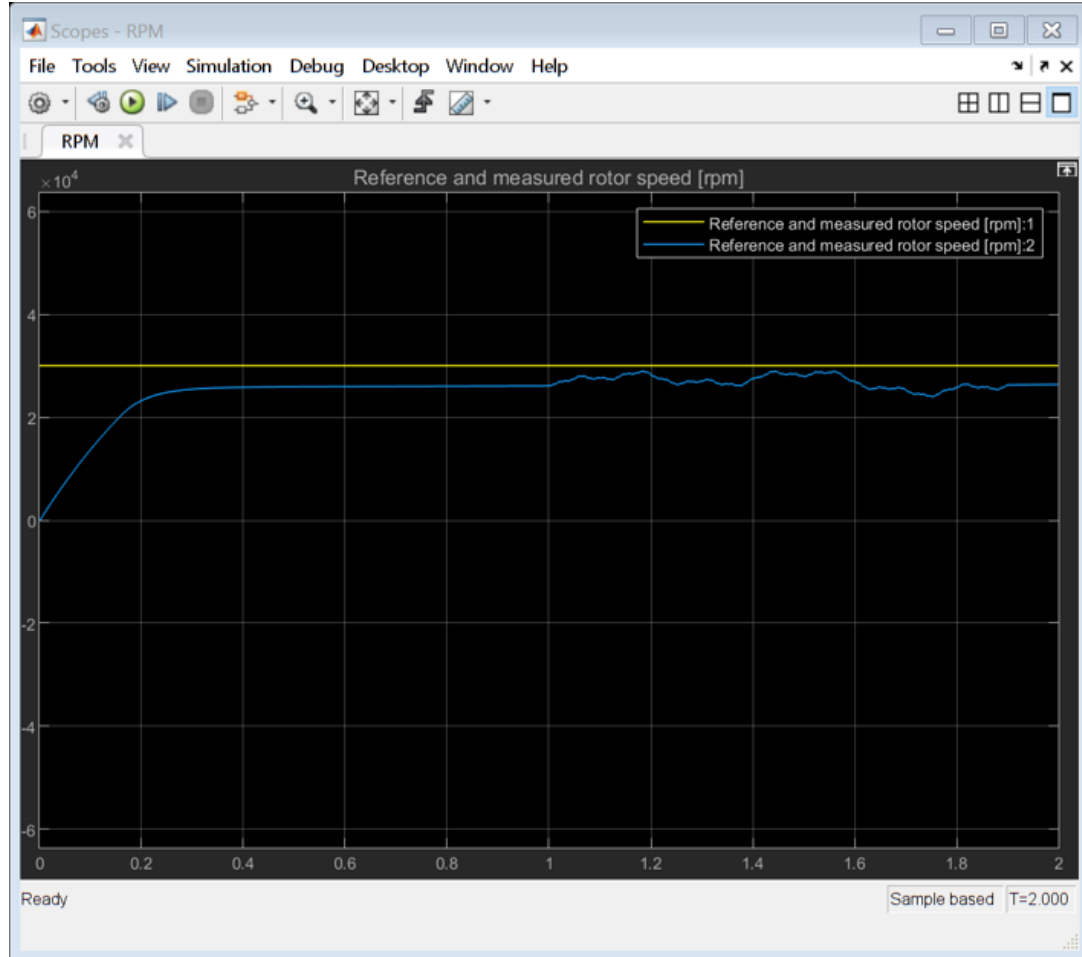
test = 1; % Step input
tune = 0; % Tuning flag
```

## Simulation Before Tuning and Tuning

```
open_system([mdl '/RPM']);
tune = 1;

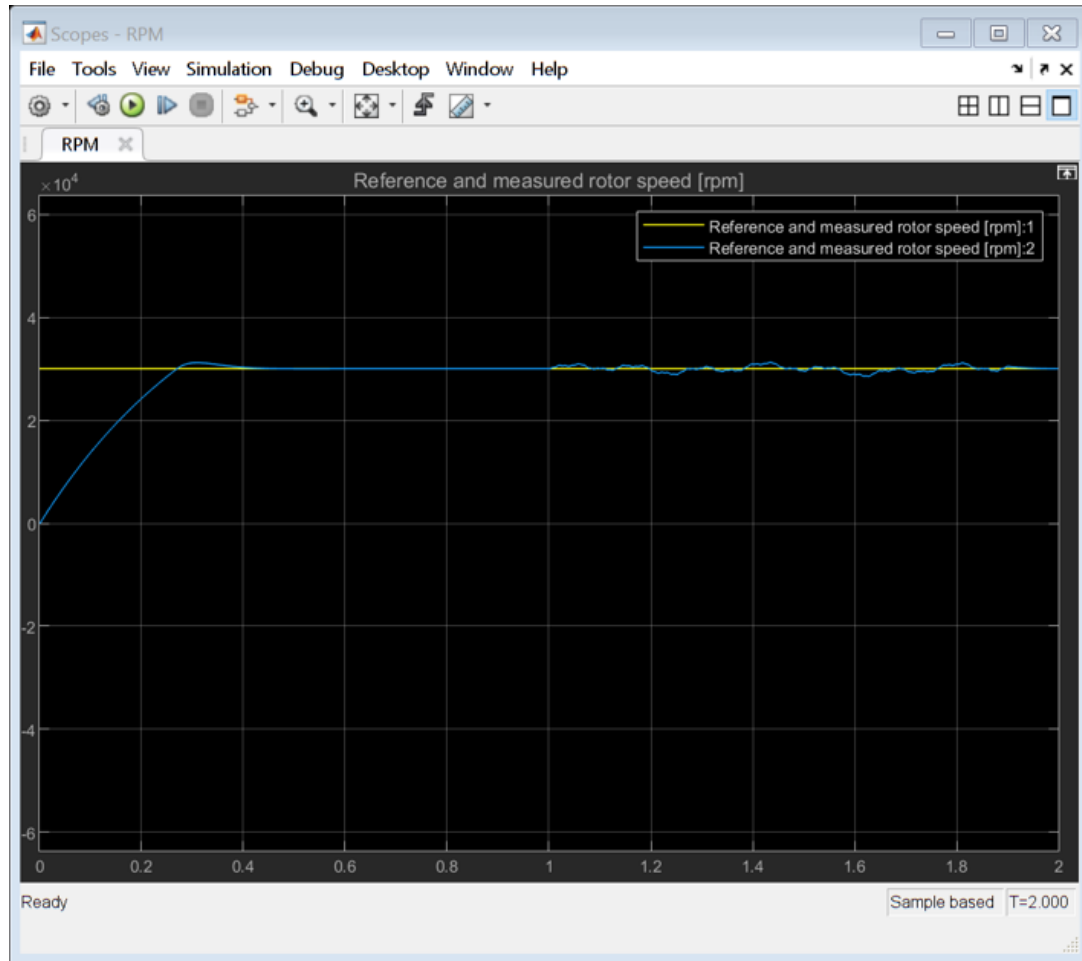
sim.mdl, 2);
simout_rpm0 = simout_rpm;

Kp = SpeedLoopGains(1);
Ki = SpeedLoopGains(2);
```



## Simulation After Tuning

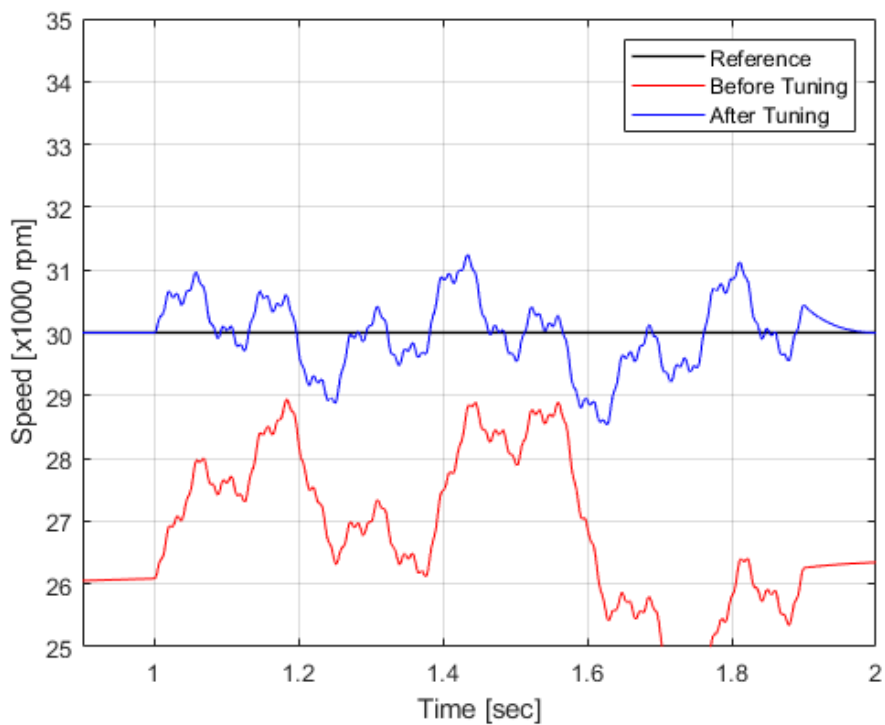
```
sim(md1, 2);
simout_rpm1 = simout_rpm;
```



## Results, Random Noise

```
figure(1)
plot(simout_rpm0.time,simout_rpm0.data(:,1)/1000,'k-','LineWidth',1)
hold on
plot(simout_rpm0.time,simout_rpm0.data(:,2)/1000,'r-','LineWidth',.5)
plot(simout_rpm1.time,simout_rpm1.data(:,2)/1000,'b-','LineWidth',.5)
hold off

grid on
axis([.9 2 25 35])
xlabel('Time [sec]')
ylabel('Speed [x1000 rpm]')
%title('Controller Tuning Experiment')
legend('Reference','Before Tuning','After Tuning')
saveas(gcf,'4_Tuning/TuningExperiment.png')
```

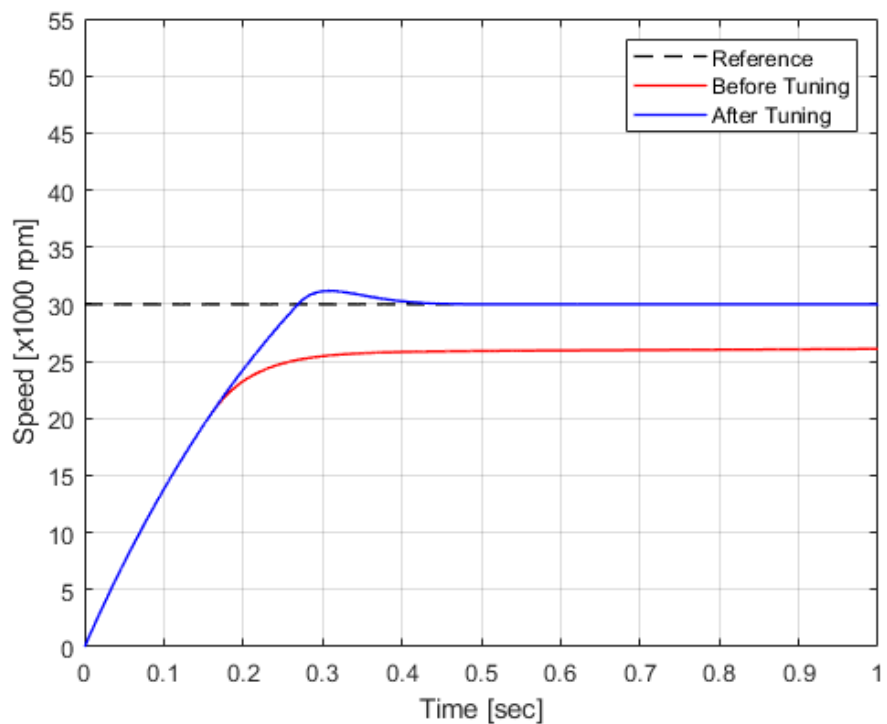


## Results, Step Response

```
figure(2)
plot(simout_rpm0.time,simout_rpm0.data(:,1)/1000,'--k','LineWidth',1)
hold on
plot(simout_rpm0.time,simout_rpm0.data(:,2)/1000,'-r','LineWidth',1)
plot(simout_rpm1.time,simout_rpm1.data(:,2)/1000,'-b','LineWidth',1)
hold off

grid on
axis([0 1 0 55])
xlabel('Time [sec]')
ylabel('Speed [x1000 rpm]')
%title('Tuning Results')
legend('Reference','Before Tuning','After Tuning')

saveas(gcf,'4_Tuning/TuningResults.png')
```



*Published with MATLAB® R2019a*

## E-2. Torque Boundary Simulation Script

```
% BLDC Motor Control - Torque Boundary
% Nick Bonafede
% 4/29/2020
clc; clear;
```

### System Setup

```
mdl = 'scdbldcspeedcontrolThesis4';
open_system(mdl);
```

### System Parameters

```
L_s = 0.0671; % Armature inductance [mH]
T_s = 15.6; % stall torque [mN*m]
w_m = 57100; % No-load speed [rpm]
v_r = 24; % Rated DC supply voltage [V]
i_nl = 67.3; % No load current [mA]
v_nl = 18; % Volatge at no load current [V]

J_r = 0.0691; % Rotor inertia [g*cm^2]
J_w = 9.35; % wheel inertia [g*cm^2]

Ts = 5e-5; % Fundamental sample time [s]
Tsc = 2e-4; % Sample time for control loop [s]

vdc = 18; % Maximum DC link voltage [V]
wnom = 30000; % Nominal motor speed, autotuning [rpm]

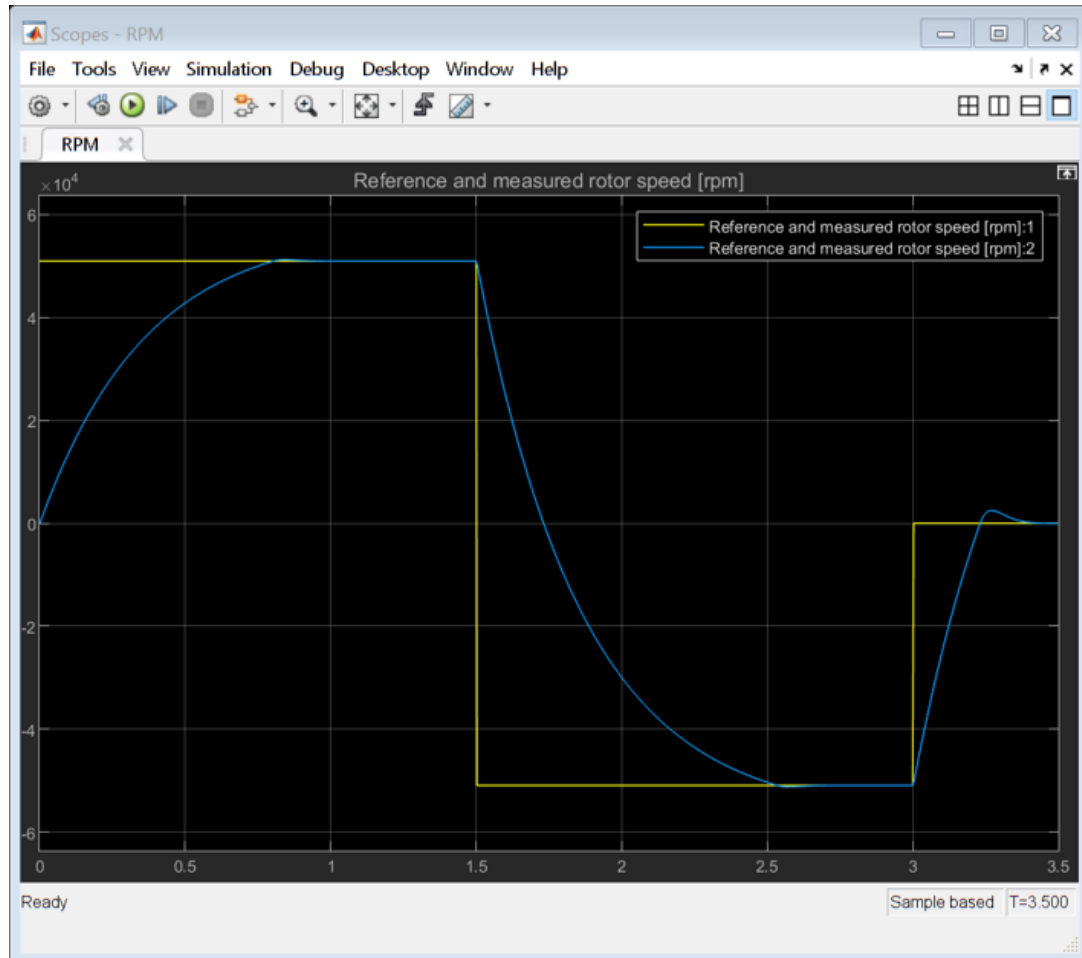
Kp = 2.63894e-4; % Proportional gain
Ki = 4.47854e-3; % Integrator gain

Tb = 50; % Target bandwidth [rad/s]

test = 2; % Max-Max input
tune = 0; % Tuning OFF
```

## Simulation

```
open_system([mdl '/RPM']);  
  
sim(mdl, 3.5);  
simout_rpm10 = simout_rpm;  
simout_torque10 = simout_torque;
```



## Results, Time Domain

```

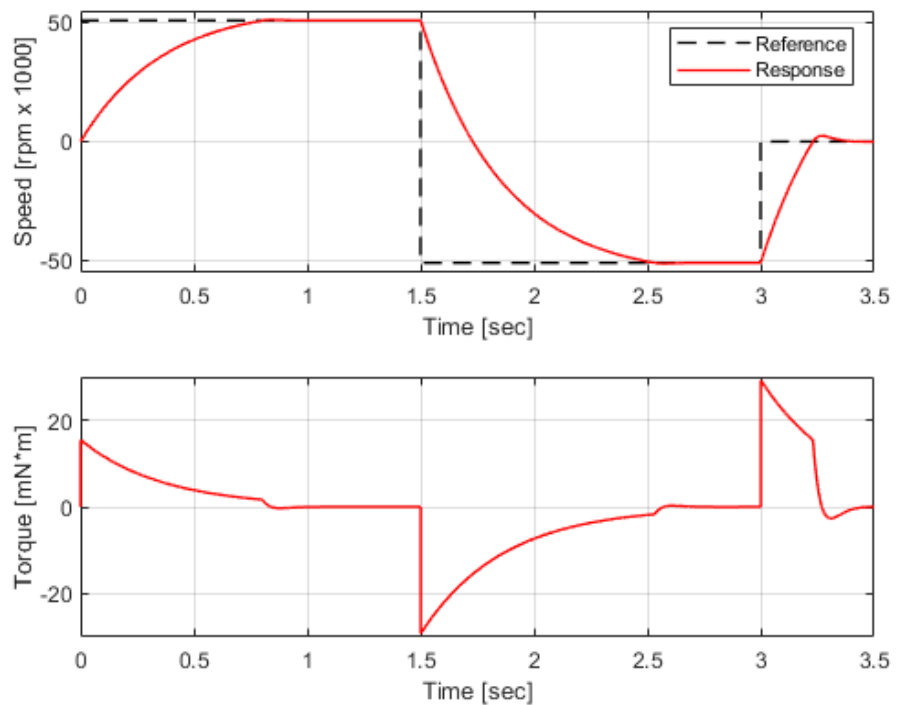
figure(10)
subplot(2,1,1)
plot(simout_rpm10.time,simout_rpm10.data(:,1)/1000,'--k','LineWidth',1)
hold on
plot(simout_rpm10.time,simout_rpm10.data(:,2)/1000,'-r','LineWidth',1)
hold off

grid on
axis([0 3.5 -55 55])
xlabel('Time [sec]')
ylabel('Speed [rpm x 1000]')
%title('Torque Bounds: Experiment')
legend('Reference','Response')

subplot(2,1,2)
plot(simout_torque10.time,simout_torque10.data(:,1)*1e3,'-r','LineWidth',1)
grid on
axis([0 3.5 -30 30])
xlabel('Time [sec]')
ylabel('Torque [mN*m]')

saveas(gcf,'4_Torque/TorqueExperiment.png')

```

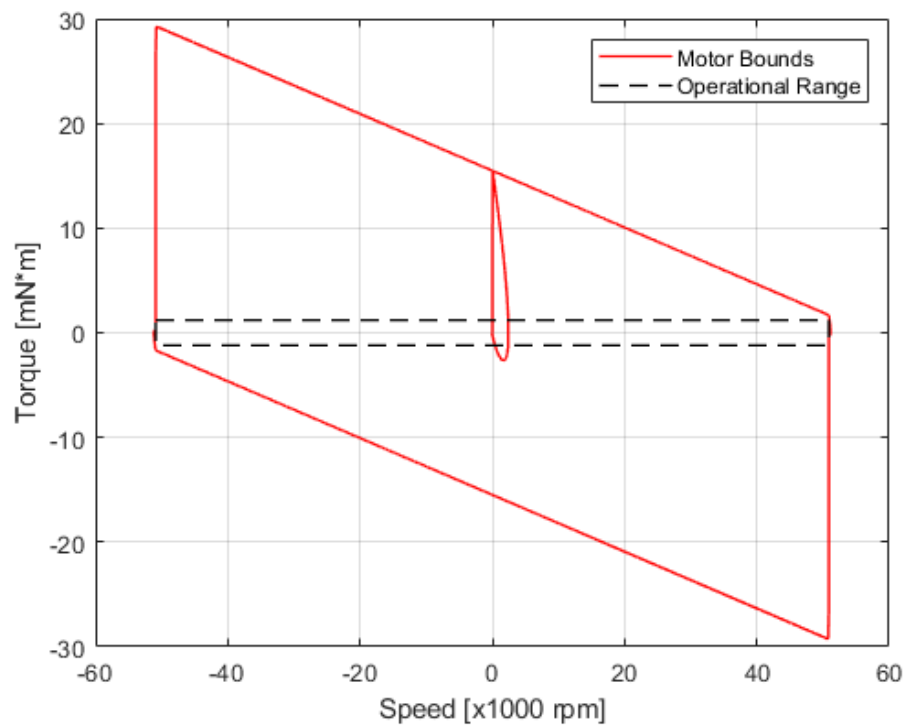


## Results, Torque Domain

```
figure(11)
plot(simout_rpm10.data(:,2)/1000,simout_torque10.data(:,1)*1e3,'-r','LineWidth',1)
hold on
plot(50.9*[-1 1 1 -1 -1],1.2*[1 1 -1 -1 1],'--k','LineWidth',1)
hold off

grid on
axis([-60 60 -30 30])
xlabel('Speed [x1000 rpm]')
ylabel('Torque [mN*m]')
%title('Torque Bounds: Results')
Legend('Motor Bounds','Operational Range')

saveas(gcf,'4_Torque/TorqueResults.png')
```



[Published with MATLAB® R2019a](#)

### E-3. Operational Range Simulation Script

```
% BLDC Motor Control - Operational Range
% Nick Bonafede
% 4/29/2020
clc; clear;
```

#### System Setup

```
mdl = 'scdbldcspeedcontrolThesis4';
open_system(mdl);
```

#### System Parameters

```
L_s = 0.0671; % Armature inductance [mH]
T_s = 15.6; % stall torque [mN*m]
w_m = 57100; % No-load speed [rpm]
v_r = 24; % Rated DC supply voltage [V]
i_n1 = 67.3; % No load current [mA]
v_n1 = 18; % Volatge at no load current [V]

J_r = 0.0691; % Rotor inertia [g*cm^2]
J_w = 9.35; % wheel inertia [g*cm^2]

Ts = 5e-5; % Fundamental sample time [s]
Tsc = 2e-4; % Sample time for control loop [s]

vdc = 18; % Maximum DC link voltage [V]
wnom = 30000; % Nominal motor speed, autotuning [rpm]

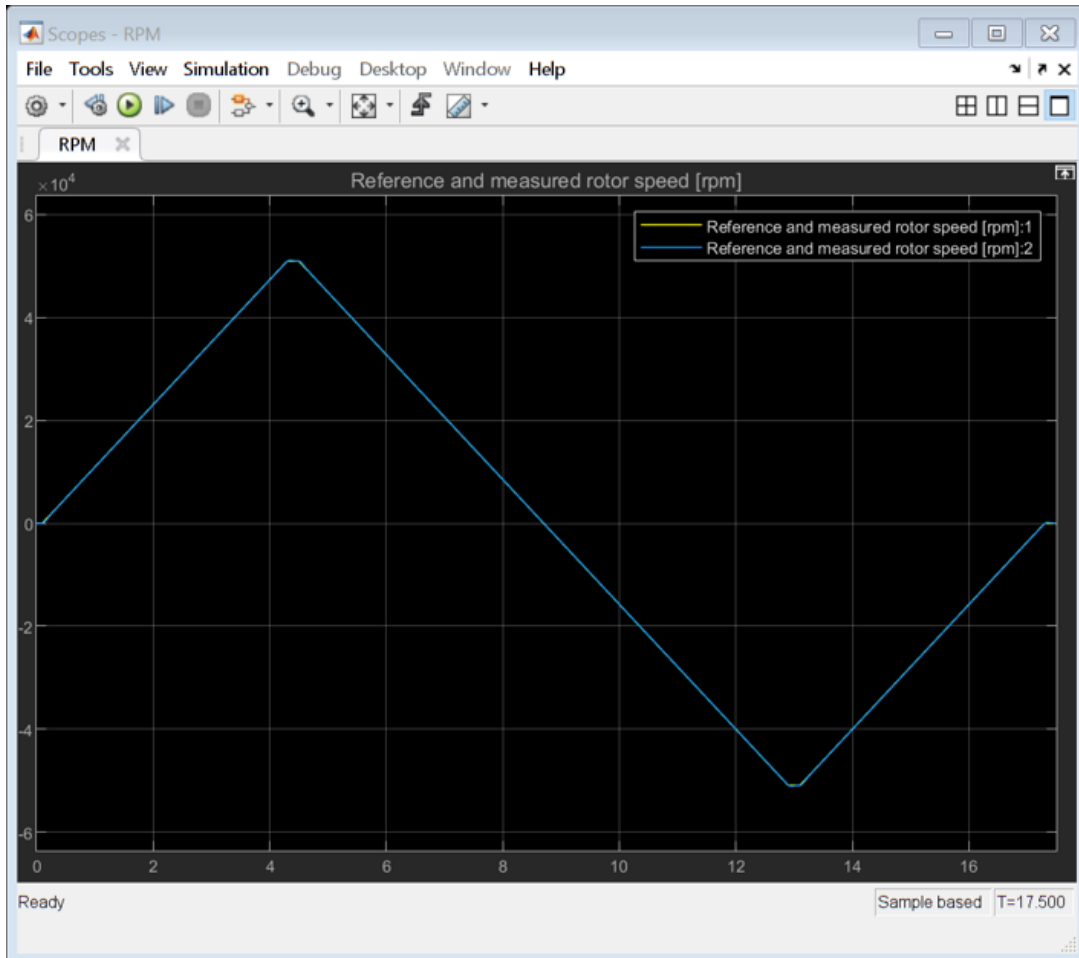
Kp = 2.63894e-4; % Proportional gain
Ki = 4.47854e-3; % Integrator gain

Tb = 50; % Target bandwidth [rad/s]

test = 3; % Ramp input
tune = 0; % Tuning OFF
```

## Simulation

```
open_system([mdl '/RPM']);  
  
sim(mdl, 17.5);  
simout_rpm20 = simout_rpm;  
simout_torque20 = simout_torque;
```



## Results, Time Domain

```

figure(20)
subplot(2,1,1)
plot(simout_rpm20.time,simout_rpm20.data(:,1)/1000,'--k','LineWidth',2)
hold on
plot(simout_rpm20.time,simout_rpm20.data(:,2)/1000,'-r','LineWidth',1)
hold off

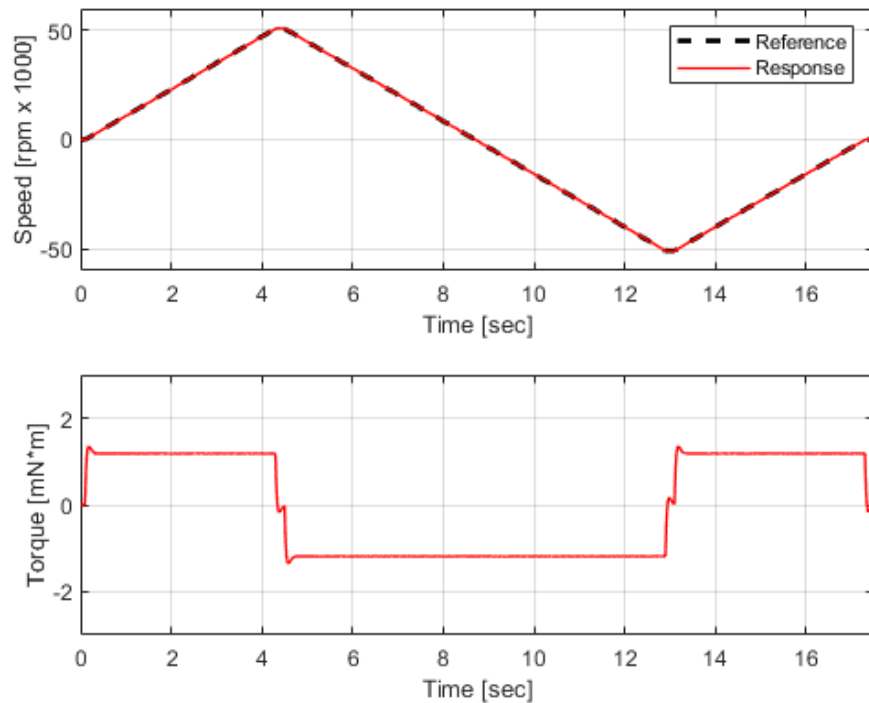
grid on
axis([0 17.5 -60 60])
xlabel('Time [sec]')
ylabel('Speed [rpm x 1000]')
%title('Operational Range: Experiment')
legend('Reference','Response')

Tavg = movmean(simout_torque20.data(:,1),round(.005/Ts));

subplot(2,1,2)
plot(simout_torque20.time,simout_torque20.data(:,1)*1e3,'-r','LineWidth',1)
grid on
axis([0 17.5 -3 3])
xlabel('Time [sec]')
ylabel('Torque [mN*m]')

saveas(gcf,'4_Operational/OperationalExperiment.png')

```

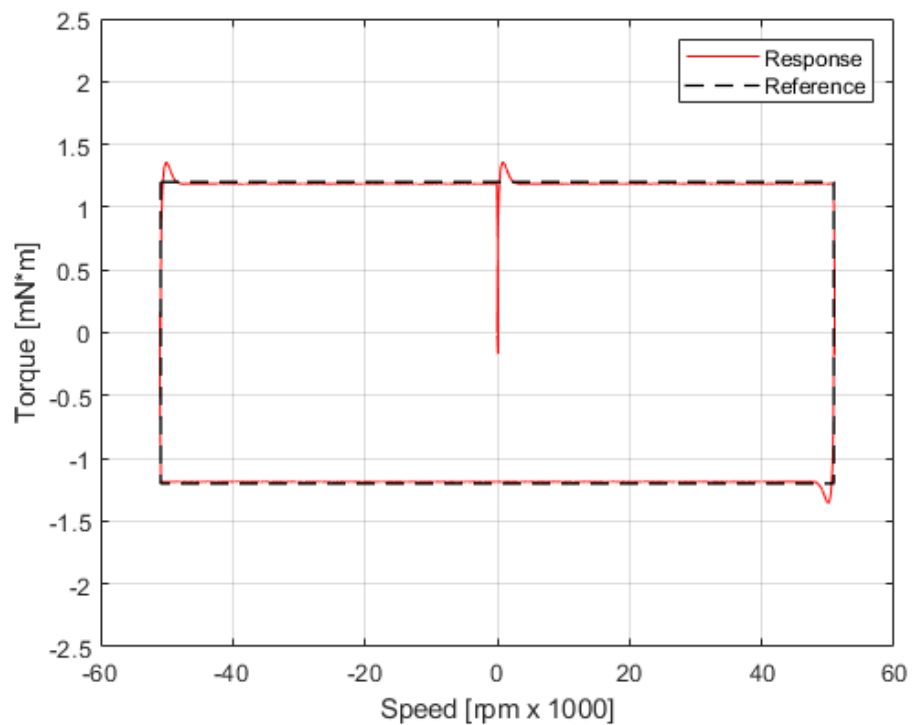


## Results, Torque Domain

```
figure(21)
plot(simout_rpm20.data(:,2)/1000,simout_torque20.data(:,1)*1e3,'-r','Linewidth',0.5)
hold on
plot(50.9*[-1 1 1 -1 -1],1.2*[1 1 -1 -1 1],'--k','Linewidth',1)
hold off

grid on
axis([-60 60 -2.5 2.5])
xlabel('Speed [rpm x 1000]')
ylabel('Torque [mN*m]')
%title('Operational Range: Results')
Legend('Response','Reference')

saveas(gcf,'4_Operational/OperationalResult.png')
```



*Published with MATLAB® R2019a*

#### E-4. Typical Maneuver Simulation Script

```
% BLDC Motor Control - Typical Maneuver
% Nick Bonafede
% 4/29/2020
clc; clear;
```

#### System Setup

```
mdl = 'scdbldcspeedcontrolThesis4';
open_system(mdl);
```

#### System Parameters

```
L_s = 0.0671; % Armature inductance [mH]
T_s = 15.6; % stall torque [mN*m]
w_m = 57100; % No-load speed [rpm]
v_r = 24; % Rated DC supply voltage [V]
I_nl = 67.3; % No load current [mA]
v_nl = 18; % Volatge at no load current [V]

J_r = 0.0691; % Rotor inertia [g*cm^2]
J_w = 9.35; % wheel inertia [g*cm^2]

Ts = 5e-5; % Fundamental sample time [s]
Tsc = 2e-4; % Sample time for control loop [s]

vdc = 18; % Maximum DC link voltage [V]
wnom = 30000; % Nominal motor speed, autotuning [rpm]

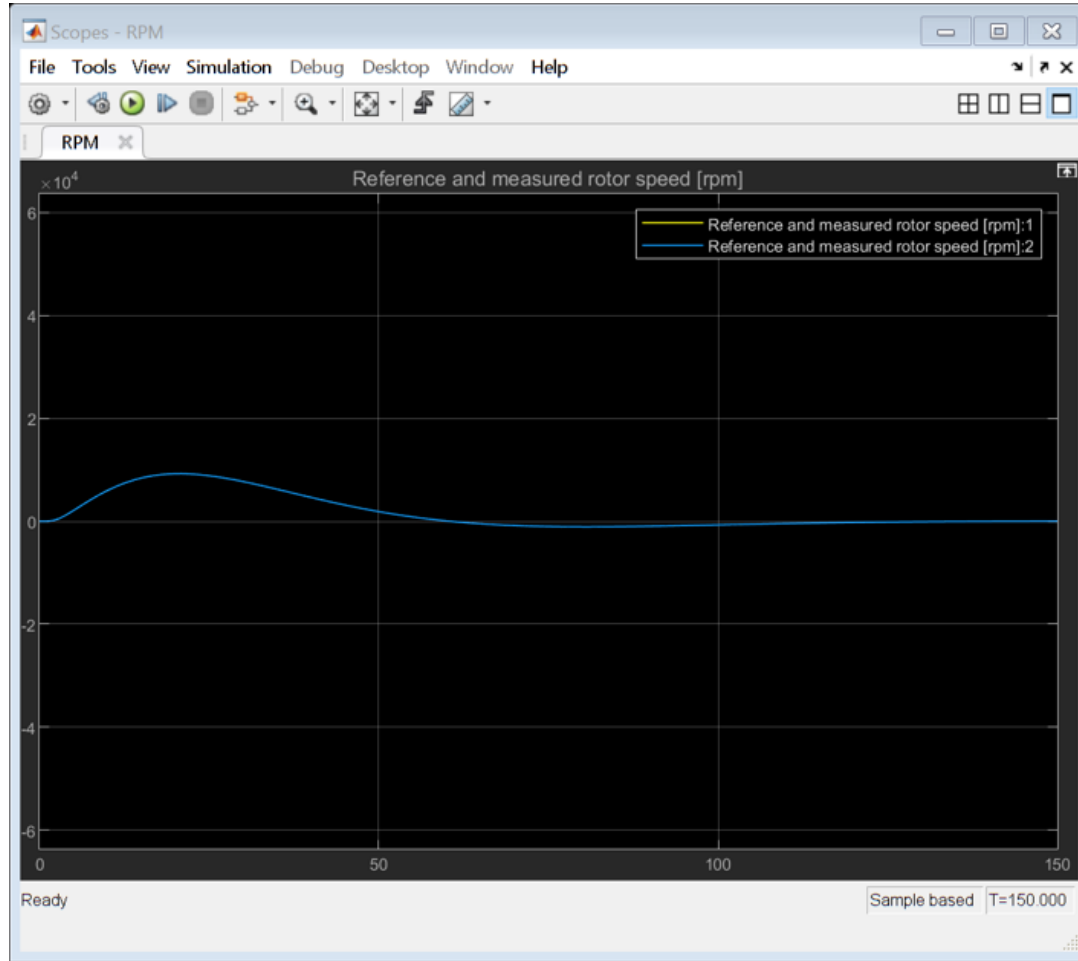
Kp = 2.63894e-4; % Proportional gain
Ki = 4.47854e-3; % Integrator gain

Tb = 50; % Target bandwidth [rad/s]

test = 4; % Ramp input
tune = 0; % Tuning OFF
```

## Simulation

```
open_system([mdl '/RPM']);  
  
sim(mdl, 150);  
simout_rpm30 = simout_rpm;  
simout_torque30 = simout_torque;
```



## Results, Time Domain

```
figure(30)  
subplot(2,1,1)  
plot(simout_rpm30.time,simout_rpm30.data(:,1)/1000,'--k','LineWidth',2)  
hold on  
plot(simout_rpm30.time,simout_rpm30.data(:,2)/1000,'-r','LineWidth',1)  
hold off
```

```

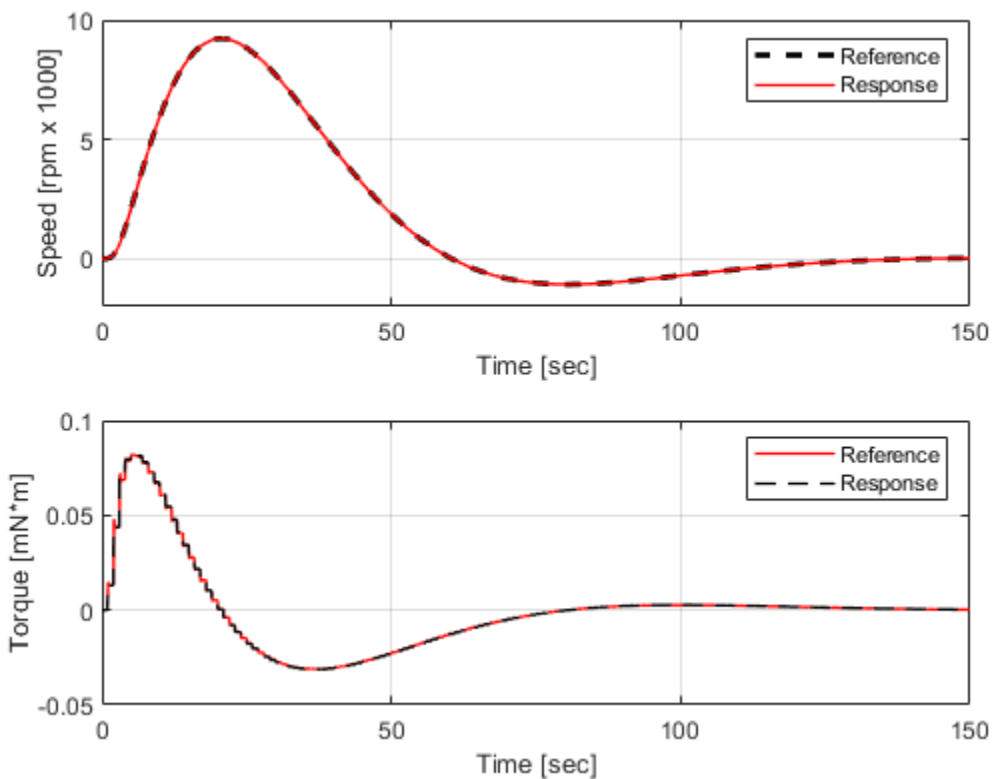
grid on
axis([0 150 -2 10])
xlabel('Time [sec]')
ylabel('Speed [rpm x 1000]')
%title('Operational Range: Experiment')
legend('Reference', 'Response')

Tavg = movmean(simout_torque30.data(:,1),round(.005/Ts));

subplot(2,1,2)
plot(simout_torque30.time,simout_torque30.data(:,1)*1e3,'-r','Linewidth',1)
hold on
plot(simout_torqueSetpoint.time,simout_torqueSetpoint.data(:,1), '--k','Linewidth',1)
hold off
grid on
axis([0 150 -.05 .1])
xlabel('Time [sec]')
ylabel('Torque [mN*m]')
legend('Reference', 'Response')

saveas(gcf, '4_Maneuver/ManeuverExperiment.png')

```

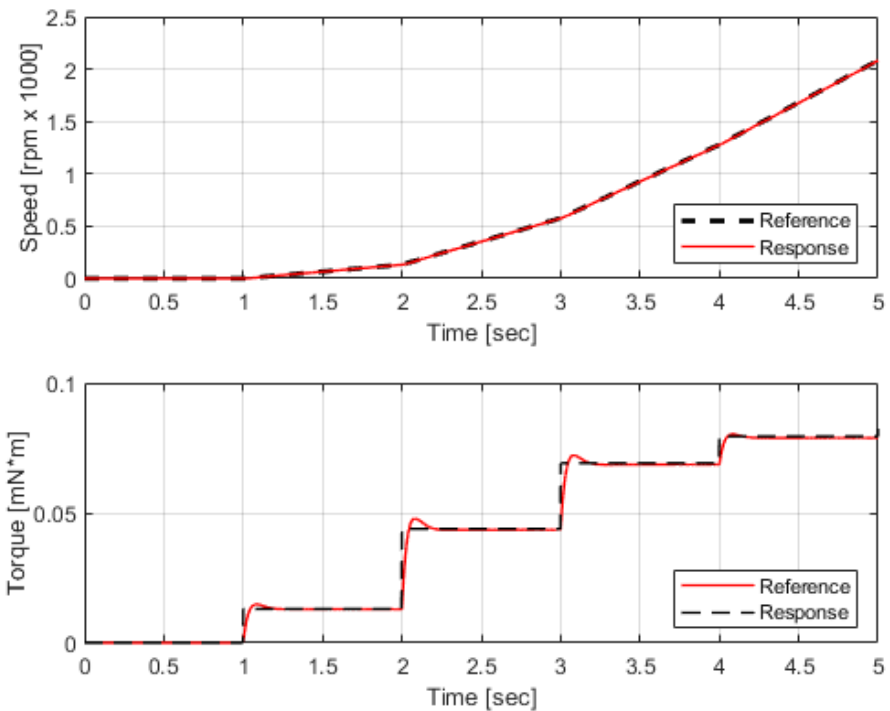


## Results, Time Domain (Detail)

```
subplot(2,1,1)
axis([0 5 0 2.5])
legend('Location', 'SouthEast')

subplot(2,1,2)
axis([0 5 0 .1])
legend('Location', 'SouthEast')

saveas(gcf, '4_Maneuver/ManeuverExperimentZoom.png')
```

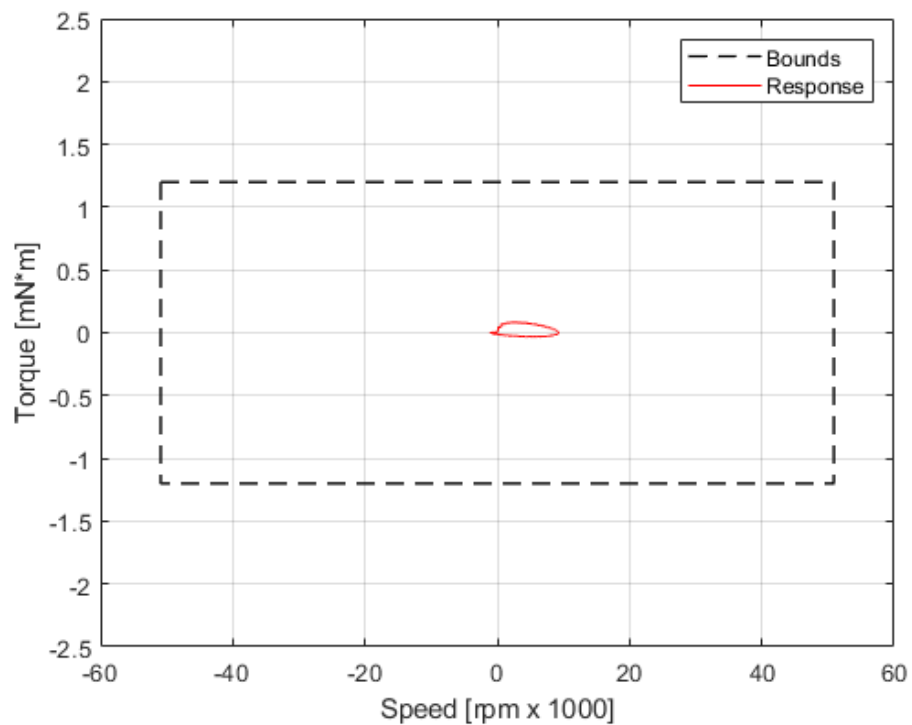


## Results, Torque Domain

```
figure(31)
plot(50.9*[-1 1 1 -1 -1],1.2*[1 1 -1 -1 1], '--k', 'LineWidth', 1)
hold on
plot(simout_rpm30.data(:,2)/1000,simout_torque30.data(:,1)*1e3, '-r', 'LineWidth', 0.5)
hold off

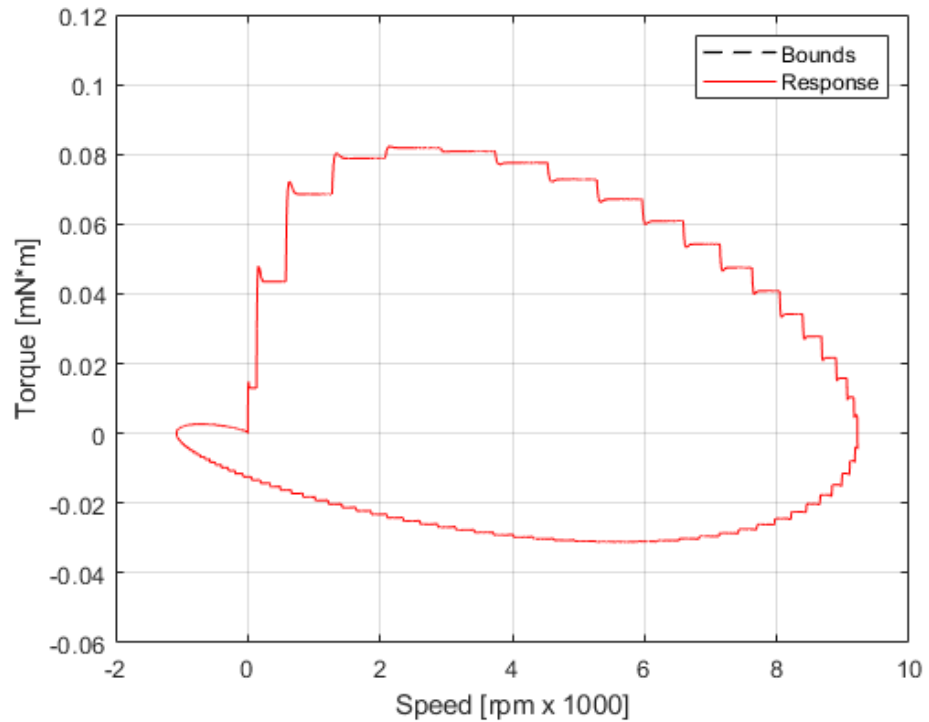
grid on
axis([-60 60 -2.5 2.5])
xlabel('Speed [rpm x 1000]')
ylabel('Torque [mN*m]')
%title('Operational Range: Results')
legend('Bounds', 'Response')

saveas(gcf, '4_Maneuver/ManeuverResult.png')
```



## Results, Torque Domain (Detail)

```
axis([-2 10 -0.06 0.12])
saveas(gcf, '4_Maneuver/ManeuverResultZoom.png')
```



*Published with MATLAB® R2019a*

## APPENDIX F

### TYPICAL MANEUVER TORQUE REQUESTS

typical\_torque\_request.csv

| Time [sec] | Torque [mN m] |
|------------|---------------|------------|---------------|------------|---------------|------------|---------------|
| 0          | 0.0000E+00    | 45         | -2.7051E-02   | 90         | 2.1768E-03    | 135        | 7.6803E-04    |
| 1          | 1.3093E-02    | 46         | -2.6188E-02   | 91         | 2.2895E-03    | 136        | 7.1900E-04    |
| 2          | 4.3855E-02    | 47         | -2.5283E-02   | 92         | 2.3864E-03    | 137        | 6.7174E-04    |
| 3          | 6.9104E-02    | 48         | -2.4343E-02   | 93         | 2.4685E-03    | 138        | 6.2628E-04    |
| 4          | 7.9437E-02    | 49         | -2.3377E-02   | 94         | 2.5366E-03    | 139        | 5.8263E-04    |
| 5          | 8.2423E-02    | 50         | -2.2391E-02   | 95         | 2.5915E-03    | 140        | 5.4076E-04    |
| 6          | 8.1446E-02    | 51         | -2.1390E-02   | 96         | 2.6340E-03    | 141        | 5.0068E-04    |
| 7          | 7.8129E-02    | 52         | -2.0381E-02   | 97         | 2.6651E-03    | 142        | 4.6235E-04    |
| 8          | 7.3343E-02    | 53         | -1.9369E-02   | 98         | 2.6855E-03    | 143        | 4.2576E-04    |
| 9          | 6.7615E-02    | 54         | -1.8358E-02   | 99         | 2.6959E-03    | 144        | 3.9089E-04    |
| 10         | 6.1301E-02    | 55         | -1.7353E-02   | 100        | 2.6971E-03    | 145        | 3.5770E-04    |
| 11         | 5.4657E-02    | 56         | -1.6358E-02   | 101        | 2.6898E-03    | 146        | 3.2616E-04    |
| 12         | 4.7875E-02    | 57         | -1.5375E-02   | 102        | 2.6746E-03    | 147        | 2.9625E-04    |
| 13         | 4.1102E-02    | 58         | -1.4409E-02   | 103        | 2.6524E-03    | 148        | 2.6792E-04    |
| 14         | 3.4448E-02    | 59         | -1.3462E-02   | 104        | 2.6235E-03    | 149        | 2.4114E-04    |
| 15         | 2.8000E-02    | 60         | -1.2535E-02   | 105        | 2.5888E-03    | 150        | 2.1585E-04    |
| 16         | 2.1820E-02    | 61         | -1.1632E-02   | 106        | 2.5487E-03    | 151        | 1.9203E-04    |
| 17         | 1.5953E-02    | 62         | -1.0754E-02   | 107        | 2.5038E-03    | 152        | 1.6962E-04    |
| 18         | 1.0432E-02    | 63         | -9.9031E-03   | 108        | 2.4546E-03    | 153        | 1.4858E-04    |
| 19         | 5.2764E-03    | 64         | -9.0797E-03   | 109        | 2.4017E-03    | 154        | 1.2887E-04    |
| 20         | 4.9805E-04    | 65         | -8.2853E-03   | 110        | 2.3454E-03    | 155        | 1.1043E-04    |
| 21         | -3.8990E-03   | 66         | -7.5207E-03   | 111        | 2.2863E-03    | 156        | 9.3200E-05    |
| 22         | -7.9164E-03   | 67         | -6.7865E-03   | 112        | 2.2247E-03    | 157        | 7.7200E-05    |
| 23         | -1.1560E-02   | 68         | -6.0832E-03   | 113        | 2.1611E-03    | 158        | 6.2300E-05    |
| 24         | -1.4840E-02   | 69         | -5.4110E-03   | 114        | 2.0958E-03    | 159        | 4.8500E-05    |
| 25         | -1.7767E-02   | 70         | -4.7700E-03   | 115        | 2.0291E-03    | 160        | 3.5700E-05    |
| 26         | -2.0356E-02   | 71         | -4.1602E-03   | 116        | 1.9614E-03    | 161        | 2.4000E-05    |
| 27         | -2.2623E-02   | 72         | -3.5816E-03   | 117        | 1.8930E-03    | 162        | 1.3100E-05    |
| 28         | -2.4584E-02   | 73         | -3.0338E-03   | 118        | 1.8242E-03    | 163        | 3.2500E-06    |
| 29         | -2.6256E-02   | 74         | -2.5164E-03   | 119        | 1.7552E-03    | 164        | -5.8400E-06   |
| 30         | -2.7657E-02   | 75         | -2.0290E-03   | 120        | 1.6862E-03    | 165        | -1.4200E-05   |
| 31         | -2.8803E-02   | 76         | -1.5710E-03   | 121        | 1.6175E-03    | 166        | -2.1800E-05   |
| 32         | -2.9713E-02   | 77         | -1.1419E-03   | 122        | 1.5493E-03    | 167        | -2.8500E-05   |
| 33         | -3.0403E-02   | 78         | -7.4093E-04   | 123        | 1.4818E-03    | 168        | -3.4500E-05   |
| 34         | -3.0890E-02   | 79         | -3.6737E-04   | 124        | 1.4150E-03    | 169        | -3.9900E-05   |
| 35         | -3.1191E-02   | 80         | -2.0400E-05   | 125        | 1.3493E-03    | 170        | -4.4600E-05   |
| 36         | -3.1320E-02   | 81         | 3.0069E-04    | 126        | 1.2846E-03    | 171        | -4.8700E-05   |
| 37         | -3.1293E-02   | 82         | 5.9691E-04    | 127        | 1.2212E-03    | 172        | -5.2400E-05   |
| 38         | -3.1125E-02   | 83         | 8.6903E-04    | 128        | 1.1590E-03    | 173        | -5.5500E-05   |
| 39         | -3.0829E-02   | 84         | 1.1180E-03    | 129        | 1.0984E-03    | 174        | -5.8200E-05   |
| 40         | -3.0417E-02   | 85         | 1.3446E-03    | 130        | 1.0392E-03    | 175        | -6.0400E-05   |
| 41         | -2.9904E-02   | 86         | 1.5500E-03    | 131        | 9.8161E-04    | 176        | -6.2200E-05   |
| 42         | -2.9300E-02   | 87         | 1.7349E-03    | 132        | 9.2566E-04    | 177        | -6.3700E-05   |
| 43         | -2.8616E-02   | 88         | 1.9004E-03    | 133        | 8.7139E-04    | 178        | -6.4800E-05   |
| 44         | -2.7863E-02   | 89         | 2.0474E-03    | 134        | 8.1884E-04    | 179        | -6.5600E-05   |

typical\_torque\_request.csv

| Time [sec] | Torque [mN m] |
|------------|---------------|------------|---------------|------------|---------------|------------|---------------|
| 180        | -6.6100E-05   | 225        | -1.2500E-05   | 270        | -4.3500E-06   | 315        | -4.8600E-06   |
| 181        | -6.6300E-05   | 226        | -1.1700E-05   | 271        | -4.2800E-06   | 316        | -4.8800E-06   |
| 182        | -6.6300E-05   | 227        | -1.1100E-05   | 272        | -4.3100E-06   | 317        | -4.6600E-06   |
| 183        | -6.6000E-05   | 228        | -1.0600E-05   | 273        | -4.4300E-06   | 318        | -4.4100E-06   |
| 184        | -6.5600E-05   | 229        | -9.9200E-06   | 274        | -4.6300E-06   | 319        | -4.2600E-06   |
| 185        | -6.4900E-05   | 230        | -9.3700E-06   | 275        | -4.8800E-06   | 320        | -4.2100E-06   |
| 186        | -6.4100E-05   | 231        | -8.9600E-06   | 276        | -4.9900E-06   | 321        | -4.2600E-06   |
| 187        | -6.3200E-05   | 232        | -8.5100E-06   | 277        | -4.8600E-06   | 322        | -4.3800E-06   |
| 188        | -6.2100E-05   | 233        | -7.9700E-06   | 278        | -4.6600E-06   | 323        | -4.5600E-06   |
| 189        | -6.0900E-05   | 234        | -7.5400E-06   | 279        | -4.5400E-06   | 324        | -4.6900E-06   |
| 190        | -5.9600E-05   | 235        | -7.2700E-06   | 280        | -4.5200E-06   | 325        | -4.5800E-06   |
| 191        | -5.8200E-05   | 236        | -7.0300E-06   | 281        | -4.6100E-06   | 326        | -4.3100E-06   |
| 192        | -5.6700E-05   | 237        | -6.6600E-06   | 282        | -4.7800E-06   | 327        | -4.0900E-06   |
| 193        | -5.5200E-05   | 238        | -6.2200E-06   | 283        | -5.0200E-06   | 328        | -3.9600E-06   |
| 194        | -5.3600E-05   | 239        | -5.9000E-06   | 284        | -5.1400E-06   | 329        | -3.9400E-06   |
| 195        | -5.2000E-05   | 240        | -5.7300E-06   | 285        | -5.0300E-06   | 330        | -4.0100E-06   |
| 196        | -5.0400E-05   | 241        | -5.6900E-06   | 286        | -4.8200E-06   | 331        | -4.1500E-06   |
| 197        | -4.8700E-05   | 242        | -5.6100E-06   | 287        | -4.6800E-06   | 332        | -4.3300E-06   |
| 198        | -4.7100E-05   | 243        | -5.3400E-06   | 288        | -4.6600E-06   | 333        | -4.4600E-06   |
| 199        | -4.5400E-05   | 244        | -4.9900E-06   | 289        | -4.7300E-06   | 334        | -4.3400E-06   |
| 200        | -4.3700E-05   | 245        | -4.7300E-06   | 290        | -4.9000E-06   | 335        | -4.0600E-06   |
| 201        | -4.2000E-05   | 246        | -4.6000E-06   | 291        | -5.1200E-06   | 336        | -3.8200E-06   |
| 202        | -4.0400E-05   | 247        | -4.5900E-06   | 292        | -5.2000E-06   | 337        | -3.6800E-06   |
| 203        | -3.8700E-05   | 248        | -4.6700E-06   | 293        | -5.0400E-06   | 338        | -3.6400E-06   |
| 204        | -3.7100E-05   | 249        | -4.8000E-06   | 294        | -4.8300E-06   | 339        | -3.6900E-06   |
| 205        | -3.5500E-05   | 250        | -4.7600E-06   | 295        | -4.7000E-06   | 340        | -3.8000E-06   |
| 206        | -3.4000E-05   | 251        | -4.5000E-06   | 296        | -4.6800E-06   | 341        | -3.9700E-06   |
| 207        | -3.2500E-05   | 252        | -4.2400E-06   | 297        | -4.7600E-06   | 342        | -4.1600E-06   |
| 208        | -3.1000E-05   | 253        | -4.0800E-06   | 298        | -4.9200E-06   | 343        | -4.2000E-06   |
| 209        | -2.9500E-05   | 254        | -4.0300E-06   | 299        | -5.1300E-06   | 344        | -3.9800E-06   |
| 210        | -2.8100E-05   | 255        | -4.0800E-06   | 300        | -5.1500E-06   | 345        | -3.6900E-06   |
| 211        | -2.6700E-05   | 256        | -4.2100E-06   | 301        | -4.9500E-06   | 346        | -3.4700E-06   |
| 212        | -2.5400E-05   | 257        | -4.4100E-06   | 302        | -4.7400E-06   | 347        | -3.3500E-06   |
| 213        | -2.4100E-05   | 258        | -4.6000E-06   | 303        | -4.6100E-06   | 348        | -3.3300E-06   |
| 214        | -2.2900E-05   | 259        | -4.5700E-06   | 304        | -4.6000E-06   | 349        | -3.3800E-06   |
| 215        | -2.1700E-05   | 260        | -4.3500E-06   | 305        | -4.6900E-06   | 350        | -3.4900E-06   |
| 216        | -2.0600E-05   | 261        | -4.1400E-06   | 306        | -4.8500E-06   | 351        | -3.6500E-06   |
| 217        | -1.9500E-05   | 262        | -4.0300E-06   | 307        | -5.0400E-06   | 352        | -3.8400E-06   |
| 218        | -1.8500E-05   | 263        | -4.0400E-06   | 308        | -5.0300E-06   | 353        | -3.9700E-06   |
| 219        | -1.7500E-05   | 264        | -4.1400E-06   | 309        | -4.8100E-06   | 354        | -3.8500E-06   |
| 220        | -1.6500E-05   | 265        | -4.3100E-06   | 310        | -4.5800E-06   | 355        | -3.5400E-06   |
| 221        | -1.5600E-05   | 266        | -4.5400E-06   | 311        | -4.4600E-06   | 356        | -3.2700E-06   |
| 222        | -1.4800E-05   | 267        | -4.7500E-06   | 312        | -4.4400E-06   | 357        | -3.0900E-06   |
| 223        | -1.3900E-05   | 268        | -4.7300E-06   | 313        | -4.5200E-06   | 358        | -3.0100E-06   |
| 224        | -1.3200E-05   | 269        | -4.5300E-06   | 314        | -4.6700E-06   | 359        | -3.0100E-06   |

typical\_torque\_request.csv

| Time [sec] | Torque [mN m] |
|------------|---------------|------------|---------------|------------|---------------|------------|---------------|
| 360        | -3.0800E-06   | 405        | -3.0300E-06   | 450        | -1.0600E-06   | 495        | -1.6100E-06   |
| 361        | -3.2000E-06   | 406        | -3.0500E-06   | 451        | -1.0700E-06   | 496        | -1.2100E-06   |
| 362        | -3.3600E-06   | 407        | -2.8000E-06   | 452        | -1.1100E-06   | 497        | -8.9900E-07   |
| 363        | -3.5400E-06   | 408        | -2.4400E-06   | 453        | -1.1700E-06   | 498        | -6.7800E-07   |
| 364        | -3.7100E-06   | 409        | -2.1200E-06   | 454        | -1.2500E-06   | 499        | -5.3300E-07   |
| 365        | -3.6700E-06   | 410        | -1.9000E-06   | 455        | -1.3300E-06   | 500        | -4.4600E-07   |
| 366        | -3.3800E-06   | 411        | -1.7700E-06   | 456        | -1.4300E-06   | 501        | -4.0200E-07   |
| 367        | -3.0700E-06   | 412        | -1.7200E-06   | 457        | -1.5300E-06   | 502        | -3.8800E-07   |
| 368        | -2.8500E-06   | 413        | -1.7200E-06   | 458        | -1.6400E-06   | 503        | -3.9600E-07   |
| 369        | -2.7200E-06   | 414        | -1.7700E-06   | 459        | -1.7500E-06   | 504        | -4.2000E-07   |
| 370        | -2.6800E-06   | 415        | -1.8500E-06   | 460        | -1.8700E-06   | 505        | -4.5500E-07   |
| 371        | -2.7100E-06   | 416        | -1.9500E-06   | 461        | -1.9900E-06   | 506        | -4.9900E-07   |
| 372        | -2.7900E-06   | 417        | -2.0600E-06   | 462        | -2.1200E-06   | 507        | -5.4900E-07   |
| 373        | -2.9100E-06   | 418        | -2.2000E-06   | 463        | -2.2500E-06   | 508        | -6.0500E-07   |
| 374        | -3.0600E-06   | 419        | -2.3400E-06   | 464        | -2.3800E-06   | 509        | -6.6400E-07   |
| 375        | -3.2400E-06   | 420        | -2.4900E-06   | 465        | -2.5000E-06   | 510        | -7.2800E-07   |
| 376        | -3.4300E-06   | 421        | -2.6400E-06   | 466        | -2.3900E-06   | 511        | -7.9400E-07   |
| 377        | -3.4900E-06   | 422        | -2.8100E-06   | 467        | -2.0200E-06   | 512        | -8.6400E-07   |
| 378        | -3.2800E-06   | 423        | -2.8600E-06   | 468        | -1.6100E-06   | 513        | -9.3700E-07   |
| 379        | -2.9500E-06   | 424        | -2.6400E-06   | 469        | -1.2700E-06   | 514        | -1.0100E-06   |
| 380        | -2.6600E-06   | 425        | -2.2600E-06   | 470        | -1.0300E-06   | 515        | -1.0900E-06   |
| 381        | -2.4700E-06   | 426        | -1.9100E-06   | 471        | -8.6700E-07   | 516        | -1.1700E-06   |
| 382        | -2.3800E-06   | 427        | -1.6600E-06   | 472        | -7.7400E-07   | 517        | -1.2500E-06   |
| 383        | -2.3600E-06   | 428        | -1.5000E-06   | 473        | -7.3200E-07   | 518        | -1.3400E-06   |
| 384        | -2.4000E-06   | 429        | -1.4100E-06   | 474        | -7.2600E-07   | 519        | -1.4300E-06   |
| 385        | -2.4900E-06   | 430        | -1.3900E-06   | 475        | -7.4600E-07   | 520        | -1.5200E-06   |
| 386        | -2.6100E-06   | 431        | -1.4100E-06   | 476        | -7.8500E-07   | 521        | -1.6100E-06   |
| 387        | -2.7500E-06   | 432        | -1.4600E-06   | 477        | -8.3800E-07   | 522        | -1.7000E-06   |
| 388        | -2.9100E-06   | 433        | -1.5400E-06   | 478        | -9.0100E-07   | 523        | -1.8000E-06   |
| 389        | -3.0900E-06   | 434        | -1.6300E-06   | 479        | -9.7300E-07   | 524        | -1.9000E-06   |
| 390        | -3.2600E-06   | 435        | -1.7300E-06   | 480        | -1.0500E-06   | 525        | -2.0000E-06   |
| 391        | -3.2300E-06   | 436        | -1.8500E-06   | 481        | -1.1300E-06   | 526        | -2.1100E-06   |
| 392        | -2.9400E-06   | 437        | -1.9700E-06   | 482        | -1.2200E-06   | 527        | -2.1800E-06   |
| 393        | -2.5900E-06   | 438        | -2.1000E-06   | 483        | -1.3100E-06   | 528        | -2.0000E-06   |
| 394        | -2.3200E-06   | 439        | -2.2400E-06   | 484        | -1.4100E-06   | 529        | -1.5900E-06   |
| 395        | -2.1400E-06   | 440        | -2.3800E-06   | 485        | -1.5100E-06   | 530        | -1.1400E-06   |
| 396        | -2.0500E-06   | 441        | -2.5300E-06   | 486        | -1.6100E-06   | 531        | -7.8000E-07   |
| 397        | -2.0400E-06   | 442        | -2.6700E-06   | 487        | -1.7200E-06   | 532        | -5.0900E-07   |
| 398        | -2.0700E-06   | 443        | -2.6100E-06   | 488        | -1.8200E-06   | 533        | -3.1900E-07   |
| 399        | -2.1500E-06   | 444        | -2.2800E-06   | 489        | -1.9400E-06   | 534        | -1.9200E-07   |
| 400        | -2.2500E-06   | 445        | -1.8900E-06   | 490        | -2.0500E-06   | 535        | -1.1300E-07   |
| 401        | -2.3800E-06   | 446        | -1.5500E-06   | 491        | -2.1700E-06   | 536        | -6.7900E-08   |
| 402        | -2.5300E-06   | 447        | -1.3200E-06   | 492        | -2.2900E-06   | 537        | -4.6800E-08   |
| 403        | -2.6800E-06   | 448        | -1.1700E-06   | 493        | -2.3000E-06   | 538        | -4.2800E-08   |
| 404        | -2.8500E-06   | 449        | -1.0900E-06   | 494        | -2.0400E-06   | 539        | -5.1000E-08   |

typical\_torque\_request.csv

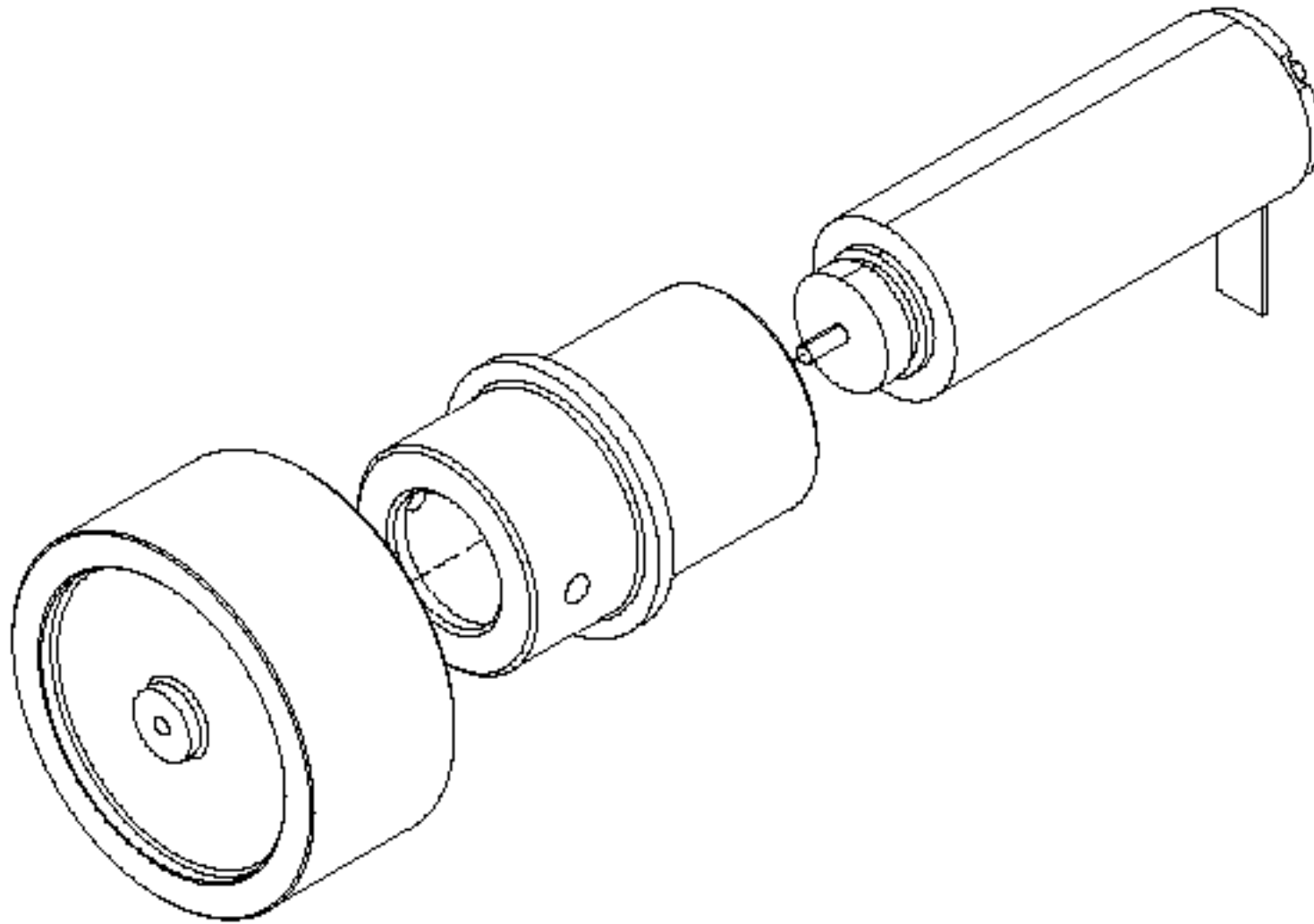
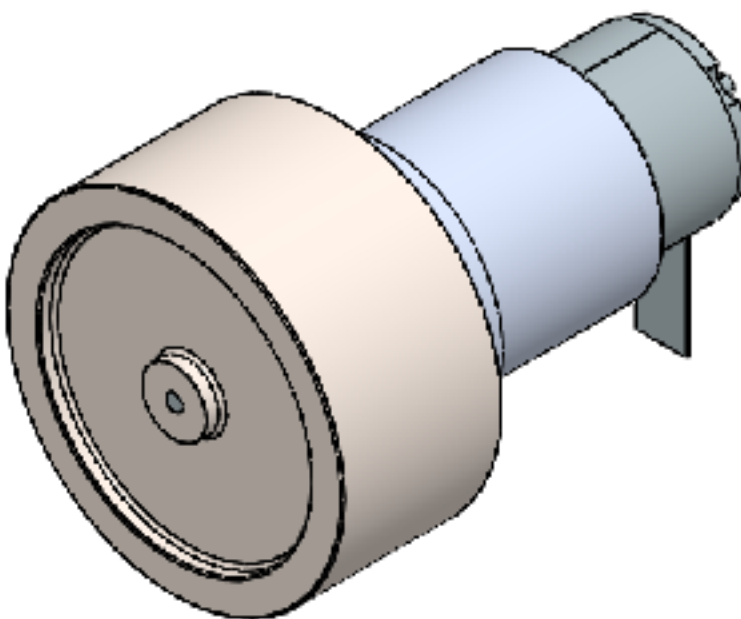
| Time [sec] | Torque [mN m] |
|------------|---------------|------------|---------------|------------|---------------|------------|---------------|
| 540        | -6.8200E-08   | 585        | 2.7800E-07    | 630        | -1.2500E-06   | 675        | -6.7000E-07   |
| 541        | -9.1900E-08   | 586        | 2.8500E-07    | 631        | -1.3200E-06   | 676        | -4.1600E-07   |
| 542        | -1.2100E-07   | 587        | 2.8500E-07    | 632        | -1.3800E-06   | 677        | -2.2800E-07   |
| 543        | -1.5400E-07   | 588        | 2.8100E-07    | 633        | -1.4500E-06   | 678        | -9.4800E-08   |
| 544        | -1.9000E-07   | 589        | 2.7400E-07    | 634        | -1.5100E-06   | 679        | -2.9800E-09   |
| 545        | -2.2800E-07   | 590        | 2.6400E-07    | 635        | -1.5800E-06   | 680        | 5.8800E-08    |
| 546        | -2.7000E-07   | 591        | 2.5100E-07    | 636        | -1.6500E-06   | 681        | 9.9200E-08    |
| 547        | -3.1300E-07   | 592        | 2.3700E-07    | 637        | -1.7200E-06   | 682        | 1.2500E-07    |
| 548        | -3.5900E-07   | 593        | 2.2100E-07    | 638        | -1.7900E-06   | 683        | 1.4000E-07    |
| 549        | -4.0700E-07   | 594        | 2.0400E-07    | 639        | -1.8600E-06   | 684        | 1.4800E-07    |
| 550        | -4.5600E-07   | 595        | 1.8500E-07    | 640        | -1.9400E-06   | 685        | 1.5100E-07    |
| 551        | -5.0800E-07   | 596        | 1.6400E-07    | 641        | -2.0100E-06   | 686        | 1.5000E-07    |
| 552        | -5.6100E-07   | 597        | 1.4300E-07    | 642        | -2.0900E-06   | 687        | 1.4600E-07    |
| 553        | -6.1600E-07   | 598        | 1.2000E-07    | 643        | -2.0400E-06   | 688        | 1.4100E-07    |
| 554        | -6.7400E-07   | 599        | 9.5900E-08    | 644        | -1.7000E-06   | 689        | 1.3400E-07    |
| 555        | -7.3300E-07   | 600        | 7.0500E-08    | 645        | -1.2200E-06   | 690        | 1.2500E-07    |
| 556        | -7.9300E-07   | 601        | 4.4000E-08    | 646        | -7.7200E-07   | 691        | 1.1600E-07    |
| 557        | -8.5600E-07   | 602        | 1.6200E-08    | 647        | -4.1400E-07   | 692        | 1.0600E-07    |
| 558        | -9.2000E-07   | 603        | -1.2800E-08   | 648        | -1.4500E-07   | 693        | 9.4900E-08    |
| 559        | -9.8700E-07   | 604        | -4.3100E-08   | 649        | 5.2700E-08    | 694        | 8.3300E-08    |
| 560        | -1.0500E-06   | 605        | -7.4500E-08   | 650        | 1.9500E-07    | 695        | 7.0900E-08    |
| 561        | -1.1200E-06   | 606        | -1.0700E-07   | 651        | 2.9800E-07    | 696        | 5.7800E-08    |
| 562        | -1.2000E-06   | 607        | -1.4100E-07   | 652        | 3.7300E-07    | 697        | 4.4200E-08    |
| 563        | -1.2700E-06   | 608        | -1.7600E-07   | 653        | 4.2900E-07    | 698        | 2.9900E-08    |
| 564        | -1.3500E-06   | 609        | -2.1200E-07   | 654        | 4.7100E-07    | 699        | 1.4900E-08    |
| 565        | -1.4200E-06   | 610        | -2.5000E-07   | 655        | 5.0400E-07    | 700        | -6.2300E-10   |
| 566        | -1.5000E-06   | 611        | -2.8900E-07   | 656        | 5.3000E-07    | 701        | -1.6800E-08   |
| 567        | -1.5800E-06   | 612        | -3.2900E-07   | 657        | 5.5200E-07    |            |               |
| 568        | -1.6600E-06   | 613        | -3.7000E-07   | 658        | 5.7000E-07    |            |               |
| 569        | -1.7500E-06   | 614        | -4.1200E-07   | 659        | 5.8600E-07    |            |               |
| 570        | -1.8400E-06   | 615        | -4.5600E-07   | 660        | 6.0000E-07    |            |               |
| 571        | -1.9200E-06   | 616        | -5.0000E-07   | 661        | 6.1300E-07    |            |               |
| 572        | -2.0100E-06   | 617        | -5.4600E-07   | 662        | 6.2400E-07    |            |               |
| 573        | -2.0800E-06   | 618        | -5.9300E-07   | 663        | 6.3500E-07    |            |               |
| 574        | -1.9300E-06   | 619        | -6.4200E-07   | 664        | 6.4400E-07    |            |               |
| 575        | -1.5100E-06   | 620        | -6.9100E-07   | 665        | 6.5300E-07    |            |               |
| 576        | -1.0500E-06   | 621        | -7.4200E-07   | 666        | 6.6000E-07    |            |               |
| 577        | -6.5500E-07   | 622        | -7.9400E-07   | 667        | 4.9800E-07    |            |               |
| 578        | -3.5400E-07   | 623        | -8.4800E-07   | 668        | 5.4700E-08    |            |               |
| 579        | -1.3600E-07   | 624        | -9.0200E-07   | 669        | -5.0400E-07   |            |               |
| 580        | 1.6100E-08    | 625        | -9.5800E-07   | 670        | -1.0100E-06   |            |               |
| 581        | 1.2000E-07    | 626        | -1.0100E-06   | 671        | -1.4300E-06   |            |               |
| 582        | 1.9000E-07    | 627        | -1.0700E-06   | 672        | -1.5500E-06   |            |               |
| 583        | 2.3500E-07    | 628        | -1.1300E-06   | 673        | -1.3300E-06   |            |               |
| 584        | 2.6200E-07    | 629        | -1.1900E-06   | 674        | -9.9000E-07   |            |               |

## APPENDIX G

### MECHANICAL DRAWINGS

## ASSEMBLY PROCEDURE

[This section has been removed in compliance with the United States International Traffic in Arms Regulations]

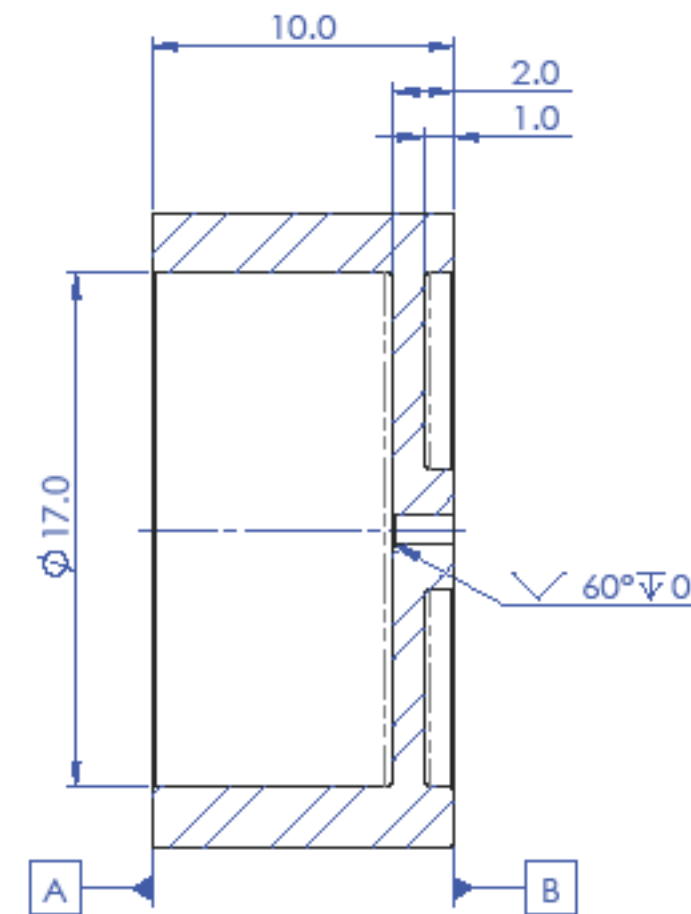


| ITEM NO. | PART NUMBER | DESCRIPTION        | QTY. |
|----------|-------------|--------------------|------|
| 1        | 315170      | MOTOR, MAXON EC10  | 1    |
| 2        | NJB-8812    | MOTOR HOUSING      | 1    |
| 3        | NJB-8811    | FLYWHEEL           | 1    |
| 4        | LOCTITE 1C  | EPOXY ADHESIVE     | 1    |
| 5        | LOCTITE 648 | PRESS FIT ADHESIVE | 1    |
| 6        | 8912K42     | EMI SHIELDING TAPE | 1    |

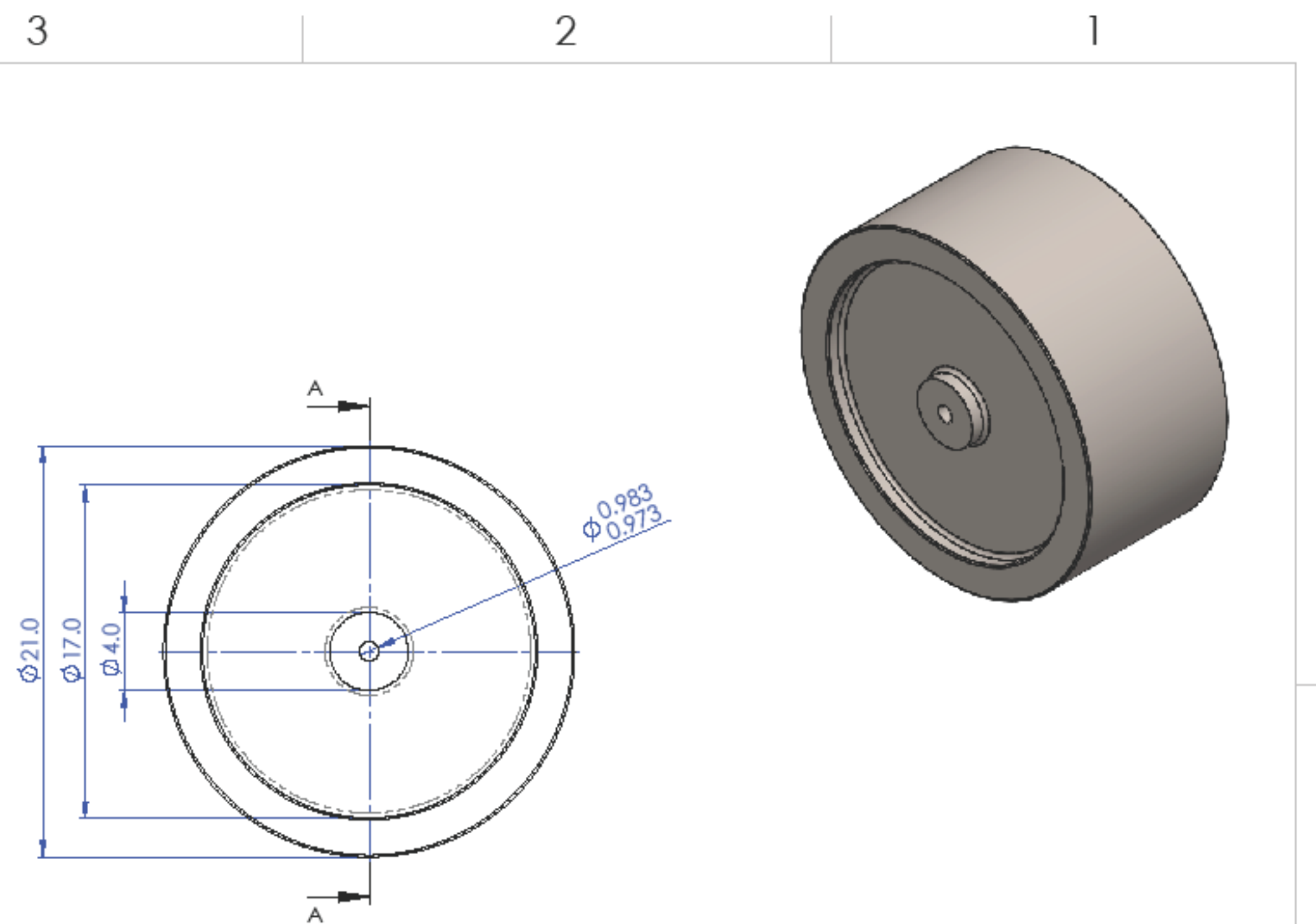
|  |  |                               |         |             |                      |                      |
|--|--|-------------------------------|---------|-------------|----------------------|----------------------|
|  |  | UNLESS OTHERWISE SPECIFIED:   |         | NAME        | DATE                 | CAL POLY CUBESAT LAB |
|  |  | DIMENSIONS ARE IN MILLIMETERS |         | DRAWN       | NJB 5/12/20          |                      |
|  |  | TOLERANCES:                   |         | CHECKED     |                      |                      |
|  |  | ONE PLACE DECIMAL $\pm 0.1$   |         | ENG APPR.   |                      |                      |
|  |  | TWO PLACE DECIMAL $\pm 0.05$  |         | MFG APPR.   |                      |                      |
|  |  | INTERPRET GEOMETRIC           |         | Q.A.        |                      |                      |
|  |  | TOLERANCING PER: ISO 1101     |         | COMMENTS:   |                      |                      |
|  |  | MATERIAL                      |         |             |                      |                      |
|  |  | N/A                           |         |             |                      |                      |
|  |  | NEXT ASSY                     | USED ON | FINISH      | N/A                  |                      |
|  |  |                               |         | APPLICATION | DO NOT SCALE DRAWING |                      |
|  |  |                               |         |             |                      | SCALE: 3:1           |
|  |  |                               |         |             |                      | WEIGHT:              |
|  |  |                               |         |             |                      | SHEET 1 OF 1         |

PROPRIETARY AND CONFIDENTIAL  
THE INFORMATION CONTAINED IN THIS  
DRAWING IS THE SOLE PROPERTY OF  
CAL POLY CUBESAT LABORATORY. ANY  
REPRODUCTION IN PART OR AS A WHOLE  
WITHOUT THE WRITTEN PERMISSION OF  
CAL POLY CUBESAT LABORATORY IS  
PROHIBITED.

B



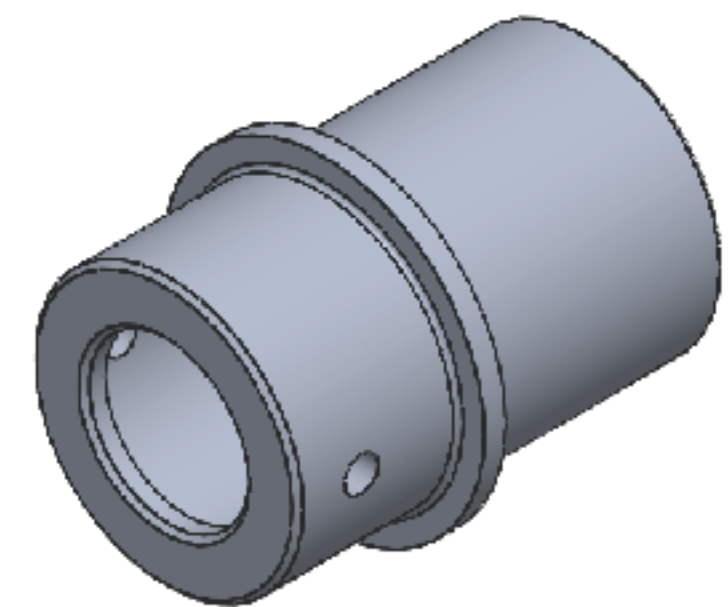
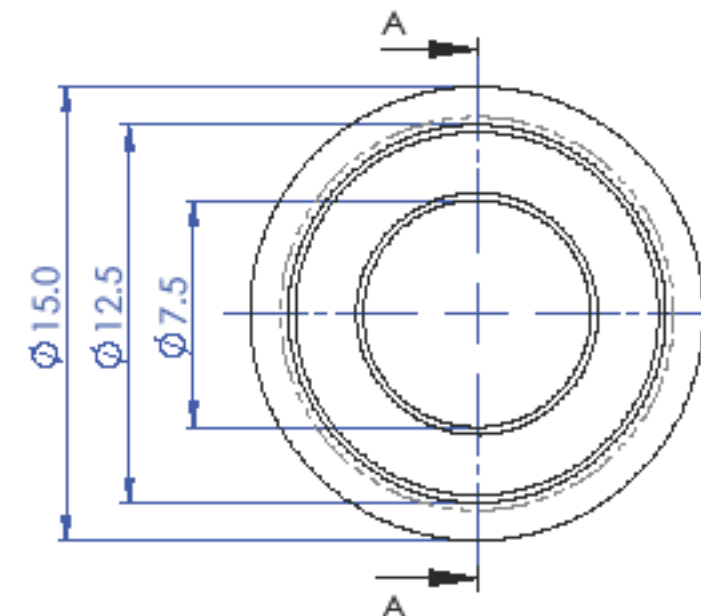
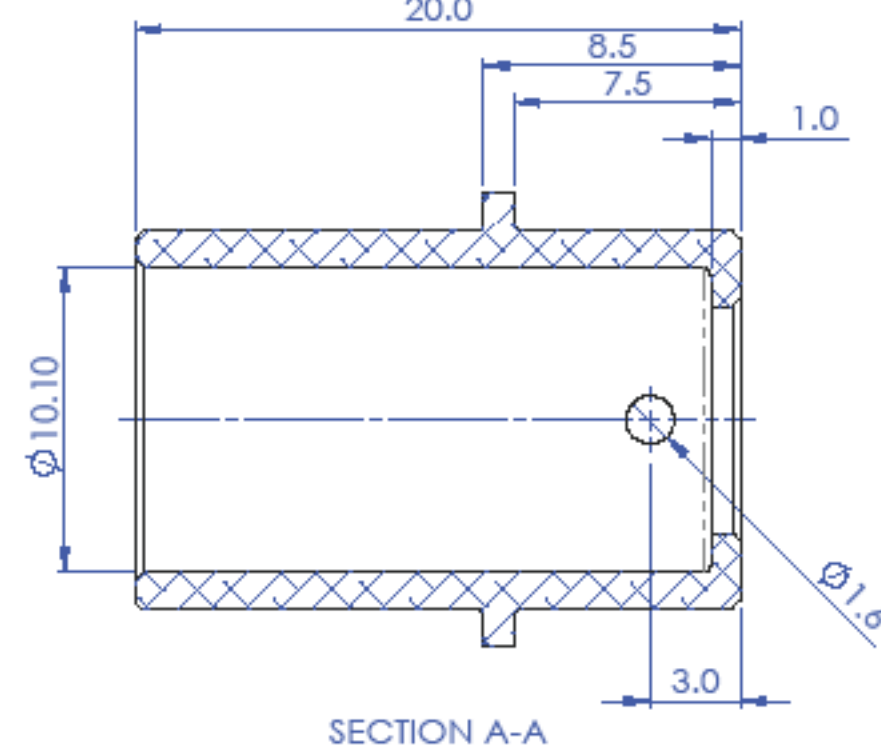
SECTION A-A



- NOTES:
1. BREAK ALL SHARP EDGES
  2. INTERNAL RADIUS: 0.1 MIN
  3. FOR BALANCING, REMOVE MATERIAL FROM BALANCE PLANE A AND BALANCE PLANE B
  4. AXIAL ROTATIONAL INERTIA:  $9.37 \text{ g} \cdot \text{cm}^2$
  5. OF-AXIS ROTATIONAL INERTIA:  $5.35 \text{ g} \cdot \text{cm}^2$

PROPRIETARY AND CONFIDENTIAL  
THE INFORMATION CONTAINED IN THIS  
DRAWING IS THE SOLE PROPERTY OF  
CAL POLY CUBESAT LABORATORY. ANY  
REPRODUCTION IN PART OR AS A WHOLE  
WITHOUT THE WRITTEN PERMISSION OF  
CAL POLY CUBESAT LABORATORY IS  
PROHIBITED.

|            |  |  |              |                      |                      |   |
|------------|--|--|--------------|----------------------|----------------------|---|
|            |  | UNLESS OTHERWISE SPECIFIED:<br>DIMENSIONS ARE IN MILLIMETERS               | NAME<br>NJB  | DATE<br>5/12/20      | CAL POLY CUBESAT LAB |   |
|            |  | TOLERANCES:<br>ONE PLACE DECIMAL $\pm 0.1$<br>TWO PLACE DECIMAL $\pm 0.05$ |              |                      |                      |   |
|            |  | INTERPRET GEOMETRIC<br>TOLERANCING PER: ISO 1101                           |              |                      |                      |   |
|            |  | MATERIAL<br>316 STAINLESS STEEL  |              |                      |                      |   |
|            |  | NEXT ASSY  | USED ON      | FINISH<br>NONE       |                      |   |
|            |  | APPLICATION  |              | DO NOT SCALE DRAWING |                      |   |
| SIZE       |  | DWG. NO.   | B NJB-8811   |                      | REV                  | A |
| SCALE: 4:1 |  | WEIGHT: 11.5 g   | SHEET 1 OF 1 |                      |                      |   |



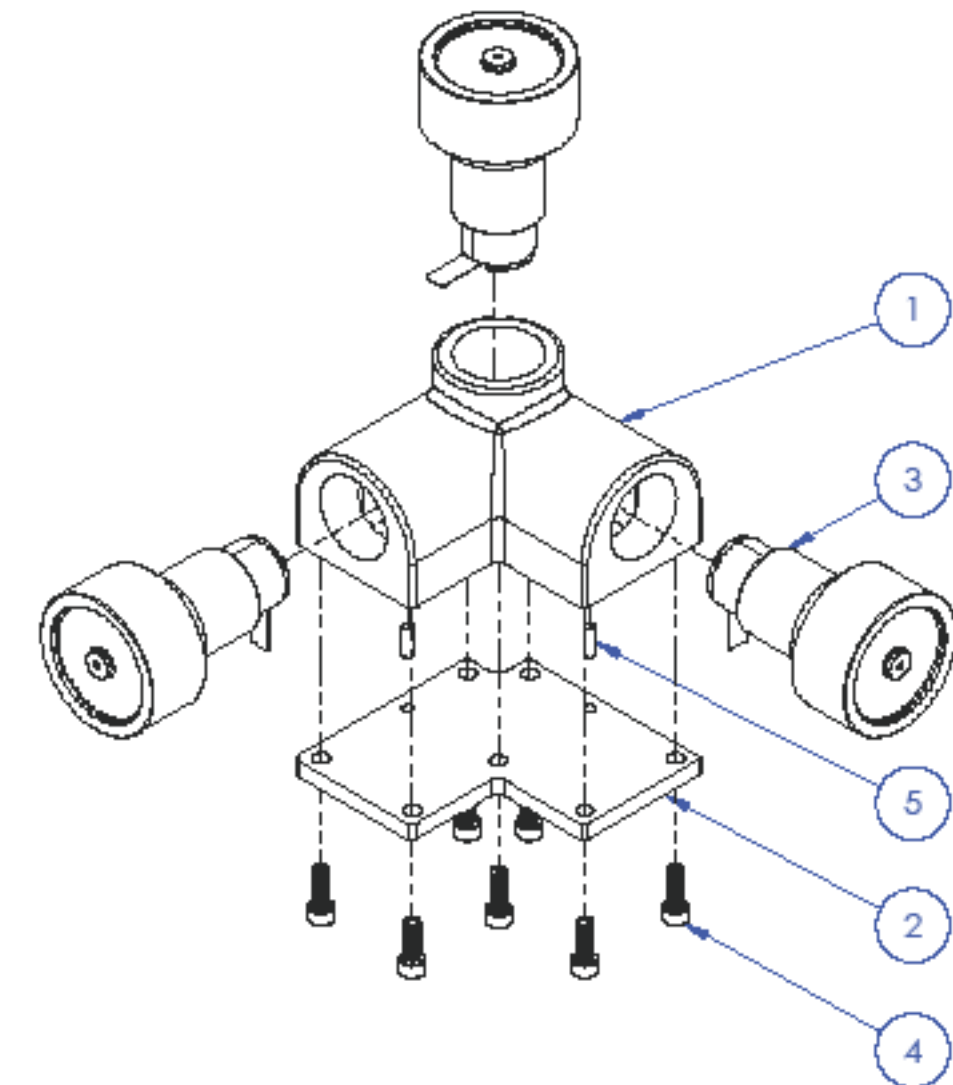
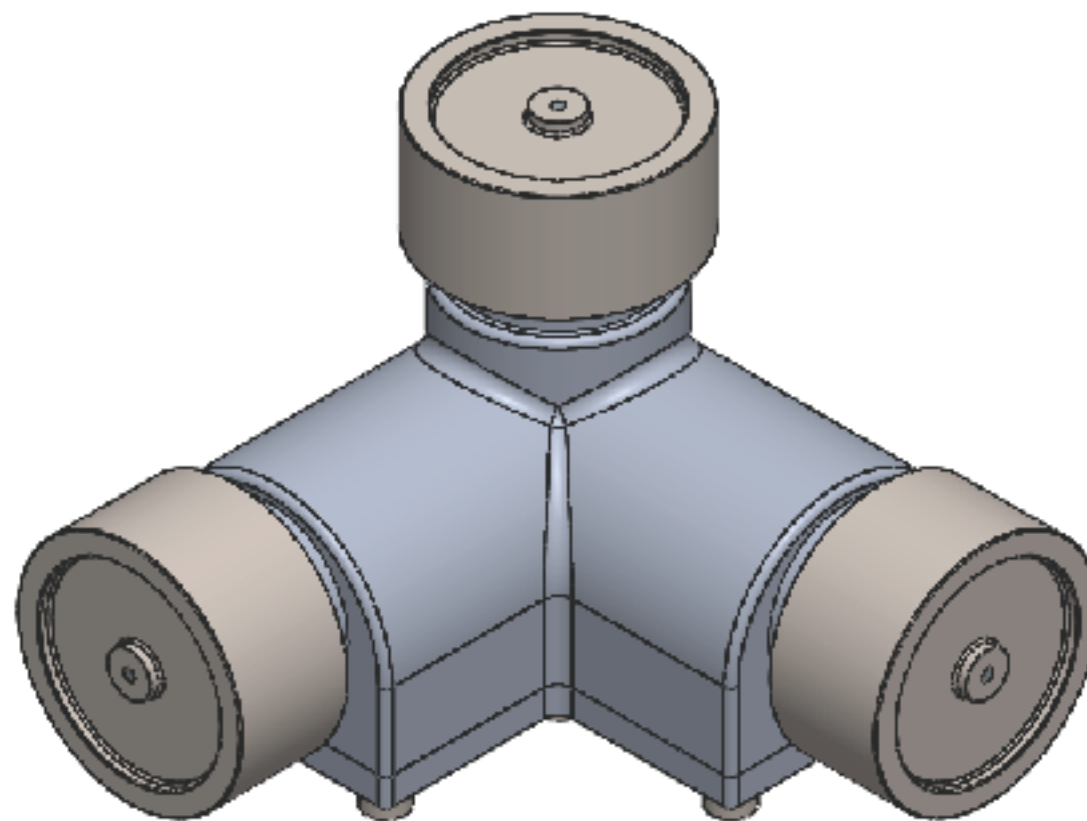
NOTES:  
 1. BREAK ALL SHARP EDGES  
 2. INTERNAL RADII: 0.25 MAX

PROPRIETARY AND CONFIDENTIAL  
 THE INFORMATION CONTAINED IN THIS  
 DRAWING IS THE SOLE PROPERTY OF  
 CAL POLY CUBESAT LABORATORY. ANY  
 REPRODUCTION IN PART OR AS A WHOLE  
 WITHOUT THE WRITTEN PERMISSION OF  
 CAL POLY CUBESAT LABORATORY IS  
 PROHIBITED.

|   |                             |  |                          |                 |
|---|-----------------------------|--|--------------------------|-----------------|
|   |                             | UNLESS OTHERWISE SPECIFIED:<br>DIMENSIONS ARE IN MILLIMETERS               | NAME<br>DRAWN<br>CHECKED | DATE<br>5/12/20 |
|   |                             | TOLERANCES:<br>ONE PLACE DECIMAL $\pm 0.1$<br>TWO PLACE DECIMAL $\pm 0.05$ |                          |                 |
|   |                             | INTERPRET GEOMETRIC<br>TOLERANCING PER: ISO 1101                           |                          |                 |
|   |                             | MATERIAL<br>HyMu 80  |                          |                 |
|   |                             | NEXT ASSY<br>USED ON<br>FINISH<br>NONE                                     |                          |                 |
|   |                             | APPLICATION<br>DO NOT SCALE DRAWING  |                          |                 |
| <b>CAL POLY CUBESAT LAB</b>                         |                             |  |                          |                 |
| TITLE:<br><b>REACTION WHEEL -<br/>MOTOR HOUSING</b> |                             |  |                          |                 |
| SIZE<br><b>B</b>                                    | DWG. NO.<br><b>NJB-8812</b> | REV<br><b>A</b>  |                          |                 |
| SCALE: 4:1  | WEIGHT: 7.9 g               | SHEET 1 OF 1   |                          |                 |

## ASSEMBLY PROCEDURE

[This section has been removed in compliance with the United States International Traffic in Arms Regulations]



| ITEM NO. | PART NUMBER | DESCRIPTION                   |   |
|----------|-------------|-------------------------------|---|
| 1        | NJB-8801    | 3-AXIS ASSY, HOUSING          | 1 |
| 2        | NJB-8802    | 3-AXIS ASSY, PLATE            | 1 |
| 3        | NJB-8810    | REACTION WHEEL ASSY           | 3 |
| 4        | 92185A077   | 2-56 SCREW, 316 STAINLESS     | 7 |
| 5        | 90145A414   | 1/16 IN DOWEL, 18-8 STAINLESS | 2 |

|  |  |  |             |                      |                      |              |
|--|--|--|-------------|----------------------|----------------------|--------------|
|  |  | UNLESS OTHERWISE SPECIFIED:                      | NAME        | DATE                 | CAL POLY CUBESAT LAB |              |
|  |  | DIMENSIONS ARE IN MILLIMETERS                    |             |                      | DRAWN                | NJB 5/12/20  |
|  |  | TOLERANCES:                                      | CHECKED     |                      |                      |              |
|  |  | ONE PLACE DECIMAL $\pm 0.1$                      |             |                      | BNG APPR.            |              |
|  |  | TWO PLACE DECIMAL $\pm 0.05$                     |             |                      | MFG APPR.            |              |
|  |  | INTERPRET GEOMETRIC<br>TOLERANCING PER: ISO 1101 | QA.         |                      |                      |              |
|  |  | MATERIAL   | COMMENTS:   |                      |                      |              |
|  |  | N/A  |             |                      |                      |              |
|  |  | NEXT ASSY  | USED ON     | FINISH               |                      |              |
|  |  |  |             | N/A                  |                      |              |
|  |  |  | APPLICATION | DO NOT SCALE DRAWING |                      |              |
|  |  |  |             |                      | SCALE: 1:1           | WEIGHT:      |
|  |  |  |             |                      |                      | SHEET 1 OF 1 |

PROPRIETARY AND CONFIDENTIAL  
THE INFORMATION CONTAINED IN THIS  
DRAWING IS THE SOLE PROPERTY OF  
CAL POLY CUBESAT LABORATORY. ANY  
REPRODUCTION IN PART OR AS A WHOLE  
WITHOUT THE WRITTEN PERMISSION OF  
CAL POLY CUBESAT LABORATORY IS  
PROHIBITED.

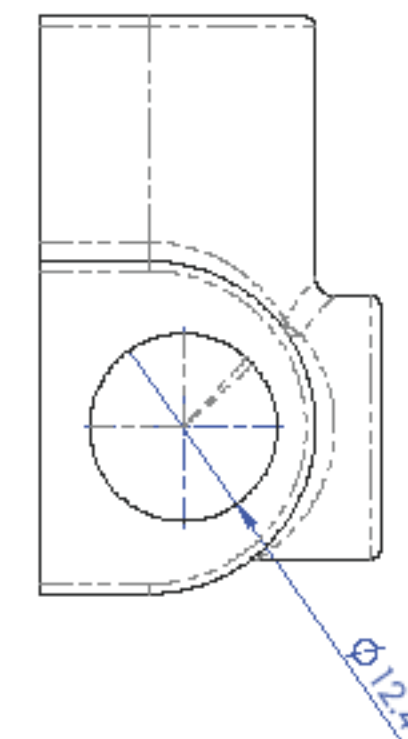
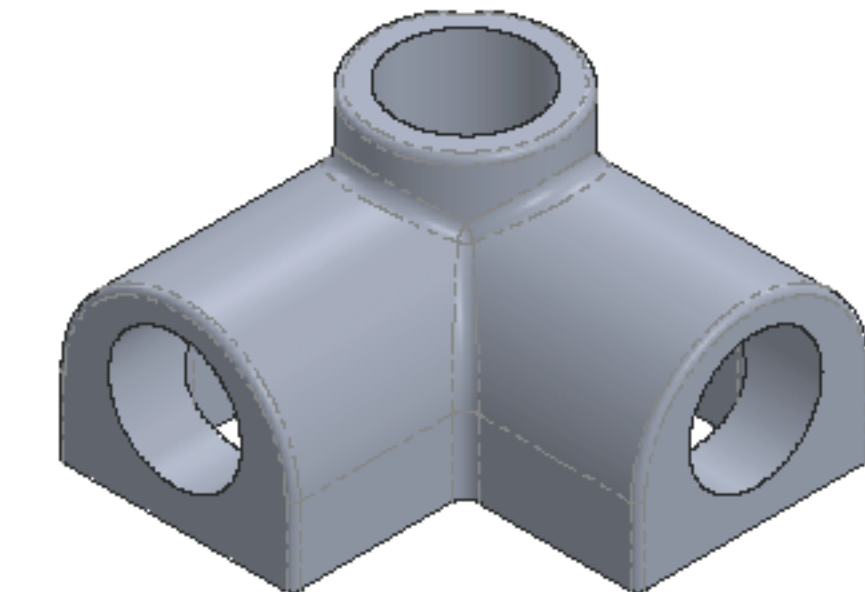
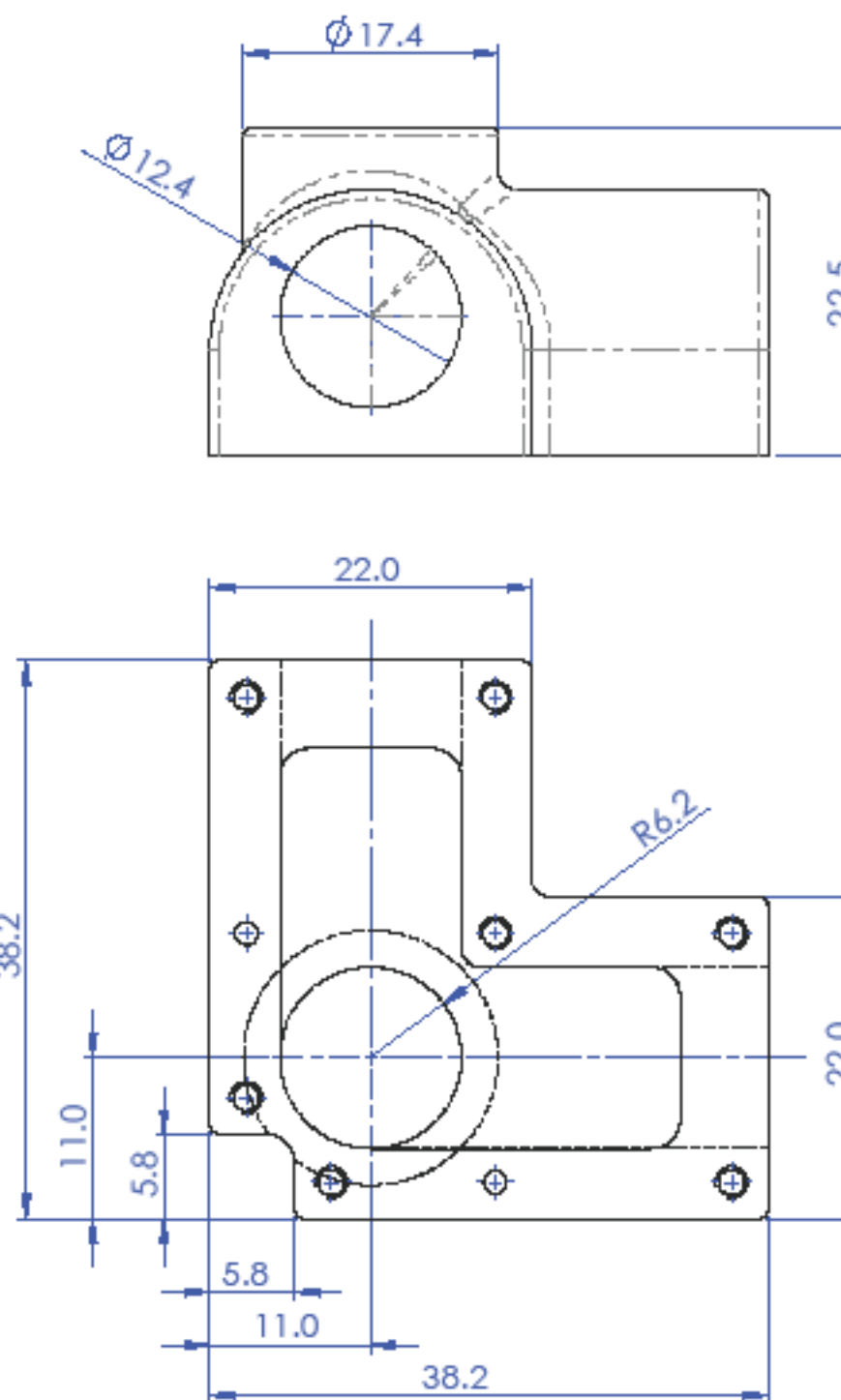
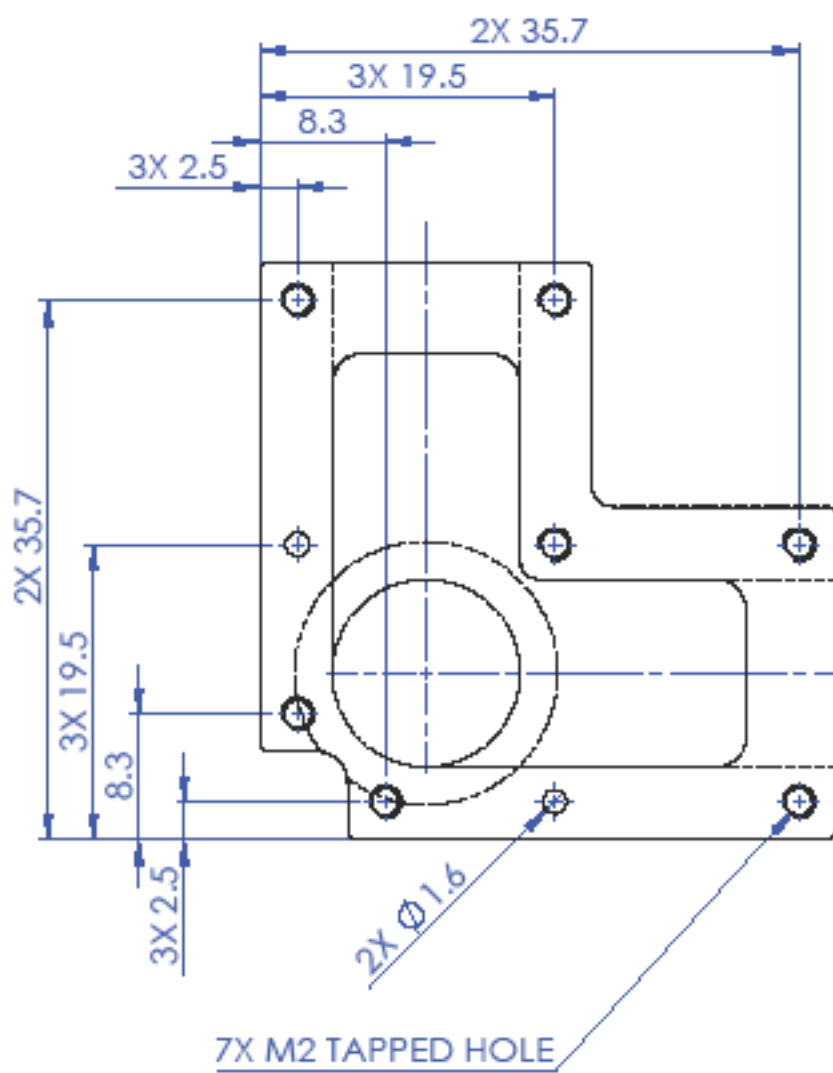
4

3

2

1

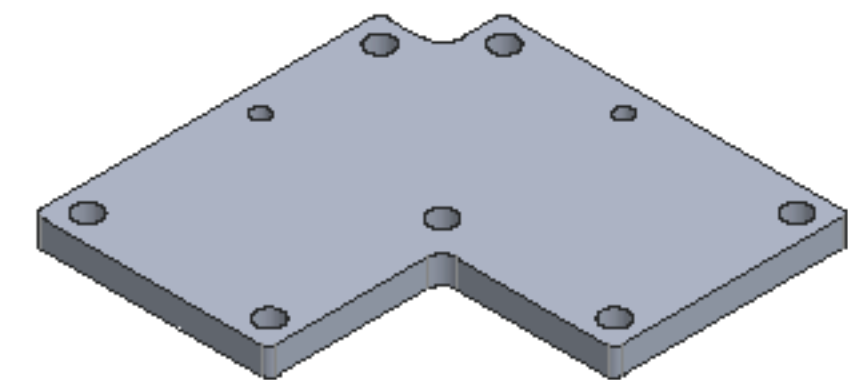
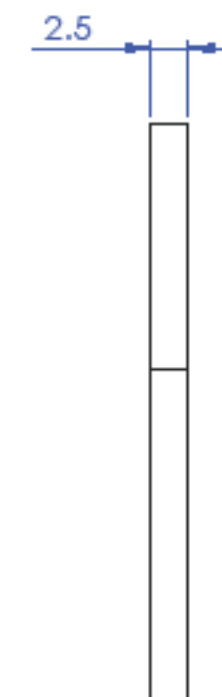
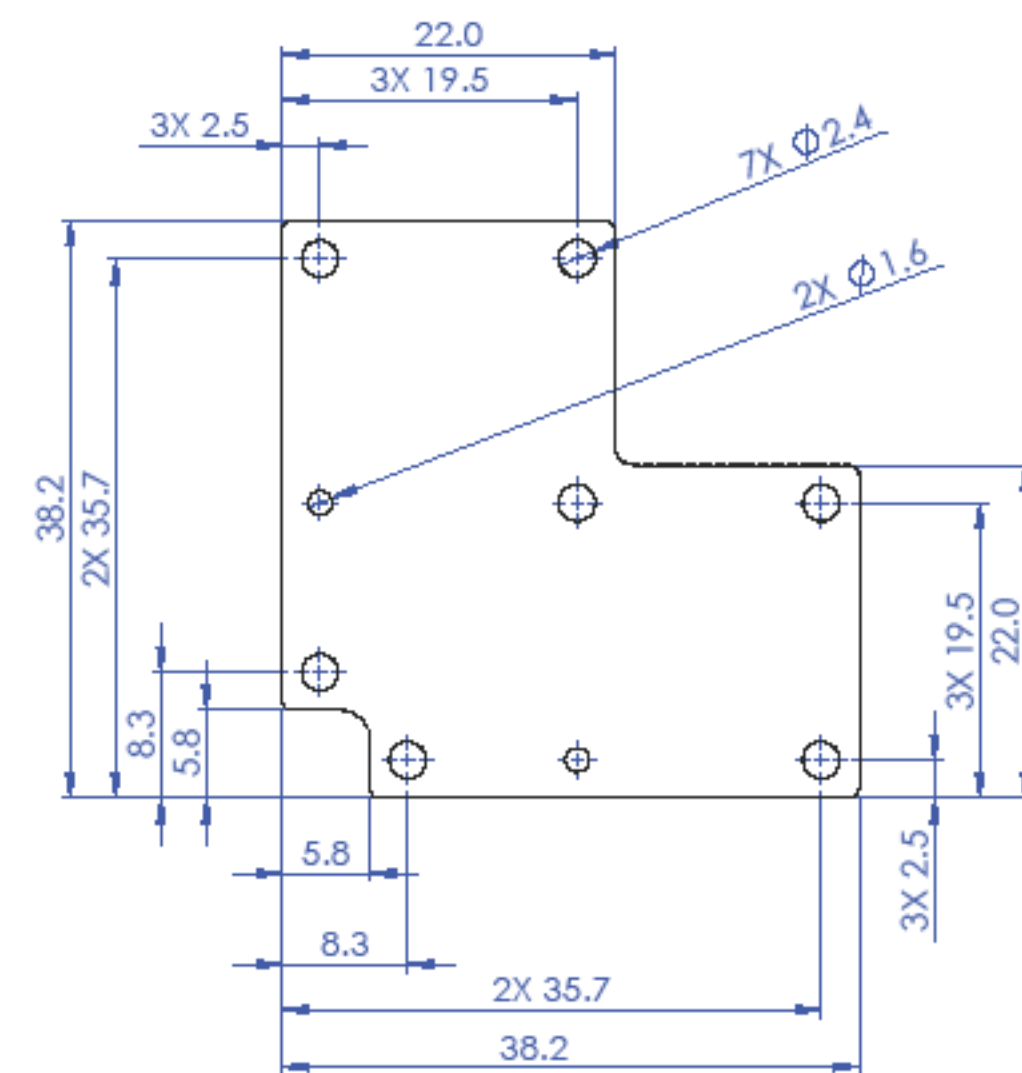
B



- NOTES:
1. BREAK ALL SHARP EDGES
  2. INTERNAL RADIUS: 0.1 MIN

PROPRIETARY AND CONFIDENTIAL  
THE INFORMATION CONTAINED IN THIS  
DRAWING IS THE SOLE PROPERTY OF  
CAL POLY CUBESAT LABORATORY. ANY  
REPRODUCTION IN PART OR AS A WHOLE  
WITHOUT THE WRITTEN PERMISSION OF  
CAL POLY CUBESAT LABORATORY IS  
PROHIBITED.

|  |                      |                |
|--|----------------------|----------------|
| UNLESS OTHERWISE SPECIFIED:                      | NAME                 | DATE           |
| DIMENSIONS ARE IN MILLIMETERS                    | NJB                  | 5/12/20        |
| TOLERANCES:                                      |                      |                |
| ONE PLACE DECIMAL $\pm 0.1$                      |                      |                |
| TWO PLACE DECIMAL $\pm 0.05$                     |                      |                |
| INTERPRET GEOMETRIC<br>TOLERANCING PER: ISO 1101 |                      |                |
| MATERIAL   |                      |                |
| 6061 ALUMINUM                                    |                      |                |
| NEXT ASSY  | USED ON              | FINISH         |
|  |                      | NONE           |
| APPLICATION                                      | DO NOT SCALE DRAWING |                |
| SCALE: 2:1                                       |                      | WEIGHT: 11.5 g |
| SHEET 1 OF 1                                     |                      |                |

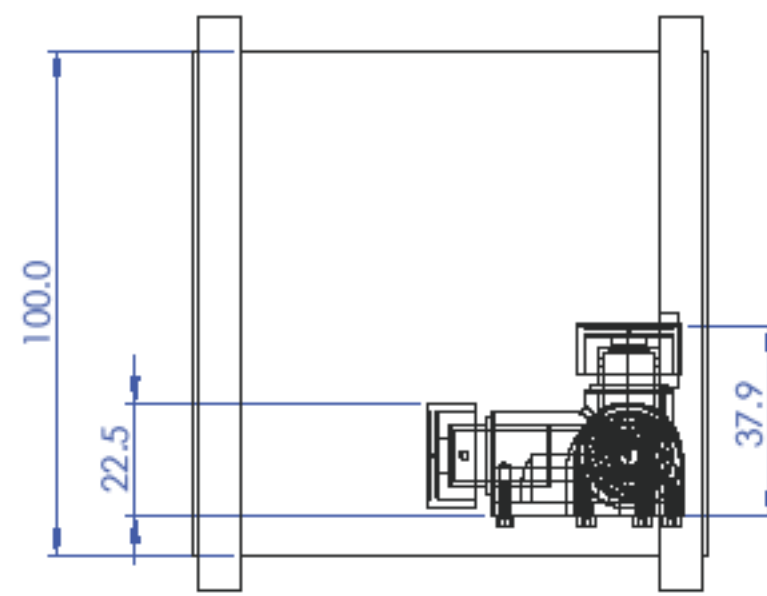
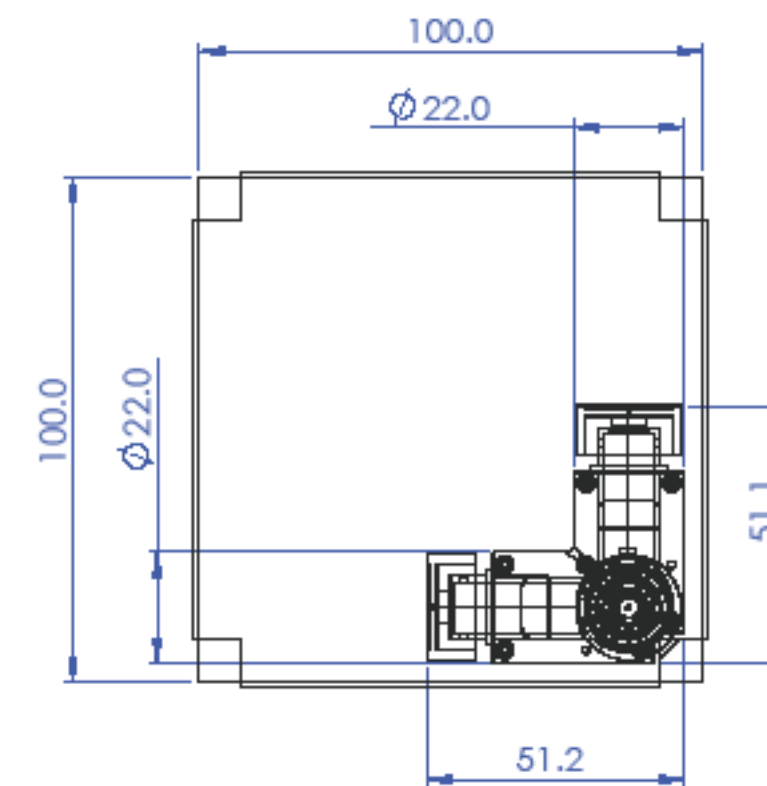


NOTES:  
 1. BREAK ALL SHARP EDGES  
 2. INTERNAL RADIUS: 0.1 MM

PROPRIETARY AND CONFIDENTIAL  
 THE INFORMATION CONTAINED IN THIS  
 DRAWING IS THE SOLE PROPERTY OF  
 CAL POLY CUBESAT LABORATORY. ANY  
 REPRODUCTION IN PART OR AS A WHOLE  
 WITHOUT THE WRITTEN PERMISSION OF  
 CAL POLY CUBESAT LABORATORY IS  
 PROHIBITED.

|            |                 |  |                |                      |                      |  |
|------------|-----------------|--|----------------|----------------------|----------------------|--|
|            |                 | UNLESS OTHERWISE SPECIFIED:<br>DIMENSIONS ARE IN MILLIMETERS               | NAME<br>NJB    | DATE<br>5/12/20      | CAL POLY CUBESAT LAB |  |
|            |                 | TOLERANCES:<br>ONE PLACE DECIMAL $\pm 0.1$<br>TWO PLACE DECIMAL $\pm 0.05$ | CHECKED        |                      |                      |  |
|            |                 |  | BNG APPR.      |                      |                      |  |
|            |                 |  | MFG APPR.      |                      |                      |  |
|            |                 | INTERPRET GEOMETRIC<br>TOLERANCING PER: ISO 1101                           | Q.A.           |                      |                      |  |
|            |                 |  | COMMENTS:      |                      |                      |  |
|            |                 | MATERIAL<br>6061 ALUMINUM  |                |                      |                      |  |
|            | NEXT ASSY       | USED ON  | FINISH<br>NONE |                      |                      |  |
|            |                 |  | APPLICATION    | DO NOT SCALE DRAWING |                      |  |
| SIZE       | DWG. NO.        |  |                |                      |                      |  |
| <b>B</b>   | <b>NJB-8802</b> |  |                |                      |                      |  |
| REV        |                 |  |                |                      |                      |  |
|            |                 |  |                |                      |                      |  |
| SCALE: 2:1 | WEIGHT: 11.5 g  | SHEET 1 OF 1   |                |                      |                      |  |

BOUNDING BOX: 51.1 x 51.1 x 37.9 MM  
VOLUME: 47.15 CM<sup>3</sup>



PROPRIETARY AND CONFIDENTIAL  
THE INFORMATION CONTAINED IN THIS  
DRAWING IS THE SOLE PROPERTY OF  
CAL POLY CUBESAT LABORATORY. ANY  
REPRODUCTION IN PART OR AS A WHOLE  
WITHOUT THE WRITTEN PERMISSION OF  
CAL POLY CUBESAT LABORATORY IS  
PROHIBITED.

|  |             |  |                          |                 |
|--|-------------|--|--------------------------|-----------------|
|  |             | UNLESS OTHERWISE SPECIFIED:<br>DIMENSIONS ARE IN MILLIMETERS     | NAME<br>DRAWN<br>CHECKED | DATE<br>5/12/20 |
|  |             | TOLERANCES:<br>ONE PLACE DECIMAL ±0.1<br>TWO PLACE DECIMAL ±0.05 |                          |                 |
|  |             | INTERPRET GEOMETRIC<br>TOLERANCING PER: ISO 1101                 | Q.A.<br>COMMENTS:        |                 |
|  |             | MATERIAL<br>N/A  |                          |                 |
|  | NEXT ASSY   | USED ON<br>FINISH<br>N/A   |                          |                 |
|  | APPLICATION | DO NOT SCALE DRAWING   |                          |                 |

**CAL POLY CUBESAT LAB**  
TITLE:  
**REACTION WHEEL  
ASSY - 1U CONTEXT**  
SIZE DWG. NO. **B NJB-8800-B** REV **A**  
SCALE: 2:3 WEIGHT: SHEET 1 OF 1

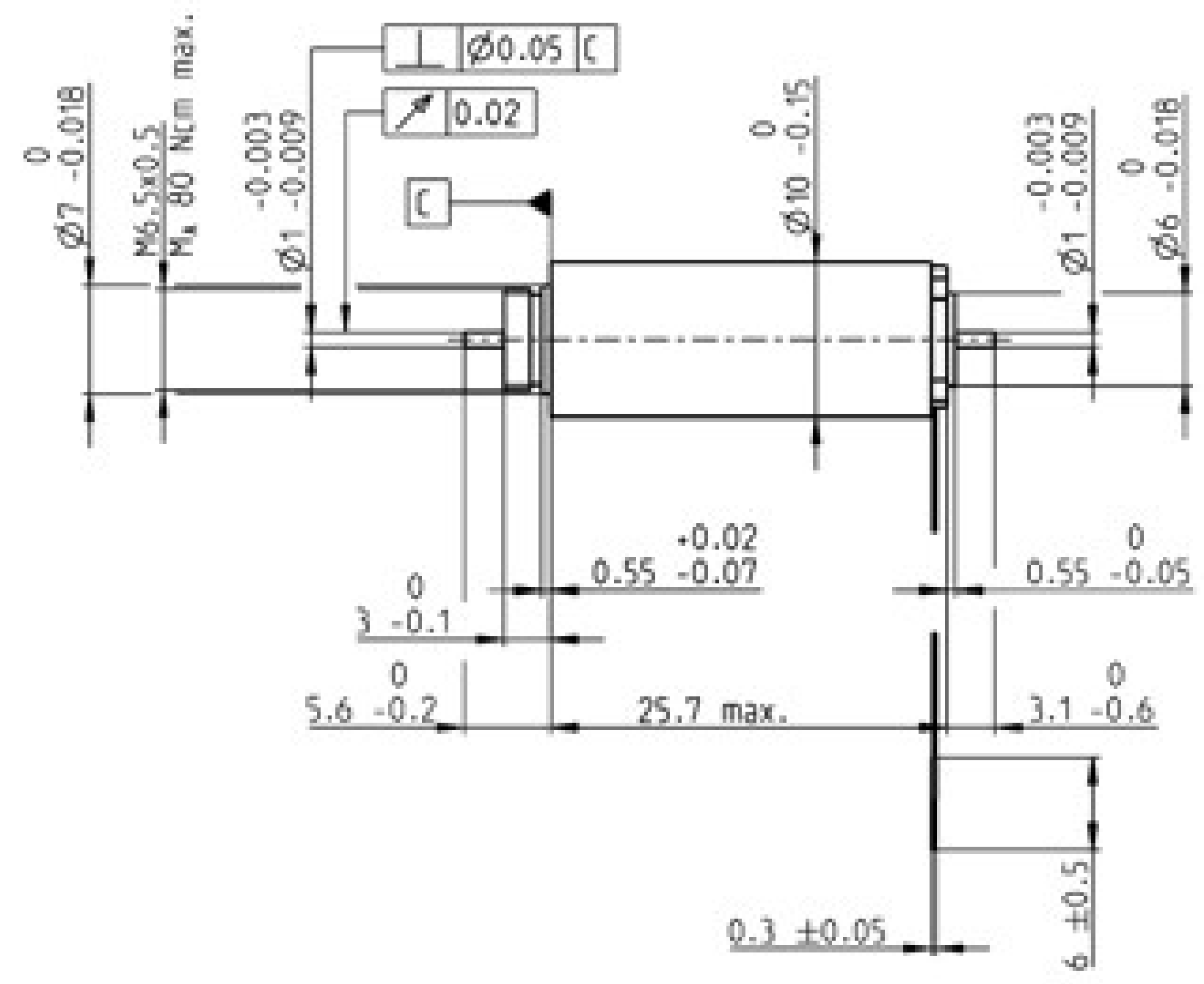
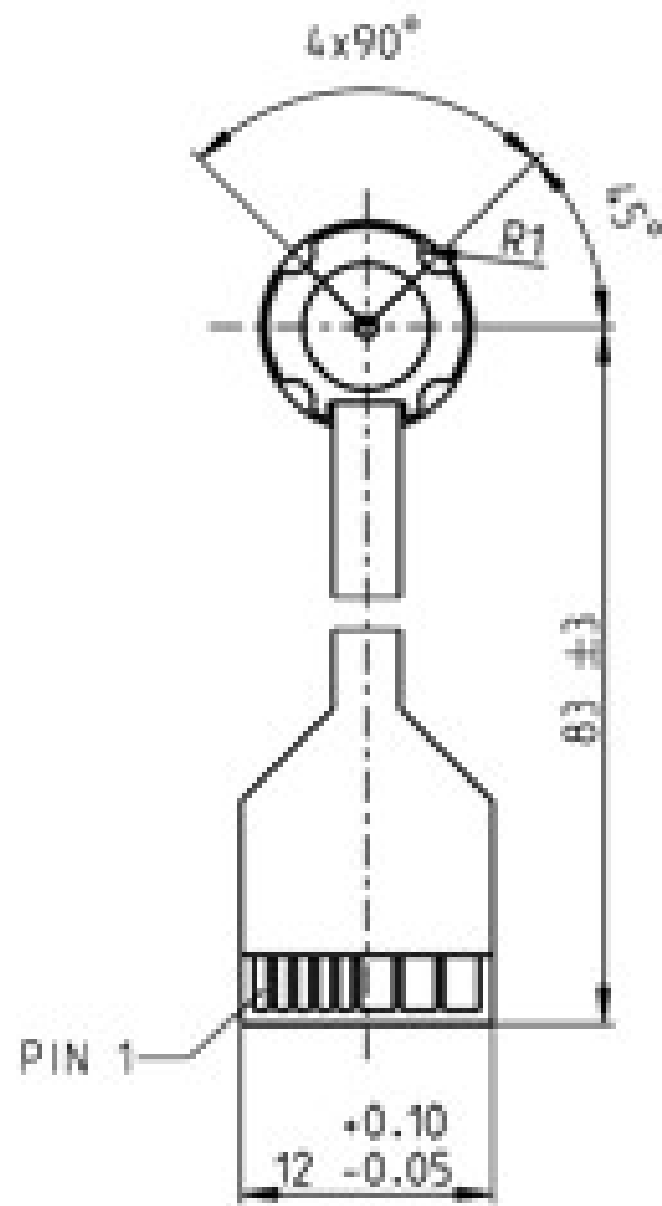


Figure F-1. EC10 Brushless DC Motor Technical Drawing [10]